Report No. 727-1
October 2002

FINAL REPORT

PROGRAM ELEMENT NO. 2.18

DEVELOPMENT OF A ROUTE OR MISSION-DEPENDENT APPROACH FOR THE CALCULATION OF RATIONAL STRUCTURAL DYNAMIC LOADS FOR HIGH-SPEED MULTIHULLS

By:

Band, Lavis & Associates
A division of CDI Government Services
900 Ritchie Highway, Suite 102
Severna Park, Maryland 21146

CCDoTT Fiscal 2001 Subcontract, DTMA91-97-H00007

CCDoTT Project Director:
Stanley Wheatley
CCDoTT
6300 State University Drive, Suite 280
Long Beach, CA 90815

Band, Lavis & Associates Program Manager:
Sathish Balasubramanian
Band, Lavis & Associates
900 Ritchie Highway, Suite 102
Severna Park, MD 21146

This program has been funded by the Center for Commercial Deployment of Transportation Technologies (CCDoTT) at California State University, Long Beach.

FOREWORD

The work described in this report was prepared by Band, Lavis & Associates (BLA) under subcontract to California State University, Long Beach Foundation (CSULB) for the Center for Commercial Deployment of Transportation Technologies (CCDoTT). The point of contact at CSULB was Mr. Stanley Wheatley.

The Program Manager for BLA was Dr. Sathish Balasubramanian. The principal contributors to this work were Andrew Eisele, Manish Gupta and Mark McCain.

TABLE OF CONTENTS

TABLE OF CONTENTS (continued)

LIST OF FIGURES

LIST OF FIGURES (continued)

LIST OF TABLES

EXECUTIVE SUMMARY

Structural design for conventional hullforms usually relies on past design experience which, today, is best represented by Classification Society Rules or U.S. Navy Design Data Sheets. However, past design experience can only apply to ships of similar type, size and speed to those of the past. In the absence of design loads for similar ships, a reliable analytical tool is needed to calculate the dynamic loads for new designs. Alternatively, expensive experimental investigations would be necessary, especially for predicting impact and slamming loads. As interest in High-Speed Sealift continues to grow, the need for reliable structural design and analysis tools becomes ever more important. The calculation of reliable structural design loads for an advanced high-speed ship is a critical part of the design cycle.

The specific program of work described in this report was proposed under Program Element 2.18 to represent the first phase of a two-phased effort to develop a ship motion and dynamic load calculation program that would be suitable for use by Designers, Classification Societies and the U.S. Navy. The resulting program was to be suitable for advanced hullforms, including slender monohulls, catamarans and trimarans, SES, and other advanced hullforms. In Phase I, the development of an overall working model of a frequency-domain ship motion and loads model that incorporates a mission profile module that provides a description of the ships' overall lifetime loads was developed. Figure 1 is a visual representation of the approach.

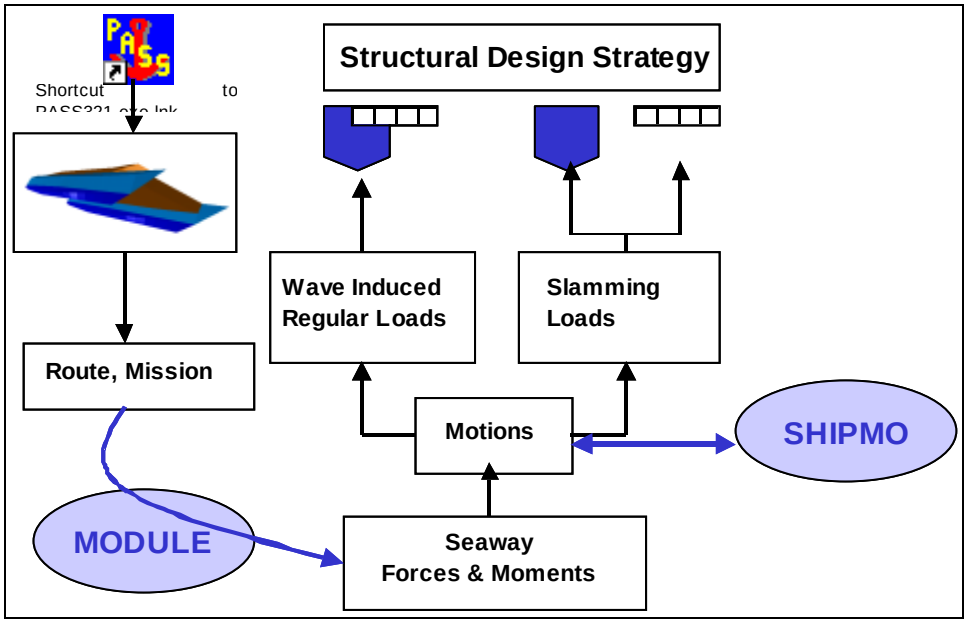

Figure 1. Schematic Representation of the Various Elements in the Development of a Route or Mission-Dependent Structural Loads Determination Program

A program framework established for tasks to be completed in Phase I included:

1. *Detailed literature survey to ensure that we have chosen the most appropriate hydrodynamic, ship motion and statistics theories.*

2. *Use of SHIPMO to model the motion characteristics of catamarans and trimarans. Compare the results of the numerical predictions with model and full-scale data. Develop analytical rationale for the differences (if any) between the experimental and numerically-predicted data. Develop modifications to the SHIPMO program to overcome any such limitations.*

3. *Use the modified SHIPMO model to predict motions and structural loads. Develop statistical descriptions of these variables. Develop a comparison of existing extreme value estimation methods as well as a method to estimate extreme loads from the calculated frequency-domain statistics. Develop a procedure and rationale for determining the load for a probability-based structural design method.*

This report summarizes the research and contributions to the state-of-the-art on rational structural design criteria accomplished in the conduct of Phase I of Program Element #2.18.

1.0 INTRODUCTION

Structural load determination is a critical part of the design spiral for high-performance vessels. Such vessels often feature high-speed capability and are, thus, inevitably weight sensitive. Therefore, it becomes essential that adequate structural strength be achieved without over-designing the structure. Such a structural design must possess a reasonable probability of surviving the environmental loads imposed on it during its lifetime.

The determination of the success of the structural design hinges on the determination of the loads to which it will be exposed and the specification of a reasonable probability level for its survival. The environmental loads imposed on the structure will have to be determined from an analysis of the modes of operation of the vehicle and its environment, and then by making use of this information to define a number of deterministic load conditions for analysis. Each of these load conditions is to be assigned a probability of occurrence and compounded to develop a single long-term probability distribution to each type of load. A failure in the accurate determination of structural loads can have significant impact on the design and operation of the vehicle. Underestimation of the loads can result in structural failure or limit operations. Overestimation of loads, on the other hand, will make the vessel carry excess structural weight, resulting in reduced operational range and payload. Hence the need for a rational approach to loads determination.

Key to the prediction of ship structural loads is the prediction of the response of the ship to the sea. Structural loads such as transverse bending and torsional moment are especially important for advanced hullforms. Therefore, there is a need for a ship motions model that can accurately model the motions of advanced hullforms. Such a motions model would have to be capable of handling high forward speed and multihull configurations such as catamarans, trimarans, SES and SWATH, and the potential impact of lifting bodies. The current state-of-the-art in frequency-domain models for ship motions is limited to low Froude numbers and has not been extensively validated for novel hullforms. Also, advanced nonlinear hydrodynamic CFD codes (such as LAMP, SWAN and USAERO) for predicting ship loads are extremely difficult to adequately validate for a wide range of hullform types, and are also very time consuming to set up, and slow and expensive to run.

The specific objective of the tasks proposed under Program Element 2.18 represents the first phase of a two-phased effort to develop a ship motion and dynamic load calculation program that is suitable for use by designers, Classification Societies and the U.S. Navy. The resulting program will be suitable for advanced hullforms, including slender monohulls, catamarans and trimarans, SES, and other advanced hullforms. In Phase I, the development of an overall working model of a frequency-domain ship motion and loads model that incorporates a mission profile module that provides a description of the ships' overall lifetime loads is being developed.

The calculated values from the frequency-domain program, developed in Phase I, will be the statistical values of ship wave-induced loads for various combinations of sea-states, ship heading angle, ship displacement and forward speed. The probability of slamming, and the loads associated with slamming, will then be predicted using a time-domain program to be developed in Phase II.

The final deliverable from this two-phased effort will be a program to quickly calculate ship motions and dynamic loads for not only monohulls, but also multihulls for operation within any specified speed and sea-state lifetime scenario. The program will be a combination of a frequency-domain program that uses the same theoretical approach as used for SMP and a time-domain program for predicting the slamming loads on high-speed ships.

At the outset, a very detailed literature survey was performed to ensure that we have chosen the most appropriate hydrodynamic, ship motion and statistics theories to describe multihull ship motions and loads. Data sources that characterize ship motion characteristics and measured structural loads on multihull vessels, including catamarans and trimarans, were identified and reviewed. Such data provided significant value in ascertaining the numerical correctness of the numerical modeling effort that was

undertaken. Following these tasks, a more detailed program framework was developed and can be described as follows:

1. Modeled the motion characteristics of catamarans and trimarans. The University of Michigan SHIPMO program was utilized to model the motion of multihulls. Compared the results of the numerical predictions with model and full-scale data. Developed analytical rationale for any differences between the experimental and numerically-predicted data.

2. Investigated modifications to the SHIPMO program to overcome limitations in its applicability.

4. Used the SHIPMO model to predict motions and structural loads. Developed statistical descriptions of these variables.

5. Used existing extreme value estimation methods to estimate extreme loads from the calculated frequency-domain statistics. Developed a procedure and rationale for determining the load for a probability-based structure design method.

The tasks outlined above were initiated and performed. Several of the tasks that followed the validation effort of the motions model were performed using the example of an east coast AutoFerry concept that was previously developed by the authors.

In preparation for the discussion of the motions and loads modeling approaches that have been conducted and are reported in the subsequent chapters of this report, we present a brief introduction to the existing paradigms in ship structural design and the naval architecture of multihulls. This is followed by a description of the state-of-the-art of experimental seakeeping assessment of multihulls.

1.1 Structural Design Methodologies

Almost all of the commercial and a fair number of military vessels, even until recently, were designed primarily using empirical approaches and “cook-book” methodologies. In the commercial sector, the Classification Societies and International Maritime Authorities provide these approaches in the form of design rules and guidelines. The military sector tends not to lean heavily on the empirical design methods, but uses first-principle approaches and model testing, to a great extent, since military vessels fall under the high-performance arena and their designs are generally pushed to the limit.

For commercial vessels, it is important that the design rules and guidelines ensure that the ships are built with an acceptable level of safety. One of the catastrophic events a ship can experience is collapse of the hull-girder. Such an event would imply a risk of loss of human lives and a risk of polluting the environment, dependent on ship type. The difference between ship types is not yet reflected in the design rules regarding the longitudinal strength. In order to avoid collapse of the hull, the design rules prescribe a maximum stress level, which must not be exceeded, under a prescribed bending moment and shear force loading. This seems to be a rather simplified methodology to avoid an extremely complex event, and it must be expected that the safety level of ships varies significantly. In order to estimate the probability of collapse of the hull, it is necessary to have a tool that can calculate the strength of the hull. Further, a probabilistic method to evaluate the probability that the loading on the hull exceeds the strength is also essential. Such a probabilistic analysis demands much computational work. Therefore, it is necessary that the calculation of the loads and strength of the hull is fast and effective.

Classification Society rules are based on analytical models for response and strength that are empirically modified to obtain agreement with observations. The safety level of existing ship structures is, hence, to a large extent, defined through registered failure statistics. Consequently, it is not straightforward to compare alternative designs if these designs are not closely related to traditional designs. Recent trends in ship design are towards more use of innovative materials and the development of new ship types. In these cases, it has become very important to estimate the actual safety level of ship structures, making it possible to compare traditional designs to new ones, aiming at the same level of safety.

The rules developed by Classification Societies have not been calibrated against a uniform reliability level. On the contrary, several analyses concerning specific structures have shown very large variations in safety and reliability levels. The two main objectives of any design tool development and calibration of partial safety factors are the determination of a method that is simple to use and yet achieves a uniform safety level for any design which is based on the method. Unfortunately, simplicity and safety become conflicting objectives when ship designers work to meet time and cost limitations.

Results of several analyses from various sources have shown that a large scatter exists presently in the design safety levels of ships, even when the unified requirements of the Classification Societies are satisfied. However, these studies have demonstrated the usefulness of a reliability-based approach in the development of ship longitudinal strength requirements. Development of a semi-probabilistic design approach compared to using empirical design rules certainly has significant merits, especially for unconventional ship types and hullforms. However, the evaluation of the target probabilities of failure can only be obtained through the results of an exhaustive set of reliability calculations carried out on a wide range of ship types and hullforms rather than using the outcome of casualty returns, which are heavily affected by the corrosion condition of structures and the different operational profiles of ships. Over the last decade, several reliability-based design methods have been proposed by the research community, which the Classification Societies are now trying to adopt in evaluating new designs. However, the inclusion of semi-probabilistic design philosophy in the rules remains to be seen.

Military vessel designs have their own sets of empirical methods, namely the U.S. Navy Design Data Sheets and NAVSEA Design Manuals. However, military ship designers also employ first-principles design philosophies featuring analytical and probabilistic approaches to complement the empirical methods. The analytical design process requires motions and loads estimation for the ship type, for a given hullform, and operational parameters. More often than not, an analytical design method needs either expensive simulation tools or experimental data. Apart from the extreme load predictions, the other side of the equation entails material property limits, which are well understood for conventional materials but, again, need design investigations for high-performance materials such as composites and new alloy grades. The commercial design community has also proposed first-principle design approaches such as the Dynamic Load Approach (DLA) of the American Bureau of Shipping (ABS), which requires hydrodynamic analyses to estimate the motions and loads in addition to performing a full-ship finite-element analysis of the ship structure to assess the design stress and safety levels.

1.2 High-Performance Multihulls

In the last two decades of the 20th Century, the realization that multihull ships possess certain attributes that offer significant advantages for certain applications has driven their increased use. This fact is borne out primarily in the arrival of catamarans in support of the high-speed fast passenger and freight market. Several other types of multihull vessels are in various levels of design and deployment.

A high-performance vessel is defined as a vessel that has performance which is significantly better than that of a typical displacement vessel. Measures of performance include high speed, better seakeeping, and greater maneuverability. This definition is difficult to use and, more often than not, high speed has become synonymous with high performance. Even so, there is no universally accepted definition of “high speed,” especially with regard to marine craft. The most common definition is the example of the planing craft, where high speed exists as soon as the support transitions from hydrostatic to predominantly hydrodynamic lift. This transition occurs around a Froude Number (F_n) of about 0.9. Thus, in general terms, this means that “high speed” is associated with a craft becoming “dynamically supported.” This is not always the case and an even broader, simpler definition of “high speed” needs to be established. Classification and Regulatory Bodies have developed varying definitions of high speed. These definitions are summarized below.

American Bureau of Shipping (ABS) - According to the ABS “Guide for Building and Classing High-Speed Craft,” when the $F_n \geq 0.9$, the vessel is classed as a high-speed craft.

Det Norske Veritas (DNV) - The DNV Rules for High-Speed Light Craft provides a definition which is not related to the geometry of the vessel. When the service speed of the vessel is greater than 25 knots, the vessel is classed as having a high speed.

Lloyds Register (LR) - LR sets forth a definition of high speed based on the speed-to-length ratio or Taylor Quotient ($V_K/L^{1/2}$), which is dimensional. A high-speed craft has a speed-to-length ratio of greater than 3.6 knots/meter$^{1/2}$ (1.99 knots/ft$^{1/2}$).

International Maritime Organization (IMO) - The IMO's Chapter X of SOLAS, "The High-Speed Craft Code," uses a modification of the volumetric Froude Number to set a minimum speed. The IMO's definition of high speed is: $V \geq 3.7*(\text{Displaced Volume})^{0.1667}$, where V is in meters/second and displaced volume is in cubic meters. This is a fairly appropriate approach as most of the existing fast ferries fall into this category.

In a later section of this report, we will highlight the differences between the approaches taken by the various Classification Society rules regarding structural design of high-performance multihulls.

Figure 1.2-1 is a graphical representation of various high-performance multihull concepts. In Figure 1.2-1, the underwater hullforms are shown to be of various types and represent a fairly comprehensive collection of hullforms. The choice of hullform, in combination with certain geometry, determines the overall design. Several unique types of hullforms have been developed to optimize the underwater hullform to maximize the potential for specific applications. Thus, one can have, for example, a combination of the SWATH hullform with a twin-hull arrangement or a four-hull arrangement. The latter is representative of the SLICE concept developed by Lockheed Martin. In the following paragraphs, we will briefly highlight the salient characteristics of some of the more developed multihull concepts.

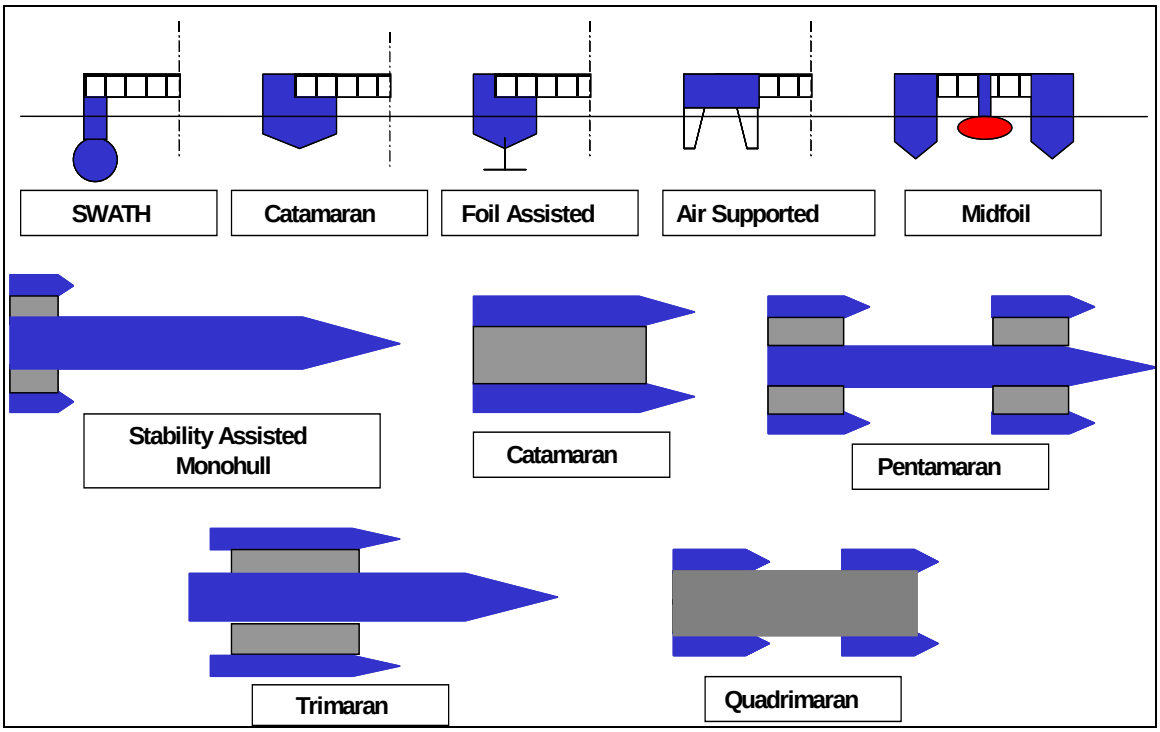

Figure 1.2-1. Schematic Description of Multihull Configurations and Hullforms

Catamarans

High transverse stability, small roll angles, large deck areas and good maneuverability, the signature of catamaran hullforms, have been exploited to good use initially for research vessels, submarine rescue vessels, and passenger and car ferries. In recent years, a new generation of catamaran vessels has emerged for high-speed passenger and car transport and is finally fully utilizing the inherent advantages of the beneficial effects of increasing aspect ratio of the hulls for decreasing the resistance to forward motion while reducing the area and longitudinal moment of inertia of a ship's waterplane to reduce ship motions.

Trimarans, Quadrimarans & Pentamarans

Trimarans are basically very slender monohulls fitted with small sidehulls or outriggers to provide them with sufficient lateral stability. The more recently proposed pentamaran concept operates on the same principle. A proper balance between the slenderness ratio of the main hull and the size and separation of the sidehulls is needed to ensure a net benefit from a speed-powering viewpoint. There has been a recent increase in interest in trimarans as viable options for ferry hullforms. There has also been interest shown by the UK and U.S. navies, including several prominent shipyards, in investigating the use of a displacement trimaran hullform for frigates and corvette size warships as well as for use as high-speed sealift platforms. Trimarans represent a highly efficient hullform allowing higher speed or lower installed power compared to equivalent monohulls as the sidehulls can easily provide adequate intact and damage stability characteristics that limit the slenderness of monohulls. Interest in this concept for large vessels, such as ferries, is recent and there is, as of yet, very little design and operational experience. The High-Speed Sealift Innovation Cell has recently been evaluating the motion characteristics of a scaled-segmented model of a trimaran type ship.

Wave-Piercers

Wave-piercing catamarans were developed to provide more comfortable high-speed passenger transport on open-ocean or other exposed routes than conventional catamarans. Like conventional catamarans, wave-piercers have twin hulls and are long and slender, but with minimal freeboard and little buoyancy in the bow section. This configuration allows the bows to cut, or pierce, the waves, reducing the tendency of the vessel to contour or ride over the waves. The pitch motions and accelerations that result are lower than in a conventional catamaran of similar deadweight. It should be noted that some wave-piercers have a half hull or third bow between the main hulls, which does not provide buoyancy since it is above the water in calm seas, but does help mitigate wave slap and slam loads on the cross-structure while operating in high sea-states.

SWATH and Semi-SWATH

The seakeeping characteristics of surface ships are significantly improved by reducing the area and changing the shape of the waterplane. However, a vessel having a small waterplane area still requires a displacement volume, and therefore the underwater shape is usually bulbous. Such a vessel, called a Small Waterplane Area Twin-Hulled vessel, or SWATH, can have excellent seakeeping characteristics, and where seakeeping is most important, this type of vessel is the most suitable. Unfortunately, a SWATH suffers from some disadvantages as well. The increased wetted surface area results in additional frictional drag, and no truly high-speed SWATH craft have yet been built. The propulsion system may be very difficult to arrange with a small waterplane shape, allowing no room for an engine room in the sidehulls, and when combined with a complex curved hull shape, the craft can be expensive to construct. Semi-SWATH craft have the features of a SWATH in the forward part, but the waist at the waterline decreases going aft such that the engine room shape is the same as a conventional catamaran. There is a small penalty to pay with increased frictional resistance, but usually a small benefit in the wave-making resistance and a substantial benefit in the seakeeping. Several of the larger fast ferries have been built with a semi-SWATH hullform.

Foil-Assisted Multihulls

A limited number of foil-assisted catamarans have been built and are in service as passenger ferries. The foils are employed to generate dynamic lift and, hence, increase the speed of the craft, and also

to minimize the craft motion and, hence, improve passenger comfort. There are two distinct types of foil-assisted concepts. A foil configuration where the foil lift is small and the hull remains in the water, and a configuration in which the foil lift is designed to lift the hull completely clear of the water. While these designs have been operationally successful, they require significant maintenance and are expensive to construct.

In the following paragraphs, we will attempt to define the characteristics of high-performance multihulls. Such an assessment is essential to develop a good understanding of the current design philosophy and expected trends for these craft. Any motion and loads modeling approach for high-performance multihulls will have to be cognizant of lessons learned from industry, the rationale for the design approaches that are currently in practice, and the trends in the most influential design parameters.

1.3 Naval Architectural Assessment of High-Performance Multihulls

The naval architectural development of multihulls for passenger and car ferry service has evolved in an era driven by market economics and differs quite significantly from the institutionally-sponsored research into the naval architecture of monohull vessels in the earlier part of the 20th century. As a result, information available on these new vessels is often limited to marketing information and glossy photographs that, while pleasing to the eye, are often intentionally incomplete as a means to avoid technology leveling amongst the competition. For example, full-load displacement data or form coefficients are seldom provided in marketing information. To develop empirical relationships between performance parameters and principal dimensions for multihulls, a mainstay of traditional naval architectural practice, one must employ deductive analytical techniques to fill the holes in information required to develop a complete naval architectural picture. The naval architectural assessment presented here is limited to the data available and represents 53 catamaran vessels and vessel designs that were available from marketing information and trade journals. The design trends for a family of 10 wave-piercing catamarans, a subset of the data under investigation, were also concurrently analyzed to determine designer bias in choice of dimensions and ratios.

Speed, Payload & Economics

In order to develop a background to provide meaning to the assessment of principal dimensions and ratios for high-performance catamarans, it is imperative to address the rationale for their design development in terms of the mission requirements that these vessels have been designed to satisfy. These requirements are best described in terms of the speed and payload carrying capacity of these vessels as well as the technical cost of accomplishing this capability, represented primarily by the installed power. As seen in Figure 1.3-1(a), the service speeds of the vessels under consideration are between 30 and 40 knots, independent of their deadweight carrying capacity. Recent investigations have shown that catamarans offer the best economic characteristics for fast ferry service for speeds less than 45 knots (see Appendix F). The power required to operate a monohull fast ferry of equivalent deadweight capacity would be substantially more and, hence, more expensive to operate. The data presented in Figure 1.3-1(a) appears to validate this trend and indicates that the narrow band of catamaran design speeds is indeed couched primarily in operational economics. The cost side of catamaran economics is presented in Figure 1.3-1(b) as the variation of installed propulsion power as a function of a novel term, the Transport Momentum. Transport Momentum is defined as the product of the individual weight of cars and passengers and the service speed, and represents the rate at which cargo is transported. Passenger only catamarans display a distinct and higher slope in comparison to vehicle carrying vessels. Propulsion power for most catamarans is based on marine diesel engines driving waterjets through mechanical gearing, with CODAG and gas turbine prime movers being the choice for installed power in excess of 45000 HP as gas turbines offer a higher power to weight ratio.

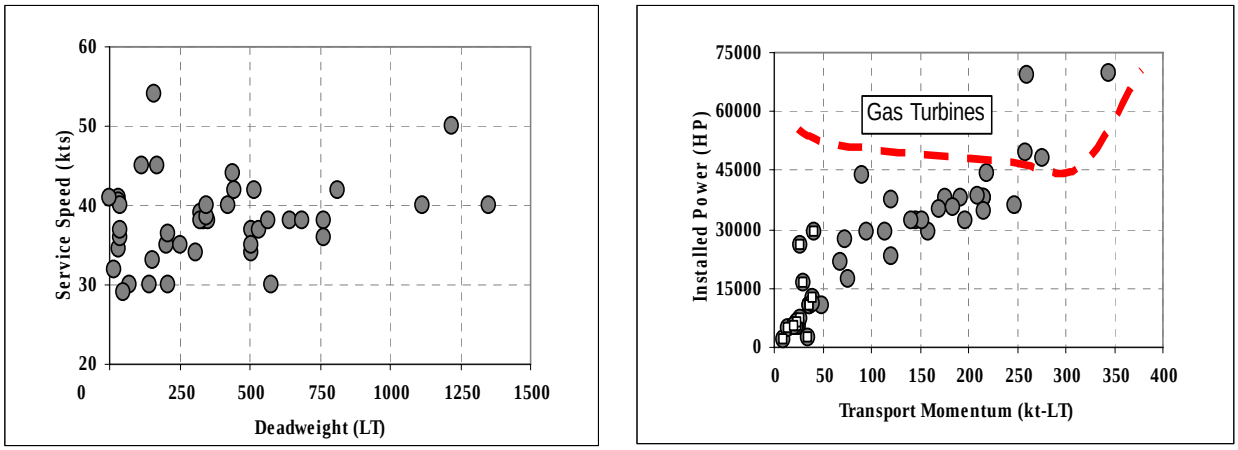

Figure 1.3-1. (a) Service Speed as a Function of Deadweight Capacity. (b) Impact of Transport Economics on Installed Power. Open squares (□) represent passenger-only catamarans.

Principal Dimensions & Hull Characteristics

The dimensions of passenger and car carrying catamarans have increased steadily and the largest in service currently are hovering around the 100m mark in overall length. Several shipyards and catamaran design houses have published marketing information for vessel designs in the 120m range, and some, in fact, have plans for 150 to 200m vessels in the future. Trends in the principal dimensions of the vessels under consideration were developed for several parameters. Of significant interest to the catamaran designer are the slenderness of the hull and the ratio of beam to draft. Figure 1.3-2(a) is a plot of the variation of demihull length-to-beam ratio as a function of waterline length. The data indicates an almost linear increase in the slenderness of the demihulls with increasing length or size of the vessel. Length-to-beam ratios in excess of 25 are projected for the largest of the catamarans and represent new ground in hull design. The data for the family of wave-piercers exhibits a colinear trend with the rest of the data and indicates no obvious designer bias. Beam-to-draft ratios have traditionally been used to assess seakeeping characteristics for monohulls, as they represent a degree of fullness of the hullform. The variation of beam-to-draft ratio for catamarans, as seen in Figure 1.3-2(b), indicates that the onus is definitely on the reduction of wetted surface area to limit frictional resistance. The data in Figure 1.3-2(b) shows substantially more scatter for the smaller vessels, with an asymptotic trend towards a limiting value of B/T ~1.50 to 1.25 emerging for the larger vessels. The family of wave-piercers appears to form the lower band of the data and displays a lower beam-to-draft ratio than other vessels of the same length.

While the Length, Beam, Draft and Block Coefficient (C_B) are sufficient to describe the geometry and principal hydrodynamic characteristics of monohull vessels, an additional variable, namely the separation between the demihulls, is required to describe the geometry and hydrodynamic characteristics of the catamaran. The separation between the sidehulls may determine the contribution of wave interference, both constructive and destructive, to the resistance of the vessel. The separation between the demihulls of the catamaran plays a significant role in determining the structural scantlings of the cross-structure between the hulls and, hence, directly affects the lightship weight of the vessel and, thus, its deadweight-to-displacement ratio.

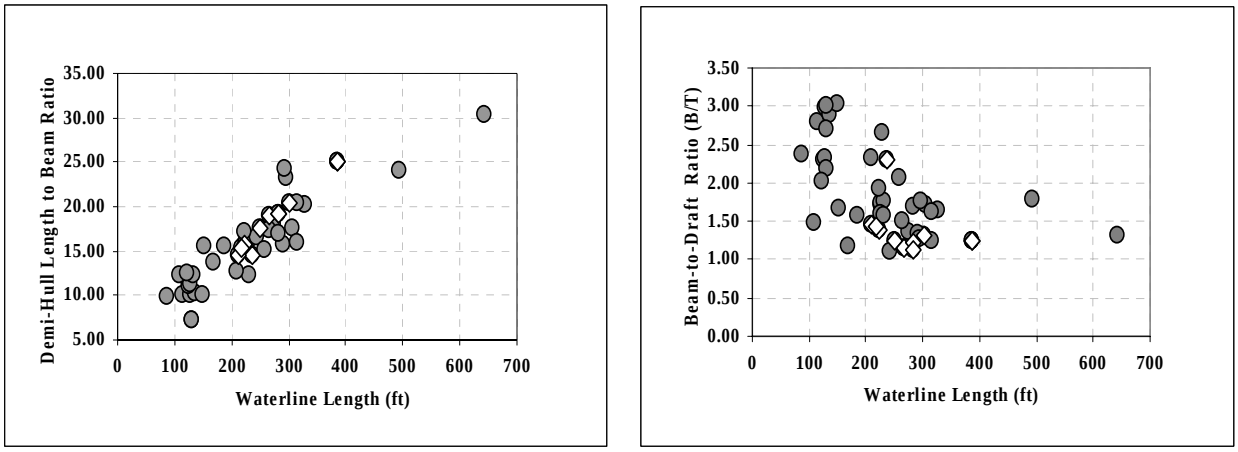

Figure 1.3-2. (a) Variation of Demihull Length-to-Beam Ratio as a Function of Waterline Length. (b) Ratio of Beam-to-Draft as a Function of Waterline Length. Open diamonds (◊) represent a family of wave-piercers.

The separation between the hulls is often represented in terms of separation ratio and is expressed as either the distance between the centerlines of the demihulls (BOA – B_{HULL}), or as the distance between the inner sides of the hulls (BOA – $2B_{HULL}$) divided by the waterline length of the craft. Figure 1.3-3(a) and 1.3-3(b) represent the variation of separation ratio (x = BOA – B_{HULL}) as a function of demihull length-to-beam ratio and Froude number, respectively. The data displays significant scatter, with a decrease in the value of separation ratio with increasing hull slenderness being visible. Data from the family of wave-piercers form the upper band of the data spread in Figure 1.3-3(a) and display an inverse linear trend. The variation of separation ratio with Froude number (Figure 1.3-3(b)) is more intriguing and suggests an increase in the separation ratio with increasing Froude number, with a maximum in separation ratio of around 0.30 at a length Froude number of 0.75. With Froude number in excess of 0.75, there appears to be a reduction in separation ratio and represents the smaller passenger-only vessels.

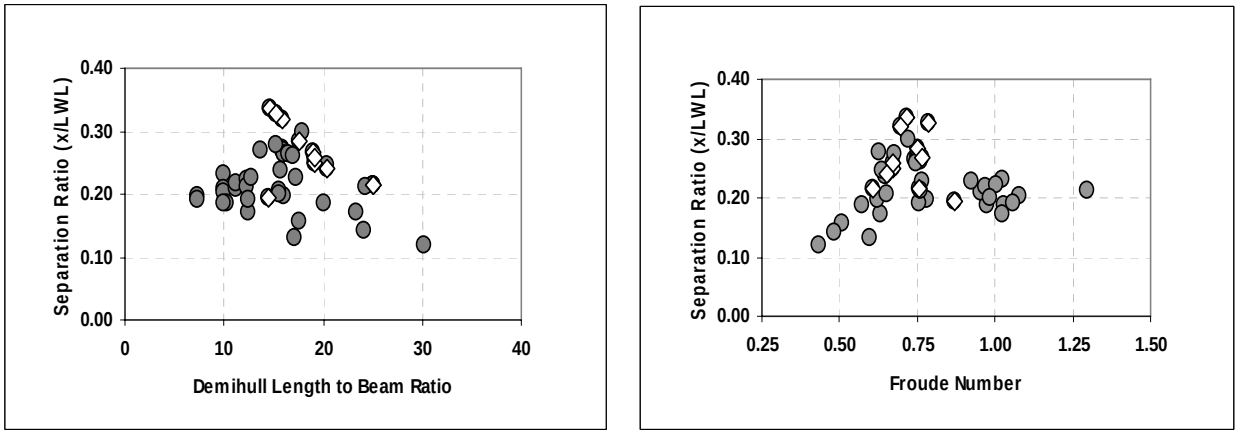

Figure 1.3-3. (a) Variation of Separation Ratio with Slenderness Ratio. (b) Variation of Separation Ratio with Froude Number. Open diamonds (◊) represent a family of wave-piercers.

In an attempt to better understand the selection of demihull separation in a catamaran, the dependence of the separation between the hulls, cast in terms of a ratio of hull beam, was also investigated, i.e. sep. ratio = (BOA – B_{HULL})/B_{HULL}. Figure 1.3-4 is a plot of the separation data in terms of hull beam as a function of hull length-to-beam ratio and Froude number. As seen in Figure 1.3-4(a), the data indicates

an increase in hull separation with increasing length-to-beam ratio and, hence, waterline length. However, the family of wave-piercers displays no variation in separation ratio as a function of both hull slenderness as well as Froude number, and indicates that the choice of hull separation is based primarily on experience and is on the order of five hull beams. It is conjectured that a detailed analysis of the data for other families of catamarans for established catamaran designs will reveal similar trends.

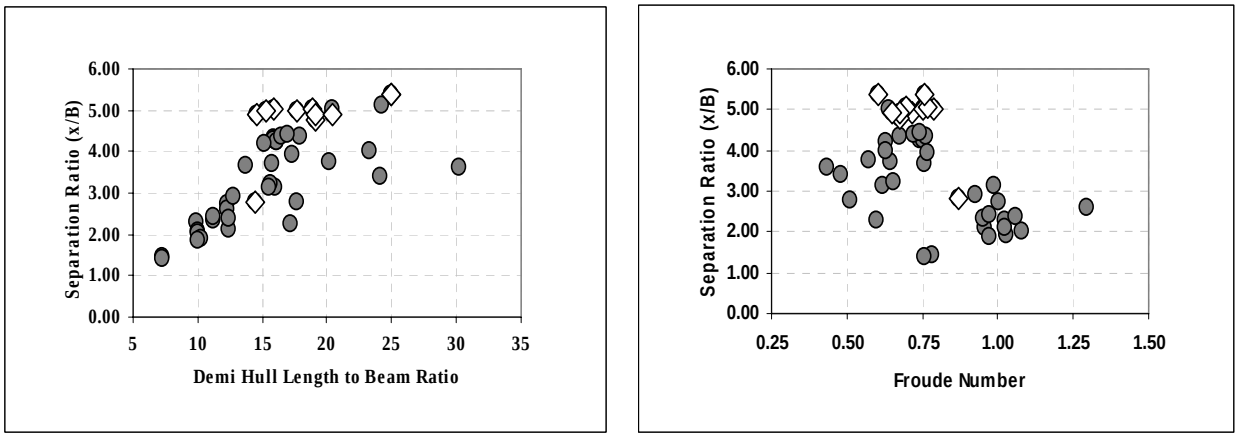

Figure 1.3-4. (a) Variation of Separation Ratio with Slenderness Ratio. (b) Variation of Separation Ratio with Froude Number. Open diamonds (◊) represent a family of wave-piercers.

Thus, for a naval architect attempting to design a catamaran based on existing vessels, there is very little guidance from historical data for the choice of suitable parameters. However, hull separation as a function of demihull beam appears to be intuitively more useful than one based on length in the development of a parametric series of high-performance catamarans. Extrapolation of the variation of the length-based separation ratio is parametrically irrelevant to the design of catamarans and could result in designs with excessive separation between the demihulls that can significantly impact the structural design of larger catamarans. The use of a beam-based separation ratio appears to limit the risk in design and would be equivalent to achieving geometric similitude for catamarans.

As mentioned earlier, very little information is currently available on full-load displacement of high-performance catamarans. An exploratory study to assess the volumetric properties of catamarans was undertaken to investigate the existence of any trends between hullform and powering. Displacement data was available for less than 20% of the data set under consideration. This data was compared to estimates of displacement for a model data set. In Figure 1.3-5(a), estimates of displacement for three models with length-to-beam ratios of 10.4, 15.6 and 20.8, with beam-to-draft ratios of 1.5, and a block coefficient of 0.50 are plotted in addition to the displacement data from actual ships. Remarkably, the available ship data is bracketed by the model data, but estimating full-load displacement can result in significant errors. An estimate of full-load displacement was made for all of the catamarans under consideration using a representative block coefficient of 0.5 based on the results described in Figure 1.3-5(a). This estimate of displacement was then used to develop an installed propulsion power-to-weight ratio and is plotted in Figure 1.3-5(b) as a function of volumetric Froude number. The data collapses in an inverse quasi-linear fashion with increasing volumetric Froude number. This data can be used to make a first estimate of the required power for new catamaran designs.

Thus, from the foregoing examination, we have established the range of geometric and mass-property related parameters for multihulls that any motion and loads predictive method should be capable of modeling.

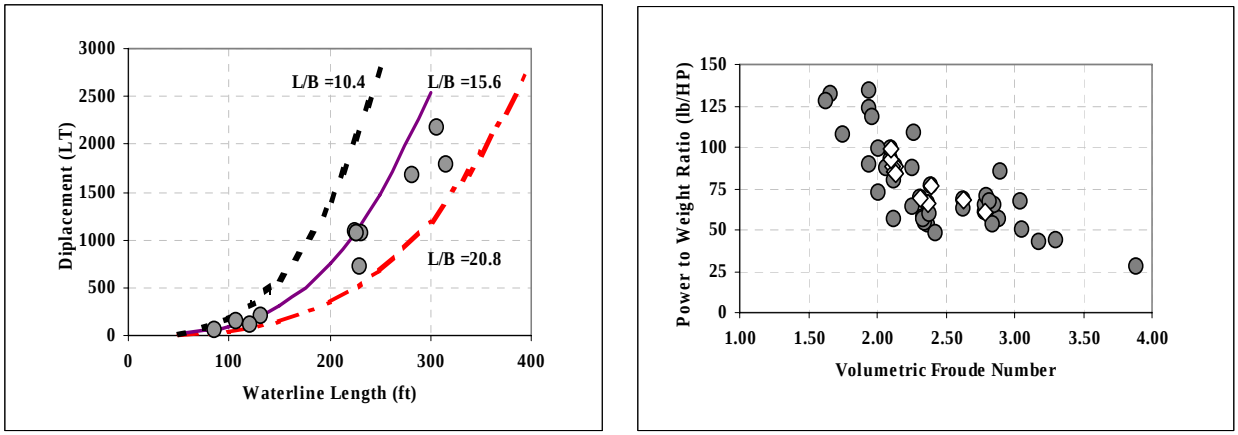

Figure 1.3-5. (a) Full-Load Displacement Data of Actual Ships in Comparison with Model Data. (b) Variation of Power-to-Weight Ratio as a Function of Volumetric Froude Number.

2.0 SEAKEEPING & MOTIONS OF MULTIHULLS

The waterplane of each hull of a catamaran or trimaran usually has a high length-to-beam (L/B) ratio and fine angles of entrance to minimize resistance in comparison to a monohull. Therefore, the longitudinal moment of inertia of the waterplane for the more slender individual hulls of a multihull is substantially smaller than that of a monohull. In addition, having two or more widely separated hulls, the transverse moment of inertia can be higher than a similar-sized monohull. Therefore, multihull craft possess motion characteristics that are quite different from those of a monohull.

For example, the rolling motion of monohull ships is characterized by the transverse motion of the water relative to the hull and, thus, results in a radial motion. The fitting of bilge keels and fins can reduce the amount of roll, although these are not desirable features for high-speed craft because of the additional frictional resistance. On the other hand, catamaran rolling is considerably less and is characterized as one hull heaving up whilst the other hull heaves down. In other words, the motion of the hull relative to the water is in a vertical direction as opposed to the radial direction of the monohull. Therefore, the most effective way to reduce roll motion on a multihull is to fit horizontal control surfaces. The seakeeping characteristics of stabilized monohulls such as trimarans may be quite different from those of catamarans. By careful design, it appears to be possible to incorporate the beneficial elements of a monohull in head seas with the beneficial elements of a catamaran in roll. The fine angles of entrance and lack of substantial flare on most multihulls result in reduced resistance to pitching motions in comparison to a monohull. The vessel may pitch and heave more than a monohull, but will have reduced acceleration levels.

A unique aspect of multihull motions that has been the subject of several investigations is termed “deck diving.” In following seas, a multihull ship may run down the face of a wave and then strike the back of the preceding wave. With the bow down attitude of the craft, striking another wave at high-speed can result in the bow of the vessel becoming buried in the wave, with green water shipped over the bow, and the vessel experiencing a severe reduction in speed. This is termed “deck diving” and has been a problem for some vessels. To avoid this problem, designs featuring a third hull between the hulls of the catamaran and having a large amount of flare and reserve buoyancy have been developed. This third hull is above the design waterline in the static load condition in order to minimize resistance, but becomes immersed should the vessel pitch down and, thus, provides a pitch reduction force.

A common method to minimize craft motions for multihull craft is to fit a fully submerged foil at the forward part of each hull containing an integral, movable trailing edge control surface, similar to elevators on the tail plane of an aircraft, commonly called a “T-foil” because of its configuration. These control surfaces are typically activated by accelerometers in order to produce forces opposing the pitching motion of the

craft. As well as the forward foil, most multihull craft have a device mounted on the transom principally to provide opposing forces to control the roll angle. These devices interact with the water flow to promote a high-pressure region to provide a lifting force on the stern. The additional drag of T-foils can be quite high because of induced drag, and the creation of vortices from foil tips, and the design of T-foils, remains a specialist area. However, lessons learned from the inclusion of such foils can be a great source of operational information to support the design of multihulls featuring lifting bodies and foils that are being studied currently.

One unfortunate characteristic of multihull craft is the need for a cross-structure to support the two or more hulls. This means that there is a structure above the waterline, which, in the case of severe motion of the craft, may come into contact with the water at high speed causing a slam. The underside of the tunnel structure is frequently a flat surface, and slamming may be an issue if the tunnel height is too low. It should be noted that the congruence of the bow waves from the multiple hulls, superimposed on the waves passing through the tunnel, can result in slamming occurring in the after part of the underside of the tunnel structure. Most high-speed craft are limited by the sea-state to a particular speed of operation. However, there is another factor unrelated to the hull design that can affect the ability to sail, and that concerns the ability to launch the life rafts.

2.1 Experimental Investigations of Multihull Motions

Several publications detailing the experimental investigations of multihull motions are available in the literature. A significant number of them focus on the impact of sidehull separation and its impact on the seakeeping behavior of catamarans. Similarly, several reports on trimaran seakeeping are also available. However, given the proprietary nature of hullform design for high-speed craft, the data from these experiments are not easily revealed. In a later section of this report, three significant contributions to the state-of-the-art in catamaran seakeeping are described. There have been several other reported experimental investigations on multihull motions. The task of compiling the salient results of all of these studies is a significant undertaking on its own. Therefore, we present here references to salient experimental multihull seakeeping studies reported in the literature as an appendix (Appendix A) to this report.

Fundamentally, the experimental investigations over the years have focused on evaluating, parametrically, the nature of hull slenderness and separation on the motion characteristics of catamarans, trimarans and other multihulls. For trimarans, the experiments have focused on the longitudinal location and geometry of the sidehulls, while for catamarans it has been more on sidehull separation. The universal truths from almost all these experiments is that:

- For catamarans, sidehull separation is not a very significant influence on vertical plane motions. Sidehull separation is driven primarily by resistance considerations, and designing to minimize interference at design speed is, thus, more important.

- For higher Froude numbers, almost all experimental investigations report response characteristics that indicate that catamaran motions in head seas are similar to those observed for monohulls.

- Catamaran motion characteristics are greatly improved when a pitch foil is incorporated between the hulls. The ideal location for the foil is forward of midship.

2.2 Numerical Motion Prediction Models

The Navier-Stokes equation (conservation of momentum) and the continuity equation (conservation of mass) are, in principle, sufficient to describe all phenomena of ship seakeeping flows. The solution of the full-bore Navier-Stokes equations is still a challenge and, very often, fundamental assumptions that simplify the flow equations are used in the field of hydrodynamics. As ship seakeeping flows are dominated by surface gravity waves in the ocean, the linearized approach to representing the ocean wave using potential flow theory has become the defacto standard to solving the ship-wave or

seakeeping problem. In such a case, the Navier-Stokes equations are simplified (by neglecting the effects of viscosity) and are referred to as the Euler equations. If one were willing to neglect the need to resolve all little turbulent fluctuations in the ship's boundary layer and wake (a reasonable simplification for most ship flows), then the approach to solving the Navier-Stokes equations is to average over time intervals, which are long compared to the turbulent fluctuations and short compared to the wave periods. This then yields the Reynolds-Averaged Navier-Stokes equations (RANSE). RANSE solvers are still computationally intensive and require a tremendous amount of computing resources, not only to run, but to adequately validate for each new application.

In practice, potential flow solvers are used almost exclusively in seakeeping predictions. The most frequent application is the computation of the linear seakeeping properties of a ship in elementary waves. In addition to the assumption for Euler solvers, potential flow assumes that the flow is irrotational. This is no major loss in the physical model, as the water adhering to the hull creates a rotational flow and this information is already lost in the Euler flow model. Potential flow solvers are much faster than Euler and RANSE solvers because potential flows have to solve only one linear differential equation instead of four non-linear coupled differential equations. Potential flow solvers are usually based on boundary element methods and need only to discretize the boundaries of the domain, not the whole fluid space. This reduces the effort in grid generation (the main cost item in most analyses) considerably.

Limitations of potential flow methods include the need for a simple, continuous free surface. Flows involving breaking waves and splashes can hardly be analyzed properly by potential flow methods. In reality, viscosity is significant in seakeeping, especially if the boundary layer separates periodically from the hull. This is definitely the case for roll and yaw motions. In practice, empirical corrections are introduced to overcome these limitations. The theoretical basics and boundary conditions of linear potential methods for ship seakeeping are treated extensively in several textbooks dedicated to ship hydrodynamics and seakeeping. Short descriptions of the more common seakeeping modeling approaches are presented herein following a brief introduction to the mathematical description of potential flow theories.

Potential Flow Methods

The flow around a ship in waves is described in terms of a velocity potential. The time and space derivatives of this velocity potential give the spatial variations of velocity and pressure of the water. The potential itself satisfies the field equation (Laplace Equation, describes continuity of mass) and boundary conditions on the surface and bottom of the ocean as well as on the surface of the ship. This potential can be considered an aggregate of several components to the ship flow and can be broken down into:

- A potential due to the (downstream) uniform flow equal to the ship speed.
- A potential due to the steady flow disturbance due to the ship.
- The wave potential (undisturbed by the presence of the ship).
- Unsteady wave potential.

The total potential (sum of the components) is, therefore, a combination of a steady component (time invariant) flow due to the ship and a periodic component due to the ocean waves. Since the field equation is linear, these contributing potentials can be linearly superimposed to generate the total potential. Different numerical techniques employ approximations to represent the wave potentials and often account for the differences in the results. The most important of the linear techniques are:

Strip Method

Strip methods have emerged as the standard tools for ship seakeeping computations. As the name suggests, the method reduces the three-dimensional problem to a set (e.g. typically 10 to 30) of two-dimensional boundary value problems. They omit the potential of the steady flow disturbance completely and approximate the remaining unsteady potential in each strip independently of the other strips. The methods originated in the late 1950s with the work of Korvin-Kroukovsky and Jacobs. Most of today's strip methods are variations of the strip method proposed by Salvesen, Tuck and

Faltinsen (1970). These are sometimes also called STF strip methods, where the first letter of each author is taken to form the abbreviation. The two-dimensional problem for each strip can be solved analytically or by panel methods. The analytical approaches use conformal mapping to transform semi-circles to cross-sections resembling ship sections (Lewis sections). Although this transformation is limited (example: submerged bulbous bow sections cannot be represented in satisfactory approximation), this approach still yields, for many ships, results of similar quality as strip methods based on panel methods (close-fit approach). Despite these inherent theoretical shortcomings, strip methods are fast, cheap and for most problems sufficiently accurate.

Insufficient accuracy of strip methods, often cited in the literature, is often due to the particular implementation of a code and not due to the strip method in principle. However, at least in their conventional form, strip methods fail (as most other computational methods) for waves shorter than perhaps 1/3 of the ship length. Therefore, the added resistance in short waves (being considerable for ships with a blunt waterline) can also only be estimated by strip methods if empirical corrections are introduced. The linear strip method is described in more detail in a later section of this report.

Unified Theory

Developed by Newman and Sclavounos at MIT, the “unified theory” is intended for slender bodies. In essence, the theory uses the slenderness of the ship hull to justify a two-dimensional approach in the near field that is coupled to a three-dimensional flow in the far field. The far-field flow is generated by distributing singularities along the centerline of the ship. This approach is theoretically applicable to all frequencies, hence, “unified”. Despite its better theoretical foundation, unified theories have failed to give significantly and consistently better results than strip theories for real ship geometries.

High-Speed Strip Theory (HSST)

Several authors have contributed to the high-speed strip theory after the initial work of Chapman (1975). HSST usually computes the ship motions in response to an elementary wave using linear potential theory. The method is often called 2 1/2 dimensional, since it considers the effect of upstream sections on the flow at a point x, but not the effect of downstream sections. Starting at the bow, the flow problem is solved for individual strips (sections). The boundary conditions at the free surface and the hull (strip contour) are used to determine the wave elevation and the velocity potential at the free surface and the hull. Derivatives in longitudinal direction are computed as numerical differences to the upstream strip that has been computed in the previous step. The computation marches downstream from strip to strip and ends at the stern just before the transom. HSST is considered an appropriate tool for fast ships with Froude numbers $F_n > 0.4$, but is often inappropriate for lower Froude numbers.

Greens Function Method (GFM)

Greens function methods distribute panels on the average wetted surface (usually for calm-water floating position, neglecting dynamical trim and sinkage and the steady wave profile) or on a slightly submerged surface inside the hull. The velocity potential of each panel (Greens function) fulfills automatically the Laplace equation, the radiation condition (waves propagate in the right direction), and a simplified free-surface condition (omitting the potential of the steady flow disturbance completely). The unknown (either source strength or potential) is determined for each element by solving a linear system of equations such that for each panel, at one point, the zero normal velocity condition on the hull is fulfilled. Some GFM approaches formulate the boundary conditions on the ship under consideration of the forward speed, but evaluate the Green function only at zero speed. This saves a lot of computational effort, but cannot be justified physically.

As an alternative to the solution in the frequency-domain (for excitation by elementary waves), GFM may also be formulated in the time-domain (for impulsive excitation). This avoids the evaluation of highly oscillating integrands, but introduces other difficulties related to the proper treatment of time history of the flow in so-called convolution integrals. Both frequency and time-domain solutions can

be superimposed to give the response to arbitrary excitation, e.g. by natural seaway, assuming that the problem is linear.

Rankine Singularity Method (RSM)

RSMs, in principle, capture the potential of the steady flow disturbance completely and also more complicated boundary conditions on the free surface and the hull. They offer the option for the best approximation of the seakeeping problem within potential theory. This comes at a price, as both the ship hull and the free surface in the near field around the ship have to be discretized by panels. Capturing all waves while avoiding unphysical reflections of the waves at the outer (artificial) boundary of the computational domain poses the main problem for RSMs. Since the early 1990s, various RSMs for ship seakeeping have been developed. By the end of the 1990s, the time-domain SWAN code (SWAN – Ship Wave ANalysis) of MIT was the first such code to be used commercially.

Combined RSM-GFM Approach

GFMs are fundamentally limited in capturing the physics when the steady flow differs considerably from uniform flow, i.e. in the near field. RSMs have fundamental problems in capturing the radiation condition for low values of the encounter frequency (often the case for high-speed ships). Both methods can be combined to overcome their individual shortcomings and to combine their strengths. "Termed Hybrid" or "Combined Boundary Integral Equation" methods match the near-field RSM solutions directly to far-field GFM solutions by introducing vertical control surfaces at the outer boundary of the near field. The solutions are matched by requiring that the potential and its normal derivative are continuous at the control surface between the near field and the far field.

It is pertinent at this point to briefly describe the Large Amplitude Motion Program (LAMP) developed by SAIC (Salvesen & Lin). LAMP is an integrated multi-level system for ship motion simulation. LAMP solves the nonlinear free-surface flow problems using a three-dimensional time-domain potential flow method. This allows its use for cases where the body motions and incident waves are very large. Again, such programs are expensive to run and validate for each application, but can be helpful when the ship design is almost complete.

Focusing attention on seakeeping computations for fast and unconventional ships, the computational methods for conventional ships are not always applicable without modification to fast ships. The HSS theory described earlier has been used successfully for both fast monohulls and multihulls, and has fared better than methods employing Greens function and Rankine Singularity techniques. As described earlier, the use of time-domain approaches is very time consuming and is an expensive approach to determining the motion properties of ships. This problem is only exacerbated by higher speed. In this investigation, we propose to employ strip theory-based models working in the frequency-domain. Frequency-domain approaches are ideal for developing statistical estimates of motions for the ship and are, thus, computationally ideal for developing structural loads descriptions for the lifetime of the ship. Equivalent time-domain approaches would require a substantially higher investment in time and computational effort. However, a time-domain code is to be developed in Phase II of this work for the purpose of predicting slamming loads to be used once the frequency-domain models have been used to determine the segments of the operational profile that are representative of nonlinear ship-wave interactions. It was this approach that Band, Lavis and Associates pioneered in the 70s and 80s for application to the 3KSES and LCAC programs.

2.2.1 Strip Theory Models

When a ship is at rest in still water, upward buoyancy and downward gravity forces are acting along its length. The longitudinal integration of these static quantities must, for equilibrium, yield equal and opposite forces and moments. When the ship is in waves, vertical forces alternately increase and decrease relative to the still water conditions. Hence, the static forces can be neglected in the calculation of ship motion in waves, and all forces and moments can be determined in relation to the still water datum. For determining shearing forces and bending moments on the hull, these static forces can be

treated separately and superimposed at any time. So, we shall refer only to the fluctuating time-dependent motions and forces.

In order to calculate the forces on a ship, it is necessary first to calculate the forces on a small section of the ship under which the wave properties will not be changing. Thus, the ship is divided into segments, as shown in Figure 2.2.1-1. The resulting theory is known as strip theory.

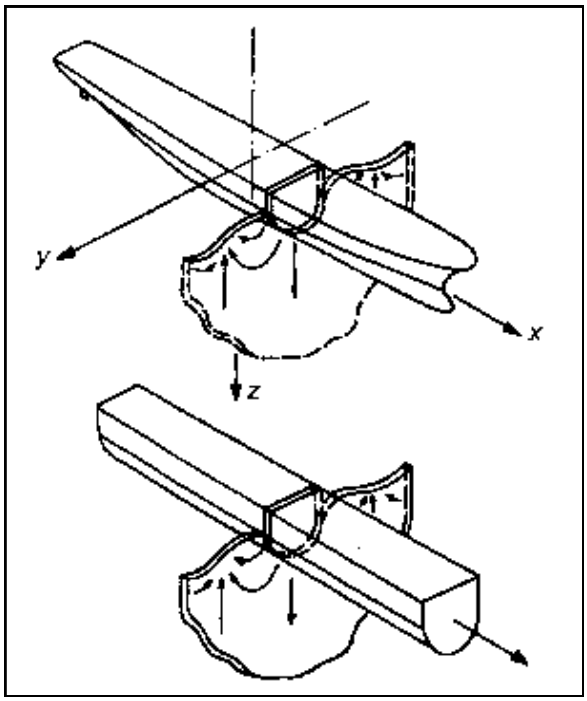

Figure 2.2.1-1. Schematic Representation of a Strip Theory Approach (From Bertram, V. Practical Ship Hydrodynamics, Butterworth Heinemann, 2000)

There are a number of different variations of the basic strip theory which are described in the literature; however, they all have the same basic features. They all require the following assumptions to be valid:

1. The ship is slender (L>> B, T & B<< L).
2. The hull is rigid and speed is moderate.
3. The motions are small relative to the wave system (so that linearity can be assumed).
4. The sections are wall-sided around the waterline region.
5. Deep water considerations where depth of water is much larger than wave length.
6. The presence of the hull has no effect on the waves - Froude-Krylov hypothesis.

The traditional way to calculate wave-induced motions and loads on a catamaran and SWATH is to use extensions of strip theory programs for monohulls. When it comes to monohulls, extensive comparisons between theory and experiments have been performed, and we have good knowledge of the limitations of strip theory calculations. The same limitations should apply to catamarans. Strip theory is a high frequency theory. That means it is more applicable in head and bow sea waves than in following and quartering seas for a ship at forward speed. The Seakeeping Committee of the 16th ITTC (International Towing Tank Conference) reports, for instance, substantial disagreement between calculated results and experimental investigations of vertical wave loads in following waves.

It should also be noted that strip theory is a low Froude number theory. It does not properly account for the interaction between the steady wave system and the oscillatory effects of ship motions. To the authors' knowledge, there is a lack of systematic investigations that show how good strip theory is at high Froude numbers; but care should be used in applying the theory for Fn >~0.4. One exception to this may be when the frequency of encounter between the ship and the waves is very high and the free surface deformation due to the hull does not matter.

Another limitation of strip theory is the assumption of linearity between response and incident wave amplitude. This means it is questionable to apply the theory in high sea-states with ship slamming and water on deck occurring. The application of strip theory is also questionable for ships with low length-to-beam ratios. The reason is that strip theory is a slender body theory. On the other hand, the Seakeeping Committee of the 18th ITTC concludes that strip theory appears to be remarkably effective for predicting motions of ships with length-to-beam ratios as low as 2.5.

Strip theory neglects all viscous effects. The most severe consequence of this is poor predictions of roll and torsional moment at roll resonance. In practical calculations, empirical viscous roll damping terms are added. For a catamaran, viscous effects will not matter much for roll predictions, but if hydrofoils are introduced between the hulls, viscous effects on the hydrofoil may influence the heave and pitch predictions. For a SWATH ship, viscous effects on the pontoons may influence the prediction of the vertical motions.

An important hydrodynamic effect for catamarans is the interaction that occurs between the two hulls. Investigations in the zero speed case indicate that, for certain frequencies, the wave energy may be trapped between the two hulls and cause small damping in pitch and heave motion. Poor agreement between theoretical and experimental values of wave bending moments between the two hulls has been reported. The correlation between theory and experiments was reported to be fair for pitch, vertical shear force, and pitch connecting moment between the two hulls.

The forward speed effect in catamaran seakeeping analytical predictions is accounted for in the same manner as for monohulls. The same limitations listed earlier for monohulls also apply to catamarans. In addition, it should be realized that the interactions between the two hulls that occur at forward speed become more complicated than for zero speed. As exemplified in research efforts, where one numerical prediction method accounts for hydrodynamic interaction and another one neglects it, the theory that neglects hydrodynamic interaction agrees best with experiments. This implies that the theory that accounts for hydrodynamic interaction is not physically correct. To the best of available knowledge, there is not available a numerical method that properly accounts for the interaction between the two hulls when a catamaran has a non-zero forward speed. This implies that the prediction of, for instance, the wave amplitude between the two hulls may be in significant error. The consequence of this is, in general, poor prediction of wave impact loads and wave-induced dynamic loads between the two hulls. However, it should be noted that Hadler et al (1974) were able to show good agreement between theory and experiment for the Hayes catamaran in head waves at 10 knots for heave, pitch and relative motion by neglecting all hydrodynamic interaction and assuming the structure had no influence on the incident waves. The rationale for doing this is questionable, and more extensive comparisons between theory and experiments are necessary.

2.3 Catamaran Motion Prediction Using SHIPMO

The primary tool utilized for the development of multihull motion and loads predictions in the first phase of this investigation was the University of Michigan seakeeping prediction program, SHIPMO.BM. SHIPMO employs a combination of strip theory, source distribution techniques, viscous roll damping calculations, and empirical corrections to predict the six degree-of-freedom linear motions and loads of displacement hulls in the frequency-domain. SHIPMO is unique in comparison to other commonly used motion prediction programs, such as the U.S. Navy Standard Ship Motion Program (SMP), in its ability to accommodate monohull *or* catamaran hullforms.

The potential theory underlying SHIPMO hinges on the slenderness of the ship's hull and on the linearity of the hydrodynamic forces. The assumption of slenderness opens up the opportunity for a 2-D 'stripwise'-solution of the hydrodynamic forces in waves. After evaluation of the hydrodynamic reaction forces and wave-induced excitation of the individual sections, the total solution is obtained by integration over the ship length. The assumption of linearity implies that the results are valid for relatively small motions and that the ship is assumed to have vertical sides.

The program is actually split up into two parts. In the first part, the hydrodynamic reaction forces, expressed in added mass, damping and wave forces, are calculated. In this part, one has the choice to use a simple Lewis transform, or a 'close-fit' mapping, or a sophisticated 2-D diffraction solution. In the second part of the program, the sectional coefficients are integrated over the ship length and the equations of motion are solved.

The integration can also be carried out for a segment of the ship, which gives the possibility to calculate the internal loads in the hull such as bending moments, shear forces and torsional moment. The added resistance in waves can be calculated by three approximation methods: Boese, Havelock and Gerritsma/Beukelman. The program was recently adapted to accommodate catamaran hullforms.

2.3.1 Collection of Experimental Data for Comparative Studies

The first step in performing a validation of computer-generated catamaran and trimaran motion predictions was the accumulation of a pool of controlled experimental data for which a series of SHIPMO match-runs could be developed. This can be a difficult task in the world of fast displacement catamarans; a highly competitive field in which access to design information and performance data is carefully controlled. However, several excellent sources of model test results were identified in a wide-ranging search of the open literature, including the three primary papers utilized for this initial study. A summary of the salient research findings of each paper is presented here.

Molland, A.F., Wellicome, J.F., Temarel, P., Cic, J., and Taunton, D.J. 'Experimental Investigation of the Seakeeping Characteristics of Fast Displacement Catamarans in Head and Oblique Seas'. Transactions of the Royal Institution of Naval Architects, 2000. pp. 78-97.

This paper summarizes an experimental investigation into the seakeeping performance of high-speed displacement catamarans with symmetric demihulls in head and oblique waves. The models tested were of round bilge hullforms with transom sterns. Three of the models were derived from the NPL Series form and one from a Series 64 form. Parametric variations investigated included length/displacement ratio and hull separation-to-length ratio. The oblique sea tests were carried out at a Froude number of 0.65 and head sea tests at a Froude number of 0.80. Measurements of pitch, heave and roll motions and vertical accelerations were made.

The results of the investigations indicate that:

- The effect of increasing forward speed was to increase the size of the resonant peaks. This effect was most pronounced when going from a Froude number of 0.2 to 0.5 and lesser when the Froude number was increased from 0.50 to 0.80.
- The catamaran RAOs in heave and pitch were found to be similar to that of monohulls with some broadening of the resonant peaks. This broadening was observed more at lower Froude numbers.
- Motions and accelerations were found to decrease slightly when going from head seas to 150 degrees. Significant decreases were found when going from 150 to 120 degrees and were found to be independent of hull spacing.

Hudson, D., Molland, A., Geraint Price, W. and Temarel, P. 'Seakeeping Performance of High Speed Catamaran Vessels in Head Seas and Oblique Waves.' Royal Institution of Naval Architects, 2001. pp. 247- 257.

In this paper, the authors study and report on the performance of a free-running catamaran based on a Series 64 hullform, with two alternative separations in head and oblique seas for one forward speed. Heave, pitch and roll responses were studied. The models used for the oblique sea tests were self-propelled and free-running, and were run at a Froude number of 0.67. Given the high speed and the small size of the tank, only 6 wave encounters per run were realized and represent a limitation of the tests. Salient results of the investigation are:

- Variation of vessel response with heading angle in shortcrested seas.

Centeno, R. Varyani, K.S., and Guedes Soares, C. 'Experimental Study on the Influence of Hull Spacing on Hard Chine Catamaran Motions'. Journal of Ship Research, Vol. 45, No. 3, September 2001, pp. 216-227.

This paper describes an experimental program on the motions of hard chine catamaran models in regular waves. Hull spacing was varied to assess the impact on wave-induced motions. The results allow the study of some aspects related to catamaran motions such as the interference between the hulls and resonance frequencies. The experimental results are also compared to calculations performed using a recently-developed code based on a two-dimensional potential flow theory in which viscous forces are included through a cross-flow drag approach. The models were tested at several Froude numbers up to a maximum of 0.75.

The results of the investigations indicate that:

- At high speeds, beyond a certain threshold encounter frequency, the heave and pitch response operators are similar to the monohull theoretical response.
- In both heave and pitch, the results at higher speeds show a tendency to obtain larger resonance peaks for the larger hull separation.

The body of work reported in the above references consists of the experimental results of model tests on three common catamaran hullforms, including two round bilge hulls (NPL Round Bilge and Series 64) and a single hard chine variant (Vosper Hard Chine). Principal characteristics of the catamaran models are contained in Table 2.3.1-1, and body plans of each of the hullforms investigated are shown in Figure 2.3.1-1.

Experimental results for all three hullforms were presented in the form of response-amplitude-operators (RAOs). RAOs are the transfer functions of motion or acceleration with respect to wave height or slope, expressed as a function of craft encounter frequency, and illustrate the physical response of the vessel at a given speed and heading in a non-dimensional format that is independent of encountered wave height and, therefore, facilitates ease of comparison. Data for all three hullforms follows the standard practice of non-dimensionalizing linear response motions by wave amplitude and angular motions by wave slope. RAOs are typically generated as a function of frequency, and, in this case, the data for both the NPL Round Bilge and Series 64 hullforms was plotted against a non-dimensional encounter frequency, whereas data for the Vosper Hard Chine hullform was plotted as a function of non-dimensional wave frequency to match the experimentally reported data format.

Data reported for each hullform largely consisted of pitch and heave RAOs at various Froude numbers for the head sea case, although limited data was included regarding response in oblique seas for the NPL Round Bilge and Series 64 models. The oblique sea data was limited to headings of 120 and 150 degrees, and roll RAOs (in addition to pitch and heave) were reported in each case. Added resistance and vertical accelerations were also reported for the NPL Round Bilge and Series 64 models.

Table 2.3.1-1

Principal Particulars of Evaluated Hullforms

Model	4b	5b	6b	5s	5b	5s	V40	V60
Hullform Type	**Round Bilge**	**Round Bilge**	**Round Bilge**	**Series 64**	**Round Bilge**	**Series 64**	**Hard Chine**	**Hard Chine**
Length, m	1.6	1.6	2.1	1.6	4.5	4.5	2.05	2.05
$L/\nabla^{1/3}$	7.4	8.5	9.5	8.5	8.3	8.3	6.07	6.07
L/B	9.0	11.0	13.1	12.8	11.0	12.8	12.97	12.97
S/L	0.2 / 0.4	0.2 / 0.4	0.2 / 0.4	0.2 / 0.4	0.2 / 0.4	0.2 / 0.4	0.195	0.30
B/T	2.0	2.0	2.0	2.0	1.9	1.9	1.86	1.86
C_B	0.397	0.397	0.397	0.537	0.400	0.540	0.695	0.695
Max. Froude No.	0.8	0.8	0.8	0.8	0.67	0.67	0.75	0.75
Tests	Head Seas	Head Seas	Head Seas	Head Seas	Oblique Seas	Oblique Seas	Head Seas	Head Seas

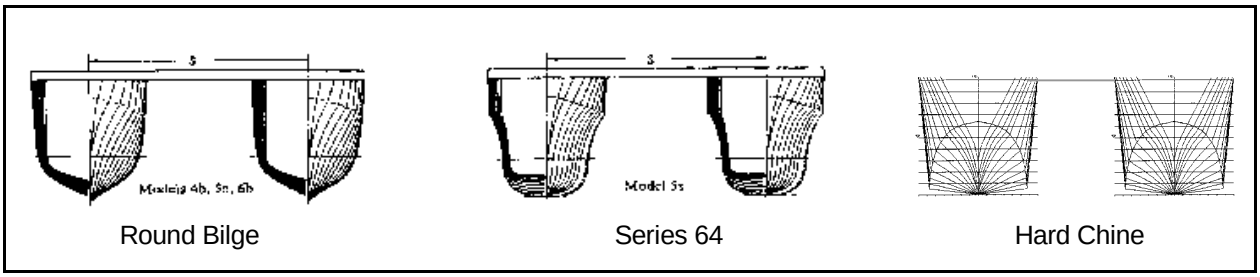

Figure 2.3.1-1. Body Plans of Evaluated Hullforms

2.3.2 Development of SHIPMO Computer Models

Following the data collection phase, SHIPMO run files were developed to reproduce the conditions recorded in the model test reports. Offsets were digitized, based on the body plans illustrated in the data sources identified above, and verified for dimensional consistency with the principal characteristics reported in the literature. The resulting SHIPMO hullforms were also verified for hydrostatic similarity with the tested models through a comparison of the predicted displacement and longitudinal center of gravity (LCG) versus the actual measured values. SHIPMO contains a built-in hydrostatic similarity check for this purpose, which prevents the program from running and returns an error if the computed displacement or LCG results in an error greater than 5% as compared to actual values supplied by the user. The models developed for this study were well within this margin of error. Figures 2.3.2-1 through 2.3.2-3 illustrate the body plans developed for use with SHIPMO for each of the hullforms (note that these offsets reflect the underwater portion of the hull only).

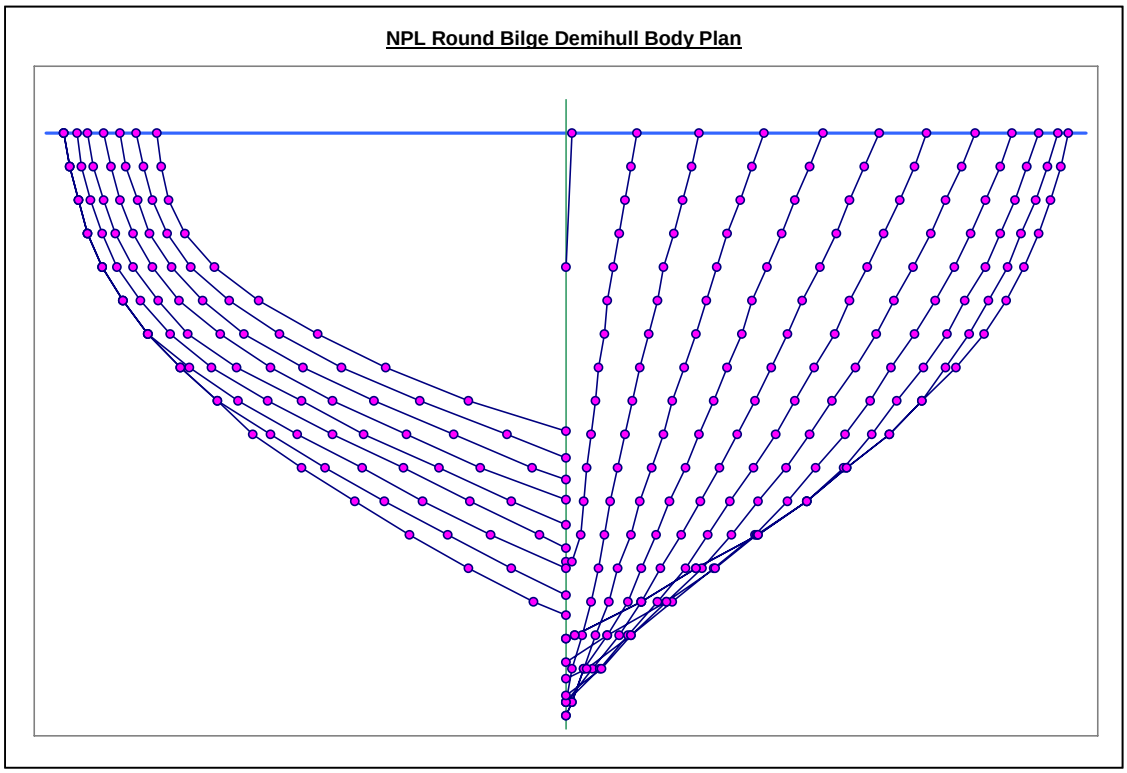

Figure 2.3.2-1. NPL Round Bilge Demihull Body Plan Developed for SHIPMO Model

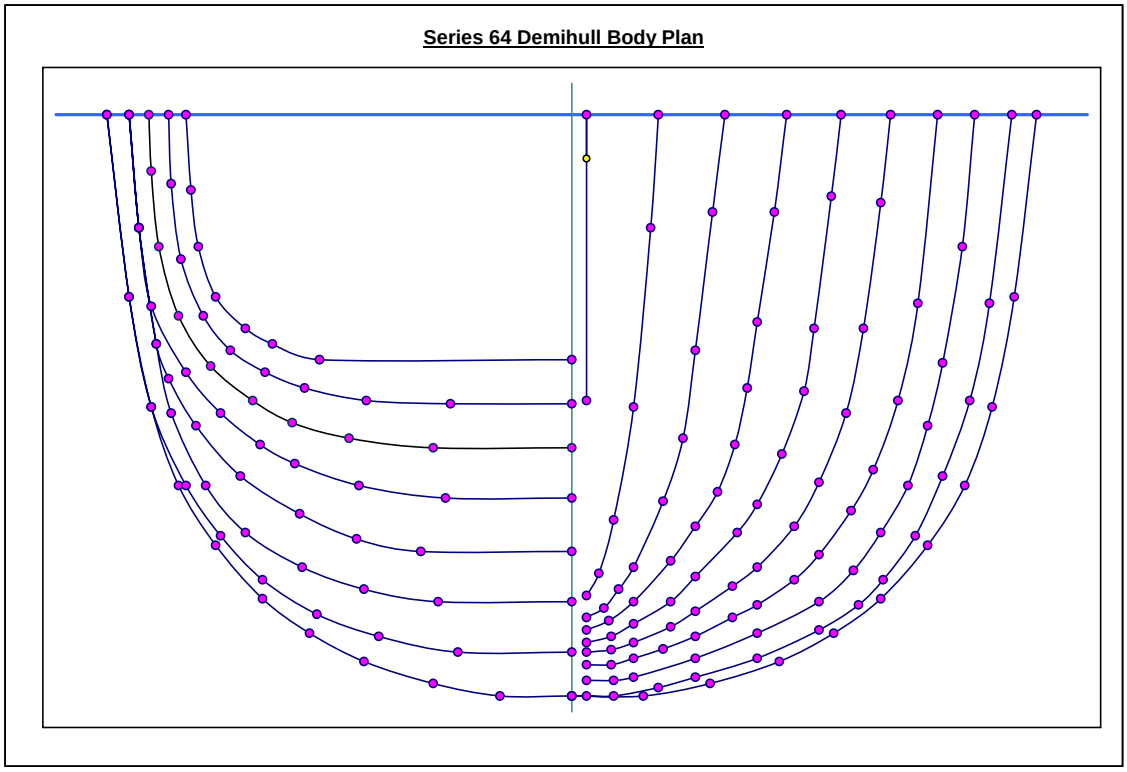

Figure 2.3.2-2. Series 64 Demihull Body Plan Developed for SHIPMO Model

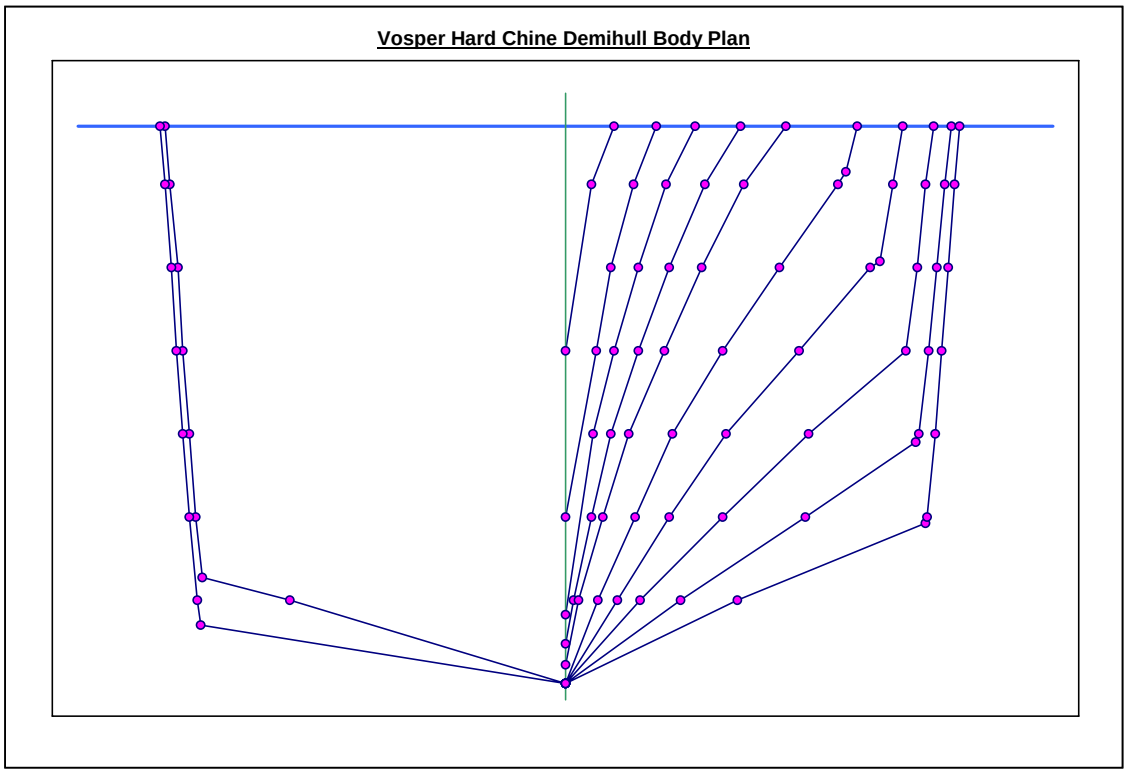

Figure 2.3.2-3. Vosper Hard Chine Demihull Body Plan Developed for SHIPMO Model

Match runs were completed for each hullform indicated in Table 2.3.1-1, with the exception of models 4b and 6b in the NPL Round Bilge series. These models were held in reserve for use in validation of any future modifications made to SHIPMO or a newly developed motion model. If empirical corrections are made based on the findings of this study, there must be independent models available (i.e. models not utilized in development of the empirical fix) to verify and validate the results.

In addition to the development of catamaran run files consistent with the experimental data, SHIPMO models were also generated for conditions in which a single demihull in each of the three hullform categories is treated as a monohull to explore the effects of the hydrodynamic interaction generated in multihull vessels.

2.3.3 Correlation of Predicted and Experimental Data

RAOs generated by SHIPMO for each match run were plotted for comparison against the actual test data. The dimensional encounter frequencies (wave frequencies in the case of the Vosper Hard Chine model) reported by the program in rad/sec^2 were non-dimensionalized for consistency with the test results. Corresponding monohull data was included on each plot to determine whether the hydrodynamic interaction between hulls is significant.

Figure 2.3.3-1 shows a sample comparative plot; this particular case illustrating the heave RAO for the NPL Round Bilge hullform in head seas at a Froude Number of 0.5. This plot shows a trend that is fairly characteristic of the hullforms investigated, particularly at higher Froude Numbers (0.5 and above). The SHIPMO-predicted catamaran response at the resonant frequency is distinctly higher than the measured data, whereas the predicted monohull response is reasonably consistent with the experimental results. Moving away from the resonant frequency in both directions, both the catamaran and the monohull predictions show reasonable agreement with the model test data. At lower Froude Numbers, the correlation of the predicted catamaran response tends to improve, while the predicted monohull response

remained generally consistent. The complete set of comparative plots is contained in Appendices B, C and D of this report for the NPL Round Bilge, Series 64 and Vosper Hard Chine hullforms, respectively.

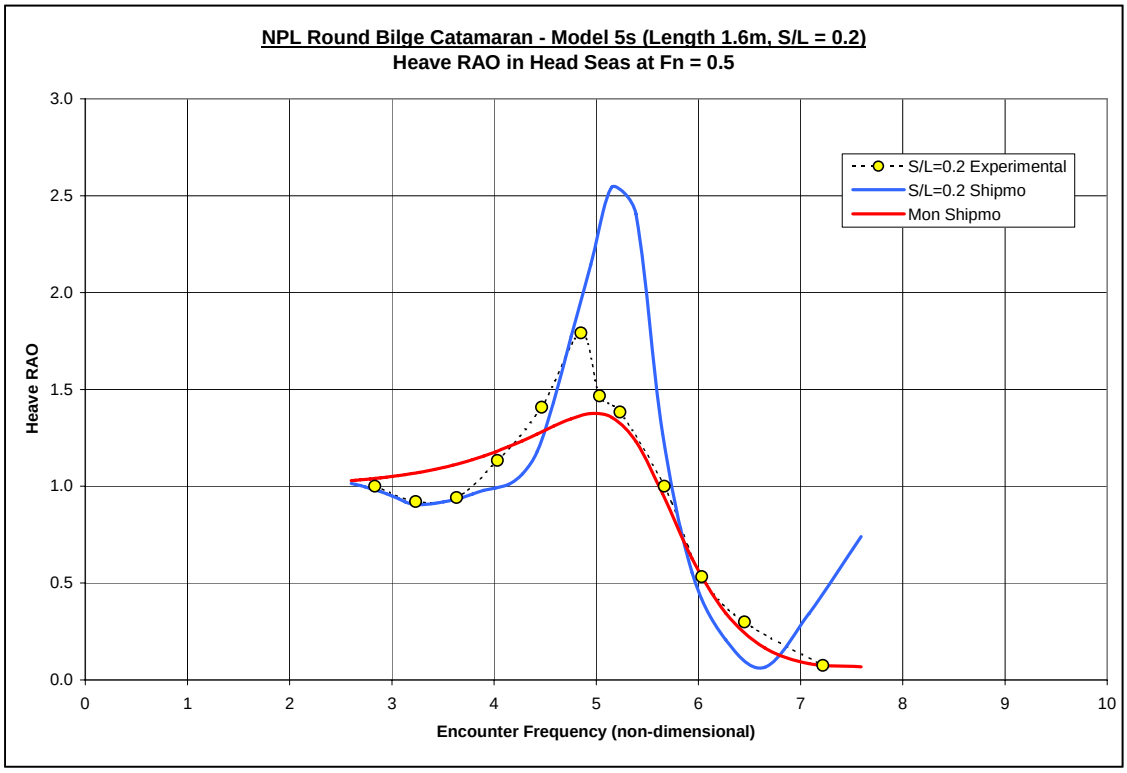

Figure 2.3.3-1. Initial Sample RAO Comparison (NPL Round Bilge in Head Seas at FN=0.5)

Following the one-to-one comparisons of the SHIPMO-predicted RAOs to the experimental data, attention was focused on capturing the large amount of information generated, in a condensed and collective manner, that would allow for the identification and analysis of trends in the data. The initial goal was to explore the ratio of predicted to experimental RAOs at the resonant frequencies, which would produce the extreme vessel response in any particular speed/heading case. The ratio of predicted to experimental frequency producing the resonant response was also studied in this same manner. These comparisons are shown in Figures 2.3.3-2 through 2.3.3-5 for the catamaran hullforms studied in head seas for motions in pitch and heave as a function of Froude Number. The solid blue line in each figure represents a ratio of predicted to experimental response of 1.0, or a perfect correlation. Any data point falling above the line represents a case in which the SHIPMO predictions are in excess of the measured model test data, whereas data points falling below the line represent cases in which the SHIPMO predictions are lower than the corresponding experimental data.

As seen in Figures 2.3.3-2 through 2.3.3-5, for these initial runs, the ratio of predicted to experimental resonant RAO values for the data set as a whole displays a tremendous amount of scatter over the entire range of speeds, with the SHIPMO predictions nearly universally higher than the corresponding model test data. The ratio of predicted to experimental frequencies of resonant response (Figures 2.3.3-3 and 2.3.3-5) shows much improved correlation, although in the case of the resonant pitch frequency (Figure 2.3.3-5), a fair amount of scatter remains evident.

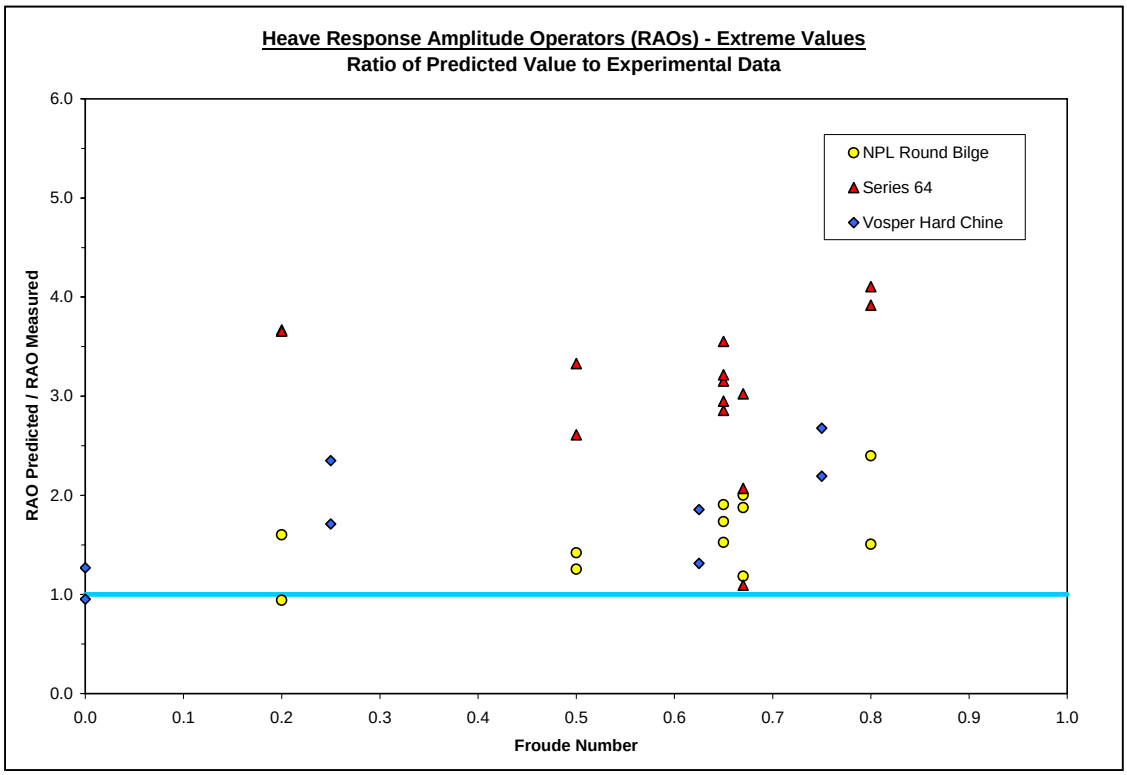

Figure 2.3.3-2. Ratio of Predicted to Experimental Heave RAO at the Resonant Frequency

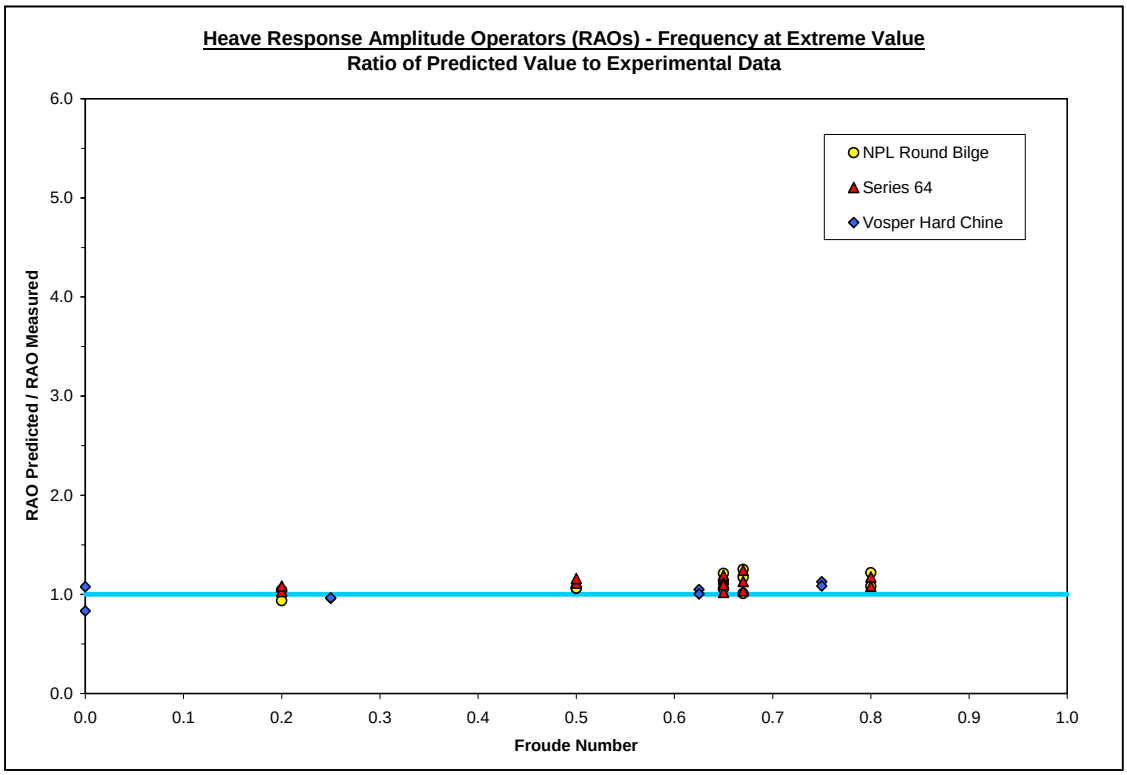

Figure 2.3.3-3. Ratio of Predicted to Experimental Frequency at the Resonant Heave Response

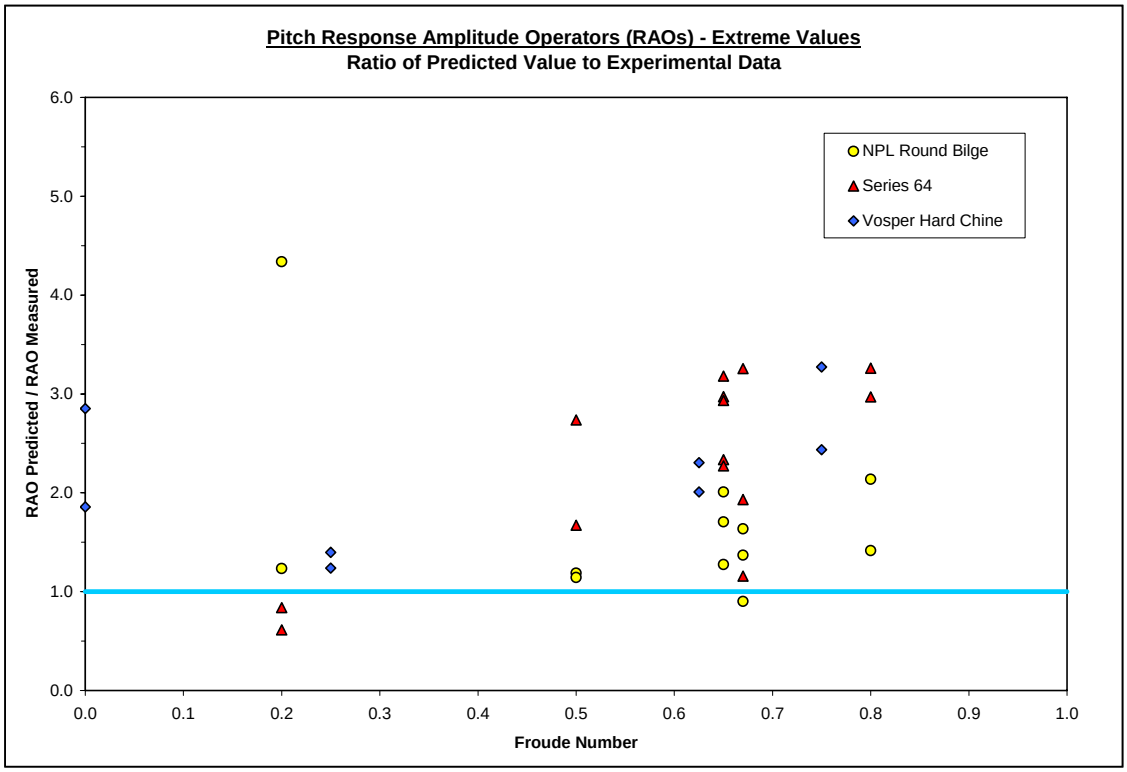

Figure 2.3.3-4. Ratio of Predicted to Experimental Pitch RAO at the Resonant Frequency

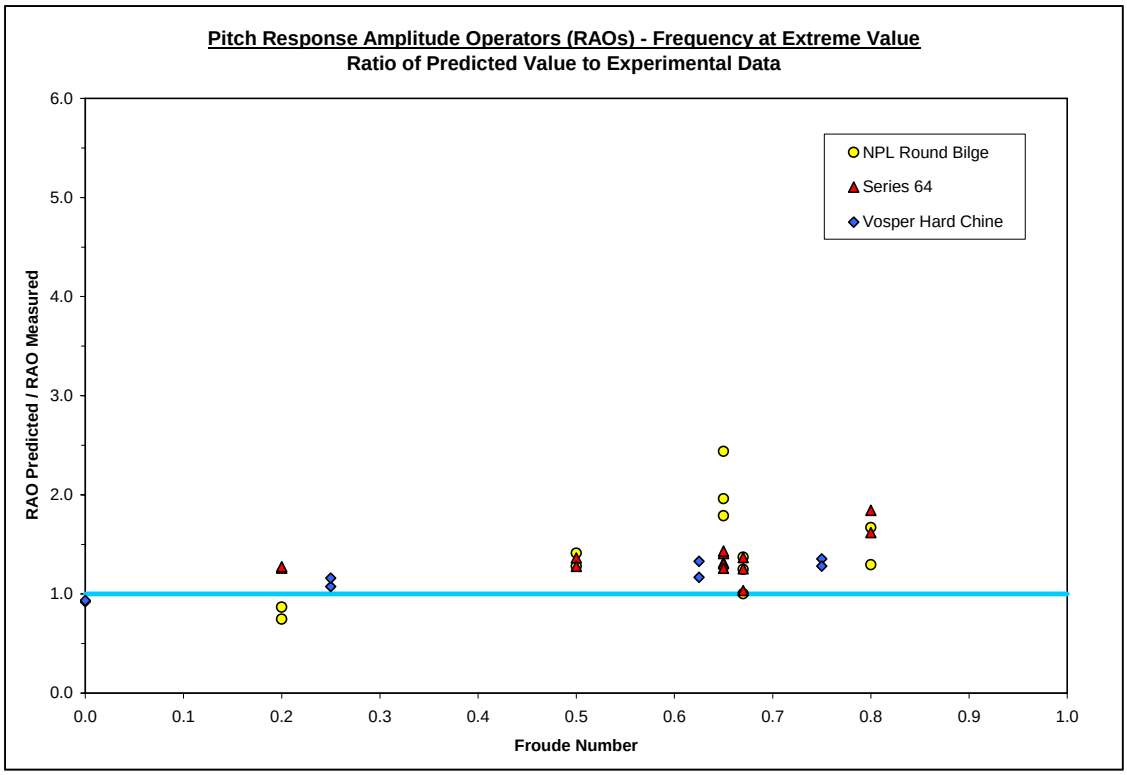

Figure 2.3.3-5. Ratio of Predicted to Experimental Frequency at the Resonant Pitch Response

In examining the plots shown in Figures 2.3.3-2 through 2.3.3-5, it was quickly realized that the process of displaying the data as ratios could be deceptive, as it eliminates the consideration of magnitude in the comparison. For instance, an error of even 50% or 100% in a very small magnitude RAO may not produce an unacceptable prediction of physical vessel motion, particularly in lower sea-states (i.e. low wave height). Likewise, a very small error in large magnitude RAOs can produce greatly exaggerated motion predictions. This is important in analyzing speed-dependent trends, because the average magnitude of RAOs at slower speeds (lower Froude Number) is generally much lower than the corresponding data at high speed. With this in mind, Figures 2.3.3-6 and 2.3.3-7 were generated to show the absolute error in the prediction of RAOs at the resonant frequency for pitch and heave in head seas. This allows the degradation of prediction accuracy with increasing speed to be observed easily, in keeping with a key hypothesis of this analysis as the linear strip theory begins to break down at high speed.

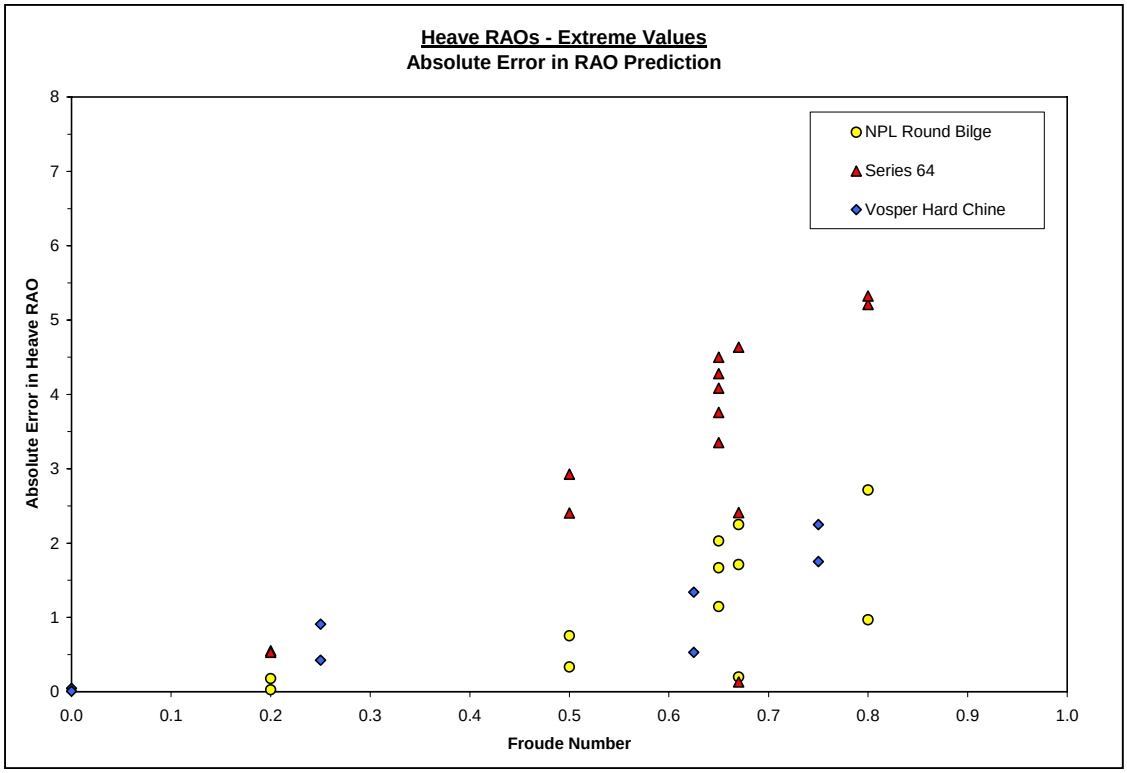

Figure 2.3.3-6. Absolute Error in Heave RAO Predictions as a Function of Froude Number

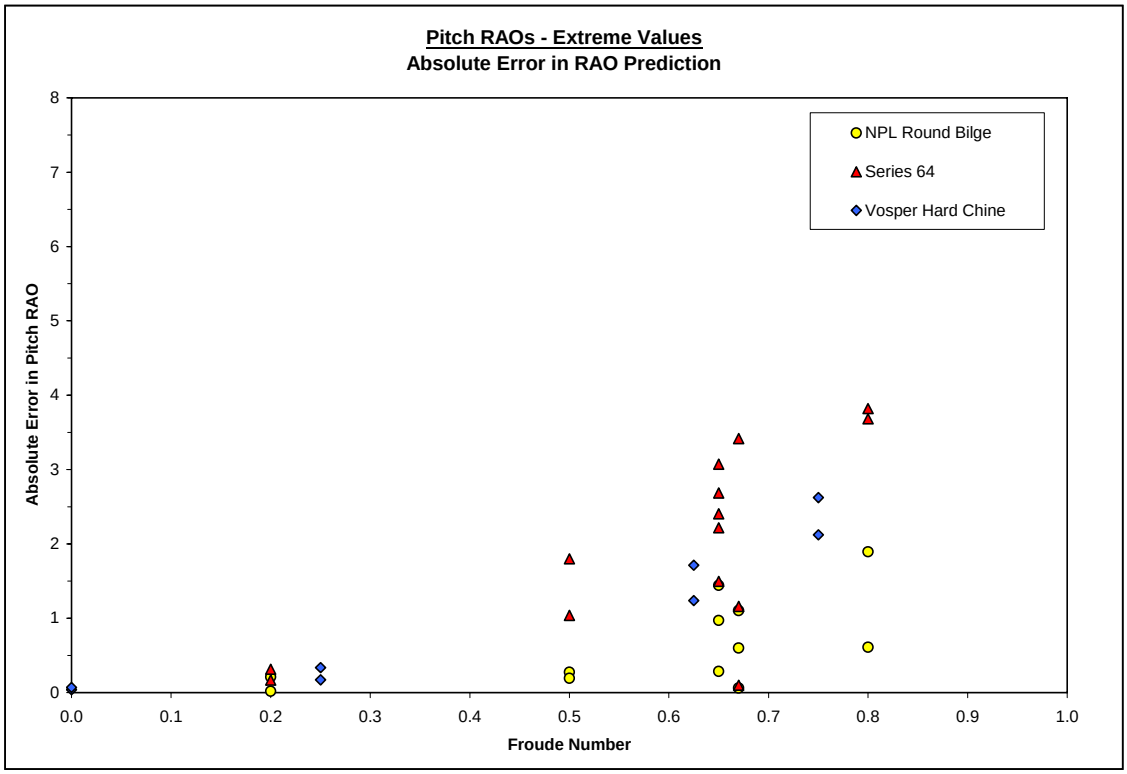

Figure 2.3.3-7. Absolute Error in Pitch RAO Predictions as a Function of Froude Number

As mentioned earlier in the discussion of Figure 2.3.3-1, one of the key observations has been the improved correlation of predicted versus experimental values when the demihulls of the tested catamarans are treated as monohulls for the purposes of pitch and heave prediction in head seas using SHIPMO. As such, the data in Figures 2.3.3-6 and 2.3.3-7 were reproduced to display the error in the SHIPMO-generated RAO predictions for the monohull configuration. This data is shown in Figures 2.3.3-8 and 2.3.3-9. The catamaran predictions are also included on the plots (small black crosses) for reference. It is easily seen from a cursory examination of these figures that the scatter in the data set is greatly decreased when the predictions are developed in this manner. The breakdown of the correlation between predicted versus experimental data as vessel speed increases can also be observed.

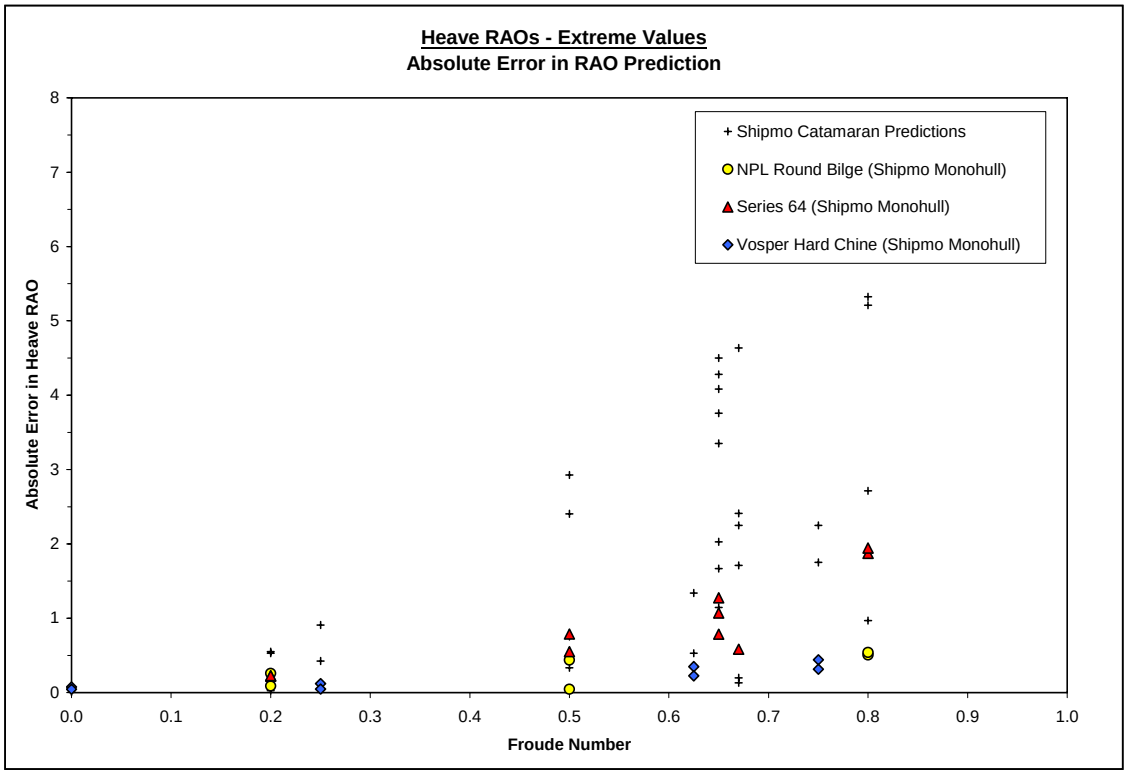

Figure 2.3.3-8. Absolute Error in Heave RAO Predictions for SHIPMO Monohulls

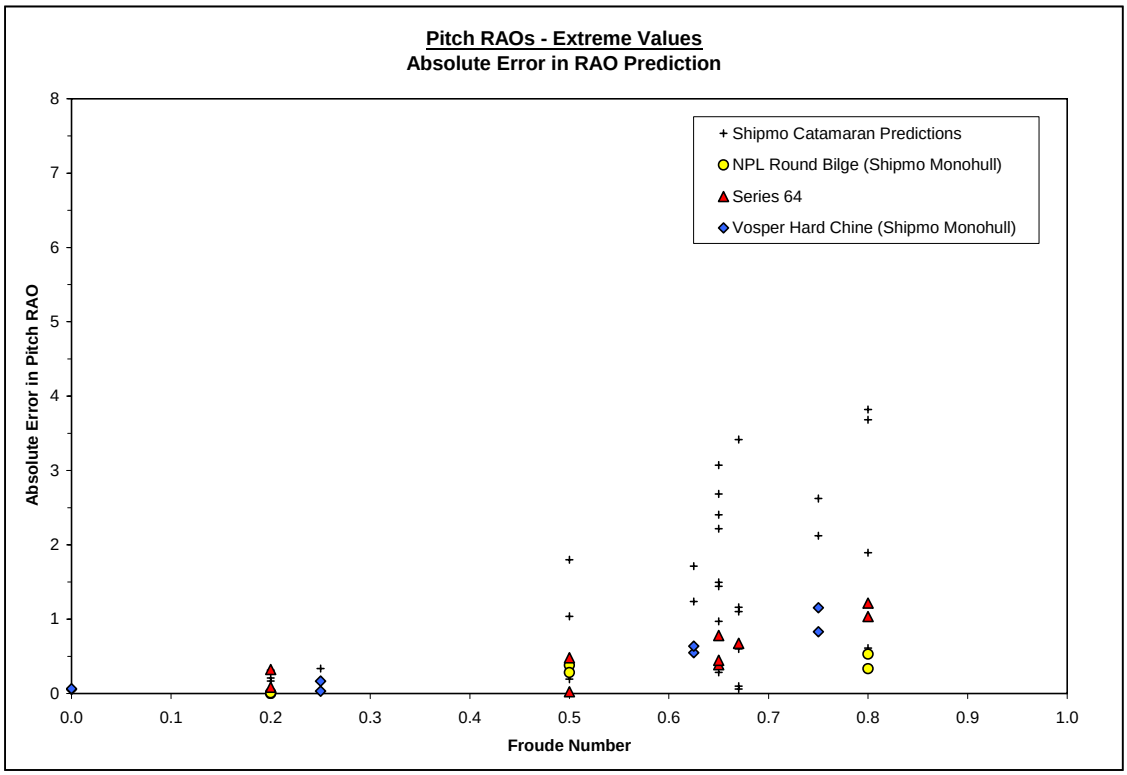

Figure 2.3.3-9. Absolute Error in Pitch RAO Predictions for SHIPMO Monohulls

2.3.4 Correlation of Added Mass & Damping Coefficients

Following the compilation of the RAO comparisons for the complete set of experimental data and the identification of the trend of response over-prediction in SHIPMO for catamaran hullforms, the analysis continued in an attempt to better understand the root of the computational discrepancies identified. In particular, the trends in two-dimensional sectional added mass and damping coefficients were explored, as these coefficients are integral to the development of the RAOs and, hence, critical to obtaining accurate motion predictions. As the added mass and damping is not typically measured and included in experimental test data (as was the case for the three hullforms studied), it was necessary to include a reasonable baseline of comparison to provide an indication of validity in the computational results. This was accomplished through the utilization of Lewis-forms, as described in the textbook on Marine Vehicle Dynamics by Rameswar Bhattacharya.

Lewis-forms consist of a two-parameter mathematical mapping function which is based on the sectional beam-to-draft ratio and the sectional area coefficient of a mathematically-developed 2-D hull section. Lewis-forms are utilized to transform the mathematical section coordinates (i.e. sectional shape) into that of a semi-circle through conformal mapping such that the known added mass and damping solutions for a circular cylinder in heave can be used to determine the solution for the actual mathematical section over a range of oscillatory frequencies. It has been proven that Lewis-form representation of conventional hulls will produce largely accurate results, assuming the beam, draft and sectional area of the experimental hull section and the Lewis-form is similar even if the sectional shape is different.

Figures 2.3.4-1 through 2.3.4-6 illustrate the correlation between the SHIPMO predictions of added mass and damping coefficient (with the case of the catamaran and that of the demihull treated independently) and the coefficient derived based on the Lewis-form approximation most appropriate to each individual hullform studied. Once again, monohull data generated using SMP is also plotted as a second baseline of comparison.

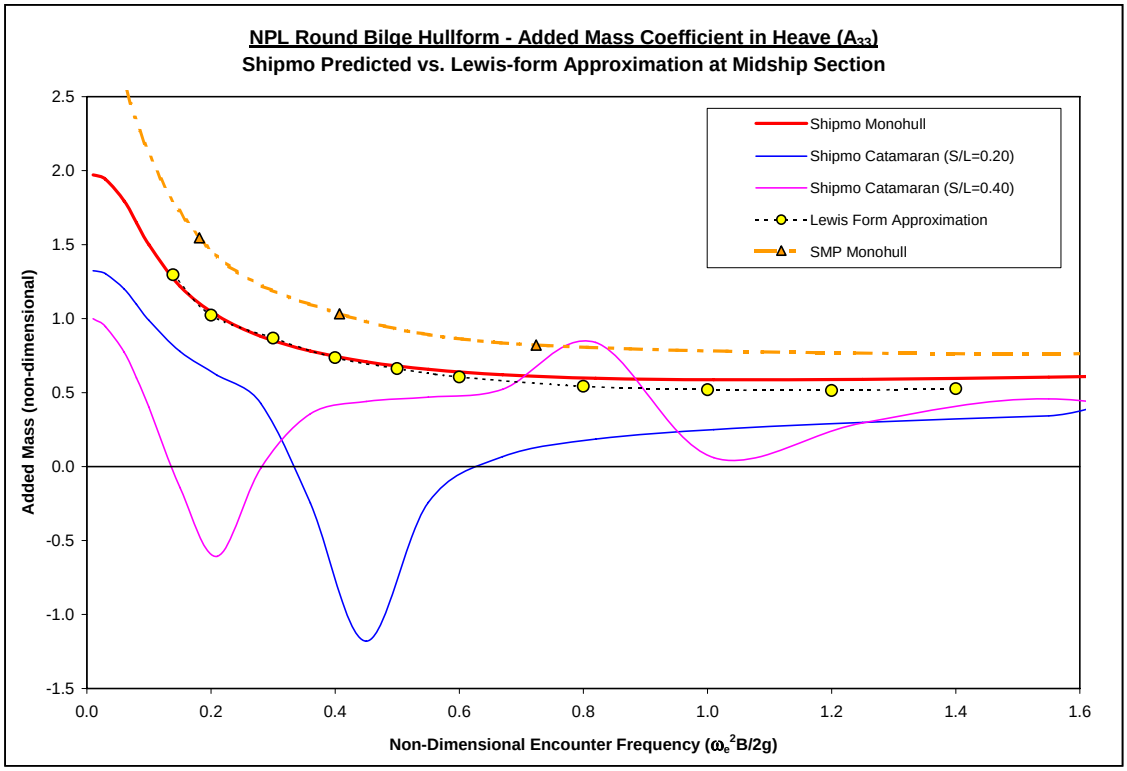

Figure 2.3.4-1. Added Mass Predictions for NPL Round Bilge Hullform, Model 5b (Midship Section)

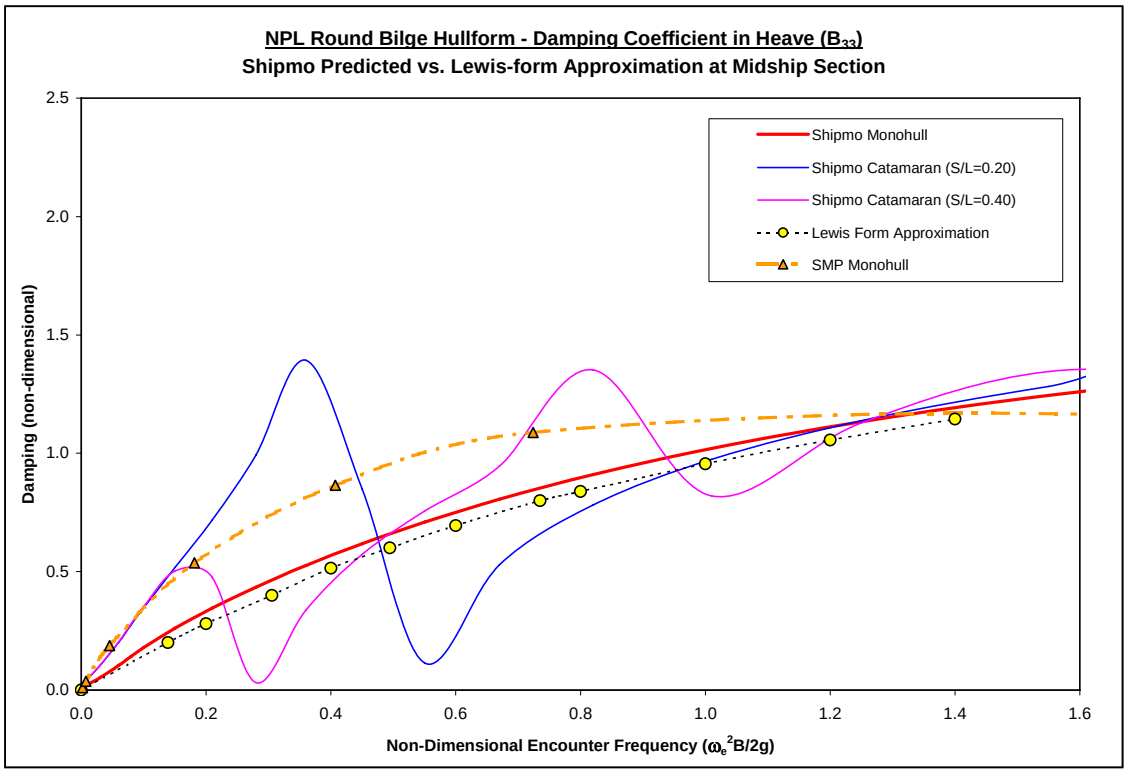

Figure 2.3.4-2. Damping Predictions for NPL Round Bilge Hullform, Model 5b (Midship Section)

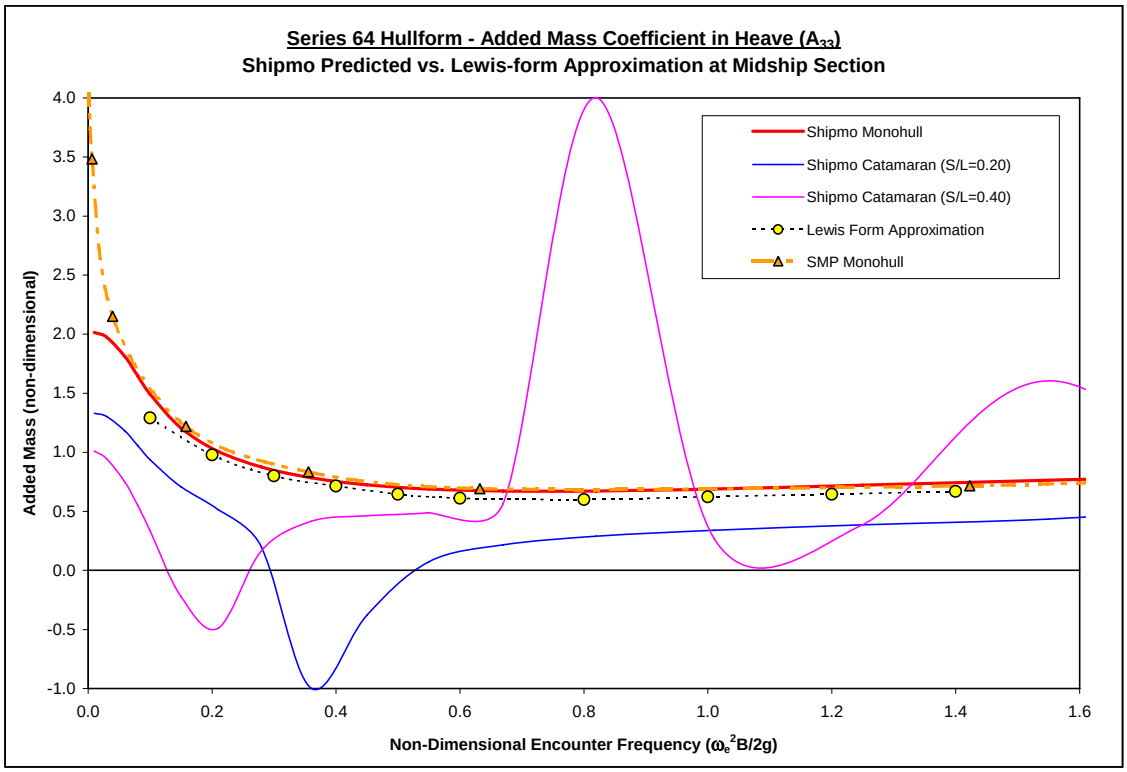

Figure 2.3.4-3. Added Mass Predictions for Series 64 Hullform, Model 5s (Midship Section)

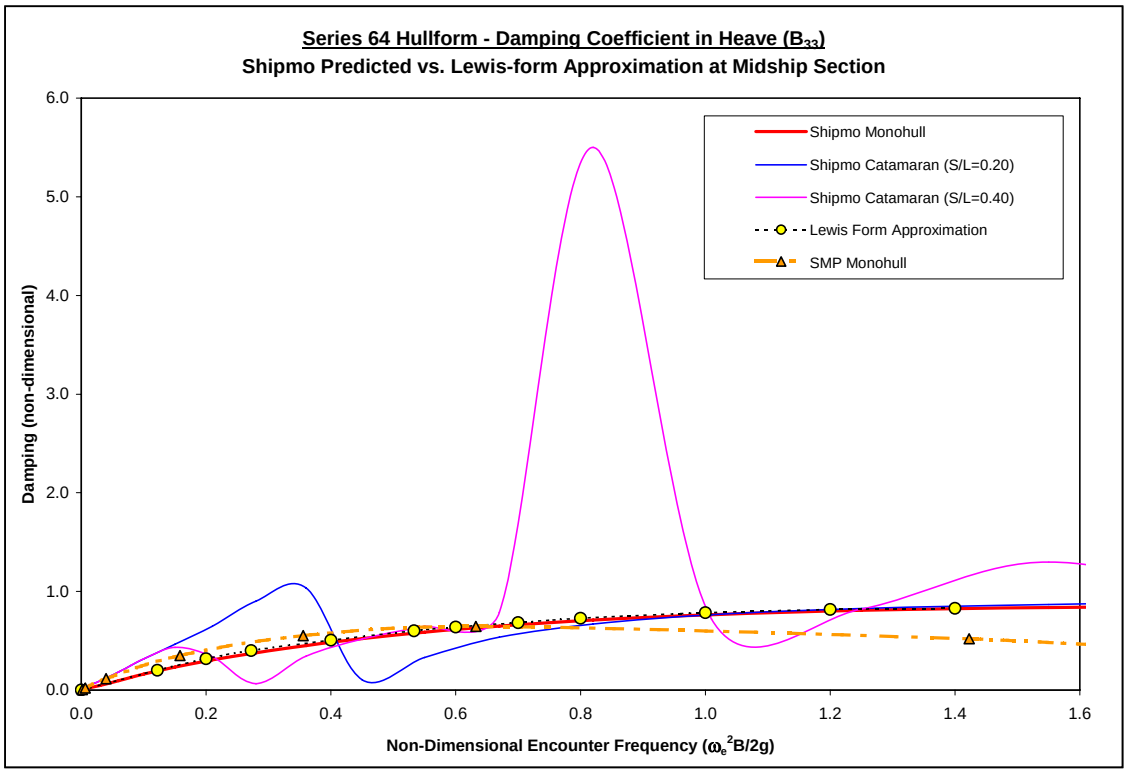

Figure 2.3.4-4. Damping Predictions for Series 64 Hullform, Model 5s (Midship Section)

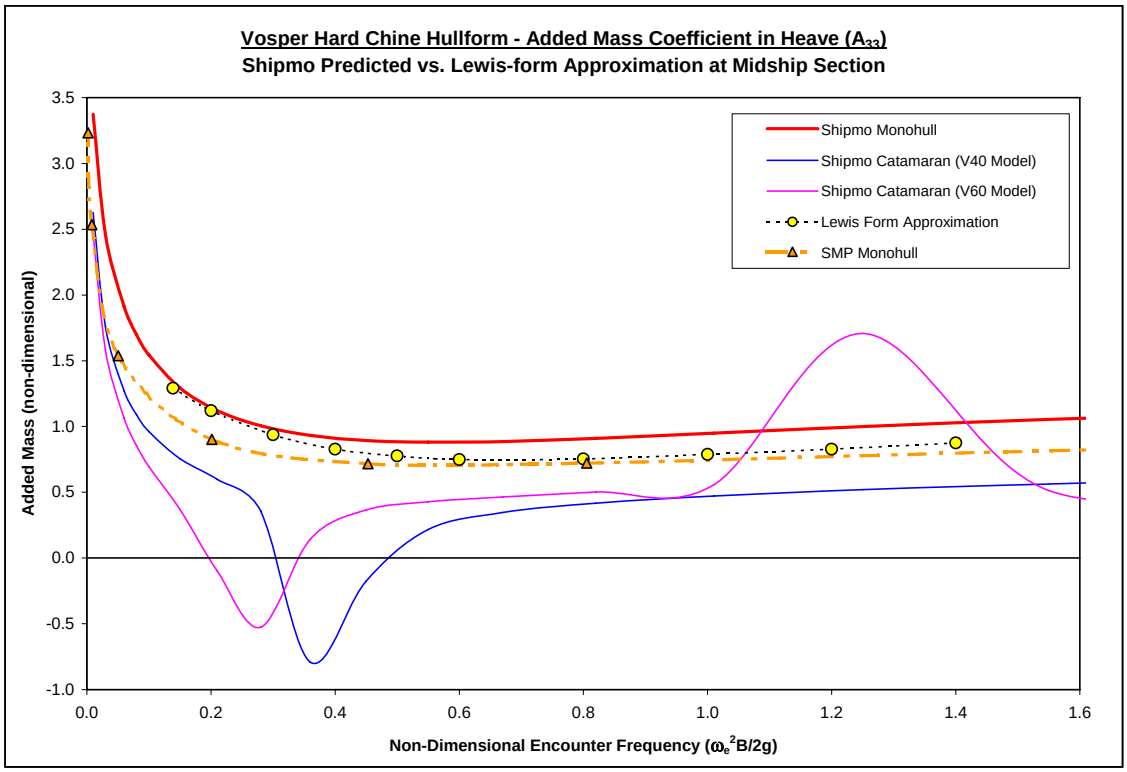

Figure 2.3.4-5. Added Mass Predictions for Vosper Hard Chine Hullform (Midship Section)

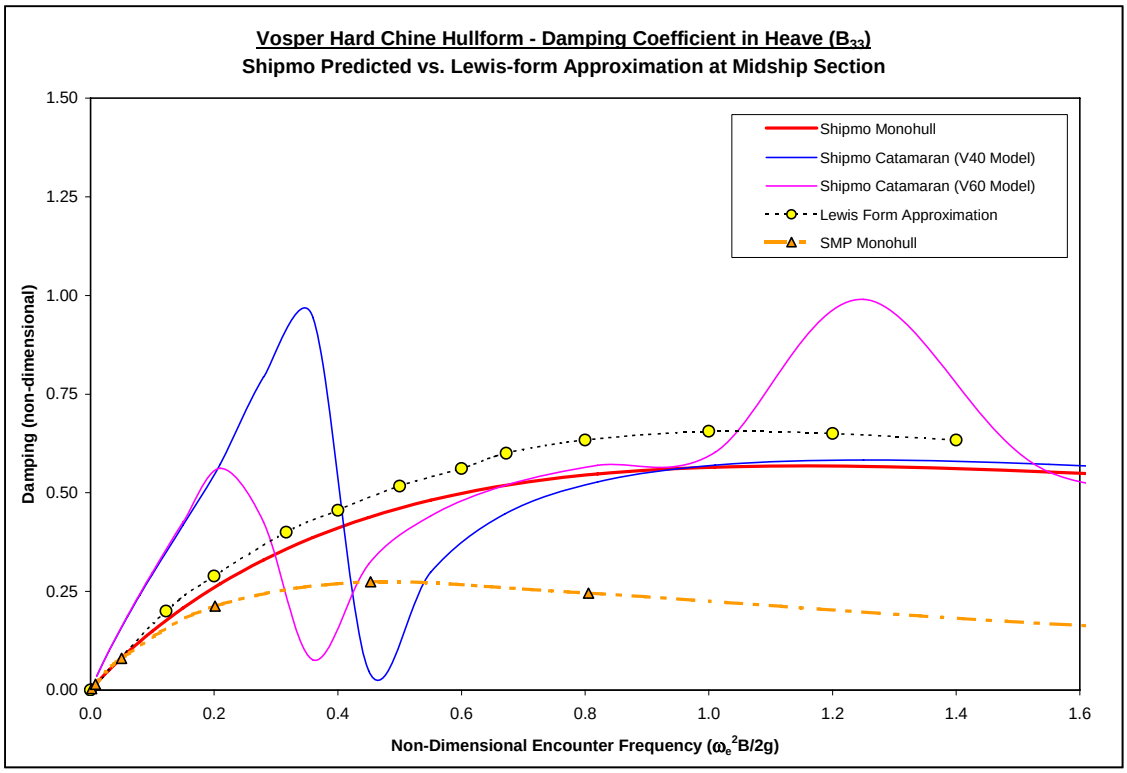

Figure 2.3.4-6. Damping Predictions for Vosper Hard Chine Hullform (Midship Section)

In examining Figures 2.3.4-1 through 2.3.4-6, several overall trends become apparent. First, the calculated catamaran values generated using SHIPMO demonstrate an oscillatory tendency in both added mass and damping, whereas the individual monohull predictions (SHIPMO and SMP) and the Lewis-form data produce a smooth curve in each case. The catamaran added mass predictions developed using SHIPMO tend to dip into negative territory at low frequencies of encounter, a phenomenon not evident in the monohull or Lewis-form data. The damping data also shows a similar tendency to dip to near zero in the low frequency range for all three hullforms.

The computational effects of separation ratio on the SHIPMO catamaran predictions can also be seen in Figures 2.3.4-1 through 2.3.4-6, as the wider separation between demihulls tends to produce a second spike in added mass and damping predictions at medium to higher frequency that is not evident in the case of the smaller separation ratios. This effect is particularly pronounced in the case of the Series 64 hullform, yet is still evident to a lesser degree in the Round Bilge and Hard Chine models.

The monohull predictions (both SHIPMO and SMP), on the other hand, tend to demonstrate very solid correlation with the Lewis-form approximations, particularly in the case of the Series 64 hullform. The only real exception is in the damping data for the Vosper Hard Chine hullform (Figure 2.3.4-6), for which the SMP monohull shows a marked decrease from both the SHIPMO predictions and the Lewis-form approximation. This is almost assuredly a direct result of the spline-fit procedure utilized by SMP to develop the hullform, which will tend to round off the chine and thereby decrease the damping associated with the sharp corner. It should be noted here that SMP was not developed to accommodate hard chine hullforms, and it is often necessary to model a small artificial bilge keel to develop the appropriate damping forces in this type of hull. This procedure has not been utilized for this study.

2.3.5 SHIPMO Performance Evaluation - Conclusions

The compilation and analysis of data presented in the previous sections results in certain general conclusions regarding the performance of the ship motions modeling program SHIPMO as applied to high-performance catamarans. It is important to note that the majority of the analysis in this study is based solely on the response at the resonant frequency (i.e. the extreme response). In many cases, correlation of the SHIPMO predictions with the experimental data is greatly improved as the analysis moves away from the resonant frequency in both directions. The salient conclusions are:

- The applicability of linear strip theory utilized in the SHIPMO motion predictions clearly begins to degrade with increased vessel speed, as was suspected at the outset of this study. The degradation is less extreme when the catamaran demihulls are treated as monohulls, but remains a concern.
- The correlation of SHIPMO-predicted RAOs to the experimental test data is significantly improved when the catamaran demihulls are treated as monohulls in the process of computer modeling for pitch and heave motions. Lending further credence to this observation, an investigation of the predicted two-dimensional sectional added mass and damping of the experimental hullforms has shown the monohull predictions, using both SHIPMO and SMP, to be solidly consistent with a benchmark Lewis-form approximation.
- The improved correlation with the experimental catamaran data in the case of the SHIPMO monohull predictions supports the hypothesis that the three-dimensional speed effects on the hydrodynamic interaction between demihulls (i.e. the decrease in wave interference and hydrodynamic interaction as speed increases) cannot be simulated by the two-dimensional linear strip theory utilized by many common motion prediction programs.
- The SHIPMO predictions developed for monohulls are reasonably consistent with the experimental data through Froude numbers approaching 0.5, particularly in lower sea-states (keeping in mind that the RAOs reported are simply multipliers of the sea conditions to arrive at a vessel response). At high speeds, confidence in the accuracy of the unaltered SHIPMO predictions is generally low. However, critical design loads generally occur in high-sea conditions when a vessel is caused to operate at low speeds.

Overall, the applicability of the linear frequency-domain ship motions model SHIPMO has been shown to possess certain limitations at higher Froude number. However, utilizing modeling procedures specifically developed to address these issues, this validation effort has demonstrated that satisfactory correlation can be achieved in modeling the motions of high-speed catamarans, within reason. More importantly, this evaluation has resulted in an increased understanding of the quantitative error in resonant response operators at high speed. Theoretically, one could provide a speed correction for the predicted RAOs.

At this time, it is also pertinent to highlight the fact that the scale-model tests of high-speed catamarans can potentially be incapable of accurately capturing the exact nature of the resonant response. In experimental investigations, the models are tested at discrete speeds and not through a finer grid of speeds, as is often the case with numerical modeling procedures. Thus, it can be argued that the peak resonant response observed in the experiments is not necessarily the maximum.

The limitations of strip theory without corrections can be overcome with modifications to the theory to account for the forward speed effects. This is an interesting challenge and will require a semi-empirical correction or validation effort for each modeling effort. In the application of most new and novel hullforms, the requirement for a model-testing program to accurately determine motion characteristics is always advisable.

Given all these factors, the recommendation based on the assessment of the performance of SHIPMO is that no modifications to the code be made without further analysis. The cause for any discrepancies between the predicted and observed maximum resonant response can be due to several reasons. The

overall good agreement between the shape of the response curves and the pre-resonant and post-resonant response amplitudes justifies the use of strip theory models as is.

2.3.6 Numerical Modeling of Trimaran Seakeeping

After the extensive validation effort of SHIPMO pertaining to catamaran motions, the analysis transitioned into the development of strategies for motions modeling of other multihull vessels, and in particular trimarans. In the pursuit of this effort, BLA visited the NSWCCD Mask facility to witness the model testing of the Innovation Cell segmented trimaran model. BLA later obtained some basic design data, in addition to the as-built hullform of the Innovation Cell model in the form of computerized 3-dimensional surface files for use in this study.

The results of this study are contained in Appendix E.

3.0 STRUCTURAL LOADS

From a structural design standpoint, the dominant global load on a ship moving through waves is vertical bending along the ship's longitudinal axis. Transverse bending and torsional loads are also important design considerations, especially for multihull vessels. When a ship is subjected to longitudinal vertical bending, it tends to respond around two distinct frequencies. The lower of the two frequencies is a narrowband spectrum of frequencies that closely matches the frequency spectrum of the waves encountered. The higher of the two frequencies is the first natural frequency of the ship's hull-girder. The low frequency component of the response is the forced vibration response of the ship to the waves, while the high frequency response is a damped free-vibration due to wave impact, called whipping, or a resonant phenomenon known as springing. For multihull vessels, similar whipping response can be observed in the transverse bending direction depending upon the structural stiffness characteristic of the vessel in the lateral direction. In addition to the wave-induced vertical and lateral global bending and whipping, pressures from hull slamming and pitching also govern the design of the bottom and side hull structures. The slamming-induced pressures can be significant on the cross-structure of multihull vessels and will dominate the global loads for small vessels.

3.1 Hull-Girder Bending Load

For a route and mission-dependent approach for load assessment, a characterization of the most probable sea-states and ship operating scenarios needs to be established first. Thereupon, using a two-dimensional strip theory based tool, a frequency-domain assessment of the motions of the vessel can be developed for the predetermined sets of sea-states and operating conditions. The input to this effort will be information such as the wave spectra, vessel operating speeds, and probable headings, and the output will be the vessel's motions response spectra and associated statistical values. Along with the motion responses, this frequency-domain assessment will also provide the vessel's low frequency ordinary wave-induced bending load spectra. The ordinary wave-induced vertical bending in both longitudinal and transverse directions and torsional bending can then be obtained. It should be noted that the other part of the global load, wave impact-induced whipping, cannot be estimated via this approach since the vessel's structural stiffness and its viscous damping characteristics are required as priors.

If a time history of the hull-girder bending moment is evaluated, especially in the longitudinal direction, it will show how the ordinary wave-induced and whipping-induced loads combine to form the total global load. Samples of the individual load components are shown in Figure 3.1-1, and the combined load after high-frequency filtering is shown in Figure 3.1-2. Extensive studies have shown that wave elevation time histories tend to have a Gaussian or normal distribution. Therefore, the ordinary wave-induced component of the total bending moment has a similar distribution. Since the ordinary wave bending moment has a narrow band response, then the extreme values of a normal random process are close to Rayleigh distributed. In practice, extreme total ship load peak amplitudes tend to follow somewhere between a Rayleigh and exponential distribution (determined by model tests), represented by a general Weibull distribution or generalized gamma distribution, as discussed later. Using these extreme value

distributions, predictions of extreme values for the route and mission-dependent operational conditions can be made.

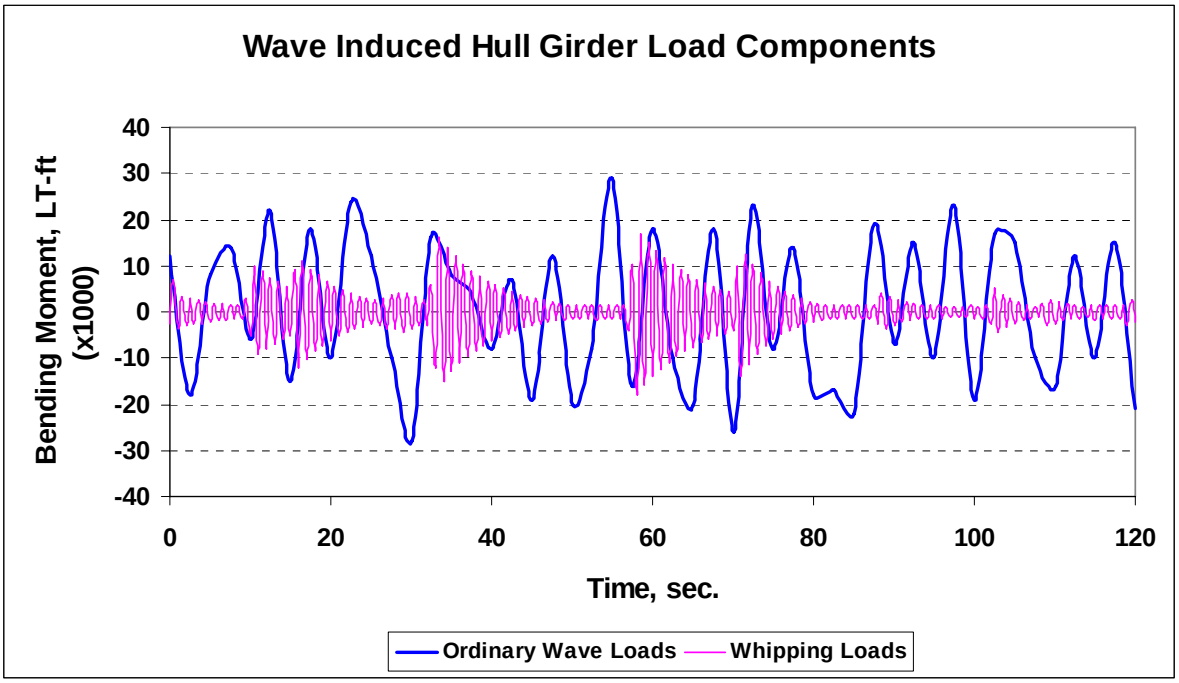

Figure 3.1-1. Wave-Induced Hull-Girder Load Component Time Series

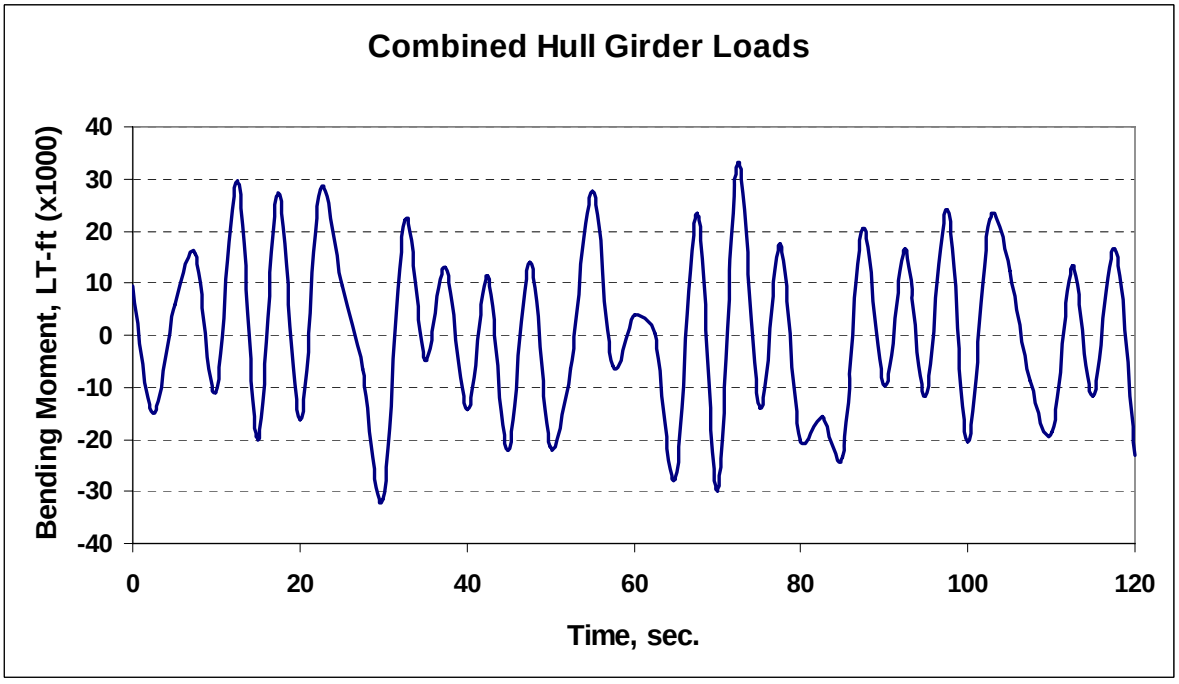

Figure 3.1-2. Combined Hull-Girder Load Time Series

3.2 Whipping and Springing Loads

The phenomena of whipping and springing occur at the hull-girder's first natural frequency mode. The lowest natural mode of vibration of a ship hull is the vertical hull-girder mode with two nodes, as shown in Figure 3.2-1. This vibration usually has a frequency too low to interact with engine and machinery vibration. However, it is low enough to interact with encountered waves. The excitation of the mode is thought to take place in two different ways. First, by a continuous low-level random vibration that may be generated by resonance with the waves. This phenomenon is known as springing, and its exact cause is still unknown in many cases. Second, slamming of the hull and bow due to pitching, as well as direct wave impacts, cause transient vibrations which occur intermittently and then decay over short periods of time, typically on the order of five to ten seconds. This phenomenon is known as whipping. Both springing and whipping response occur at the same natural frequency, and are difficult to distinguish at times for this reason. However, for high-speed ships with long slender hulls, the level of whipping loads is much larger than the level of springing loads. Also, the magnitude of the springing load does not abruptly increase as it does for whipping, which is a transient load.

The need for prior knowledge of the viscous-elastic characteristics of the hull-girder makes it impossible to predict the extreme whipping loads using the route/mission based frequency-domain analytical approach. It is envisioned that a 3-D time-domain motions prediction model will be required, with simultaneous input about the hull-girder characteristics, to predict the total global loads that include the high-frequency whipping loads. Since these 3-D time-domain models are expensive and resource-extensive, with long run times, a route and mission-based prediction approach can minimize the operational parameter ranges required to be analyzed in the 3-D time-domain model to predict the expected extreme loads and motions. In addition, the hull-girder characteristics can be obtained either via extrapolating from any existing similar full-scale prototype response data or from model test response data.

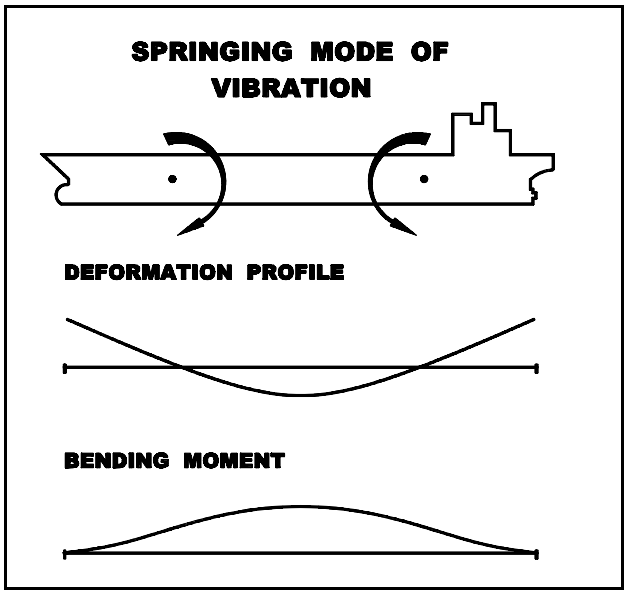

Figure 3.2-1. Springing and Whipping Vibration

A study published in 1994 investigated the effect of hull-girder characteristics, such as hull flexibility, on the wave-induced loading for high-speed monohull ships in a moderate seaway. Even if the hull flexibility normally can be ignored for ships built of steel, the use of aluminum or fiber-reinforced plastic (FRP) will lower the hull bending stiffness. Thereby, dynamic amplification of the two-node vibration mode can be significant. For a specific case, a 50-percent dynamic amplification of the standard deviation of the mid-ship bending moment was calculated for a ship made of FRP. The dynamic amplification is largest in

moderate sea-states due to the low zero-crossing periods. Therefore, the dynamic amplification of springing loads in a moderate seaway is of more concern in fatigue damage analyses than for the design values for the extreme loads.

A ship's total global load distribution is often not accurately represented by a normal distribution (Gaussian). Therefore, its extreme value prediction cannot be performed using most available statistical tools that are derived from the assumption of a Gaussian distribution. However, if the natural frequency component (the combination of whipping and springing) of the response data from the 3-D time-domain model can be extracted using the filtering technique, then it can be analyzed, but not in the same manner as the ordinary wave response. The filtering technique uses a low-band or a high-band signal filter to appropriately filter out the responses at frequencies of interest. The whipping responses are not Gaussian, but if the amplitudes of the first quarter-cycle of each of the whipping events are combined to produce a data sample, then the distribution of the amplitudes seem to follow a Weibull distribution. The whipping extreme value distribution can then be determined, and predictions of additional extreme values can be made.

Using this separation by filtering technique, the natural frequency component of a total response time history may be analyzed and the results used to make extreme value predictions for the whipping loads. However, since it is the total load that the designer is concerned about, it is necessary to find the extreme value distribution of the total load. Several factors make this difficult to determine by simply combining the ordinary wave load and whipping load. First, there is not a one-to-one correspondence between wave encounters and whipping events. This means that there is a dependent distribution of whipping with respect to wave encounter occurrence. Second, information about phasing between the low-frequency and high-frequency components is lost when the two components are separated. This means there is a distribution of phase for whipping initiation with respect to the ordinary wave component. Third, the larger the ordinary wave load is, the larger the whipping amplitude tends to be. This means there is a distribution of whipping amplitude with respect to ordinary wave load amplitude. Since there are at least three conditional distributions present, prediction of the total load using response separation and conditional probability can be extremely difficult, even impossible.

In an effort to avoid the complexities of such an analysis, the predicted amplitudes of the two components of loads, based on equal time, can simply be added together. If the phase angle tends to be nearly stable for whipping initiation with respect to ordinary wave load, then a correction can be made to the simple sum of the two components. This technique tends to be conservative for its predictions of maximum expected total load. Another method is to use an integrated procedure, proposed in 1995, for obtaining the statistics of the combined slamming and wave-induced responses and loads accounting for phasing, whipping amplitude non-linearity, whipping event clustering, and hull flexibility.

3.3 Slam Pressure Load

Slamming-induced pressure loads are generated from hull slamming resulting from pitching due to wave-induced motions. The slam pressures are considered local loads and govern the design of the bottom and side structures of the hull. For multihulls, slam pressures also dictate the design of the cross-structure, mainly in the forward sections. Several analytical and experimental studies are published explaining the nature and occurrence of slamming-induced peak pressures. The important factors concerning slam pressures are, first, the vertical acceleration at the structural location of interest; second, the relative entry velocity of the structure with respect to the water; third, the angle of entry of the structure, i.e. the shape of the structure experiencing slamming; and last, the structural unsupported panel size subjected to slam. By virtue of the third variable governing the slam pressure, it is apparent why the slam pressure on a wedge entering the water is lower than that of a flat plate. This is precisely the reason for concern for the slamming-induced pressures on the cross-structures of multihulls, since they are usually flat. Recent designs of a few high-speed catamarans have modified their forward cross-structure wet-deck section to a shallow third bow in order to reduce the slam pressures. A typical slam pressure profile along a vessel's length is shown in Figure 3.3-1. In this figure, areas I and II denote the wet-deck and internal deck of the cross-structure, whereas areas III and IV denote the same with a shallow third bow.

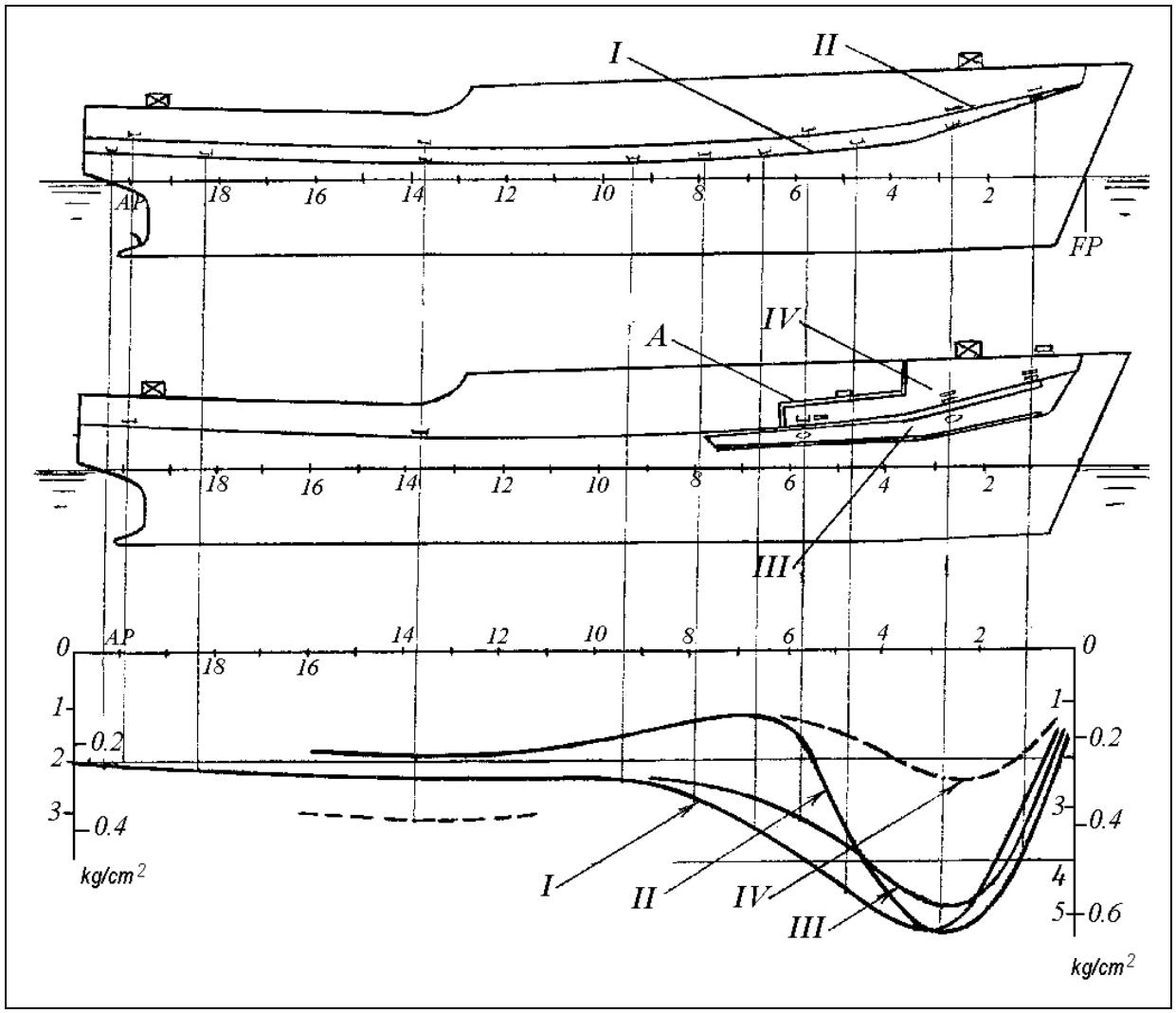

Figure 3.3-1. Slam Pressure Profile along Vessel's Length (from Multihull Ships by V. Dubrovsky & E. Lyakhovitsky)

Since slamming-induced loads are characterized as non-deterministic and more closely influence the design of the local structures than the hull-girder loads, it is imperative to accurately assess the slamming-induced loads. Designs of small high-speed vessels have shown that the local loads essentially control the total structural design, and slam pressures are an essential part of the local loads for the bottom, side and cross-structures. Traditionally, rule-based approaches have provided guidance for predicting slamming-induced pressures, which are typically based on empirical and experimental data and, therefore, provide reasonable accuracy.

For a route and mission-based load prediction approach, a frequency-domain tool to predict the vessel's motions response is not enough to estimate the slamming loads. A time-domain motions response tool is required, which can simulate the motion response time series for the desired operational conditions. Since slamming is a complex nonlinear phenomenon, it is common practice to analyze the response in random waves through time-domain simulations. In order to adequately estimate extreme responses, typically 50-70 one-hour simulations are required. A major problem is that the simulation costs grow with nonlinearity. Quadratic drag effects lead to a roughly four-fold increase in the required simulation length. Hence, several factors work against the use of time-domain simulations: (1) The number of simulations

required to adequately estimate the extreme responses, and (2) the need for response analysis over multiple sea-states. However, with a route and mission-based response prediction approach, the number of simulations required can be significantly reduced by focusing on the operational parameters and sea-states of interest.

In parallel, a slam event will need to be described in terms of a threshold relative velocity which will be attributed to the vessel's characteristics. Determining the number and characteristics of slam occurrences will help in statistically defining a slam prediction model using an extreme value distribution such as a Weibull distribution. Using such a time-domain-based statistical prediction model, slamming-induced loads can be estimated for various route/mission scenarios, as was successfully accomplished by Band, Lavis and Associates for the 80-knot 3KSES and LCAC programs in the 70s and 80s.

3.4 Load Combination

Once the individual ship structural load components are estimated, the difficulty arises in rationally combining the load components in a composite structural load. Figure 3.4-1 shows the structural loads estimating methodologies and their combination into a composite structural loading.

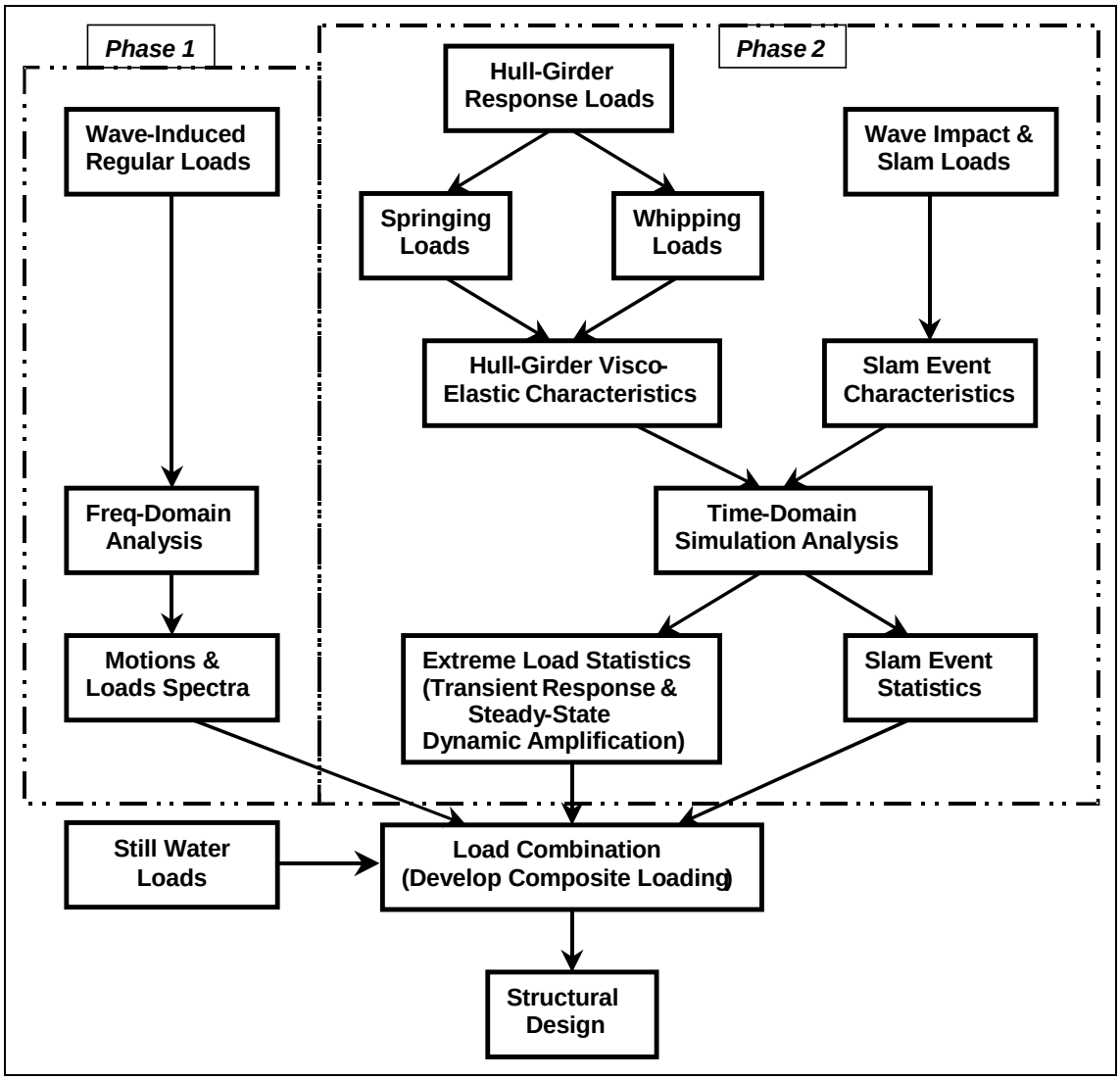

Figure 3.4-1. Structural Loads Estimating Methodology

Slam pressure loads not only govern the design of local structures, but slam-induced whipping and springing loads are global in nature. Since the extreme value wave-induced regular loads and hull-girder response loads, such as whipping, are predicted separately following different analytical procedures, their extreme value statistics have to be combined rationally to determine the composite load. As mentioned earlier, the determination of the joint statistics of the loads is quite complex, since whipping initiation and amplitude have conditional distributions with respect to the wave-induced load statistics and the presence of a phasing distribution between them.

One very conservative approach is to combine the loads off-line with a correction factor that will depend on the most probable whipping initiation phase angle. This load combination method will only be justifiable if the whipping initiation phase angle is nearly stable with respect to the wave-induced regular loads. Another load combination method is an integrated procedure proposed by a research group in 1995, which takes into consideration the whipping amplitude non-linearity and clustering, phasing, and hull-girder hydro-elastic characteristics in estimating the statistics of the combined wave-induced regular and hull-girder response loads. However, this approach was developed and validated for low-speed large vessels, and will need modifications to address high-speed slender multihull vessels. Figure 3.4.1 also highlights the overall scope of the project with phase-based development of the rationale and methodology. Eventually, all the building blocks of the integrated approach highlighted in the figure will need to be developed in order a obtain a complete route and mission-based structural load prediction program.

4.0 STRUCTURAL DESIGN OF MULTIHULLS

Multihulls, in common with other high-speed craft, are designed to withstand the static and dynamic loads that can act under the operating conditions. These loads are classified as local loads, such as the hydrostatic sea load, and those that act on the whole structure are termed global loads. The size and mission of the craft often determines the design driving criteria. The catamaran originated as two hulls joined together with two crossbeams, one aft and one forward. This same philosophy still continues with many of the smaller catamarans. The larger designs for carrying vehicles may also have a forward and an after bridging structure, but supplemented by intermediate bridging frames. The stiffening system used by almost all aluminum high-speed catamarans is closely spaced longitudinal stiffeners supported by substantial transverse web frames. For multihulls, in general, the moments and forces resulting from the vertical bending moment and shear force on the cross-structure act together with the pitch connecting moment where one hull is rotating relative to the other and the associated torsional moment have to be considered.

All of the major Classification Societies have developed rules specifically for high-speed and lightweight craft. The approach to structural design followed by the various Classification Societies is highlighted in the next section.

4.1 Rulebook-Based Design

Ship structures are today designed using rules and guidance given by the Classification Societies and the International Maritime Authorities. It is important that these design rules ensure that the ships are built with an acceptable level of safety. The rules from Classification Societies are based on analytical models for response and strength that are empirically-modified to obtain agreement with observations. The safety level of the existing ship structures is, hence, to a large extent, defined through registered failure statistics. Consequently, it is not straightforward to compare alternative designs if these designs are not closely related to traditional design. Recent trends in ship design are towards the use of more innovative materials and the development of new ship types. In these cases, it has become very important to estimate the actual safety level of ship structures, making it possible to compare traditional designs to new ones, aiming at the same safety level.

In general, local pressures generated through slamming, wave slap and hydrostatics govern Classification Society rulebook structural design. The overall procedure for a typical rulebook design is as follows:

- The craft geometry is defined and rulebook values for individual parameters are developed. Simple parameters, such as the craft length, are uniquely defined based on the particular set of rules employed (ABS, DNV, Lloyd's, etc.).
- The design accelerations due to ship motions are developed through empirical relations. The vertical acceleration at the craft LCG plays a significant role in the development of local slamming pressures.
- Upon determining the local loads, the thickness of plate elements is established. Similarly, loads on stiffening elements (girders, webs, stiffeners) are determined and the stiffeners are sized accordingly.
- Once the local design of the hull structure (and cross-structure, if applicable) is complete, the section modulus at the craft midship section (and centerline of cross-structure) is determined and compared to a minimum value that is provided by the rules. If the section established through local design is sufficient, the design is considered complete.

Generally, the rulebook-based approaches require an additional check of the local buckling strength of individual members due to global loads. The global loads are those induced through craft longitudinal bending and they induce a compressive stress in local members. By and large, the buckling check is a formality as the local design due to slamming and hydrostatic pressures govern the strength of these members. This procedure is the backbone of each of the rulebook-based design spirals. Variations exist in individual steps, and those differences make the rules for each Classification Society unique.

The development and application of global loads on the craft structure varies based on the Classification Society rules being used. The following is a brief summary of the methodology employed by each of the Classification Societies investigated.

American Bureau of Shipping (ABS)

- All craft (monohull and multihull) must meet a minimum midship section modulus (SM) requirement determined through an empirical relation based on the craft geometry and material.
- Craft of length greater than or equal to 61 m must meet an additional minimum midship SM requirement that is based on the estimated wave-induced hogging and sagging moments of the craft.
- In addition, a minimum hull-girder moment of inertia requirement at midship is imposed.
- For twin-hulled craft, the transverse bending moment, torsional moment and vertical shear acting on the cross-structure are determined. These values are then used to determine the minimum bending SM, minimum torsional SM, and the minimum shear area of the cross-structure.

Det Norske Veritas (DNV)

- The longitudinal bending moment (BM) is calculated using several different methods (crest landing, hollow landing, wave-induced hogging, and wave-induced sagging), and the maximum value obtained is taken as the rulebook BM. The same equations and approach are used for monohull and multihull craft.
- The vertical shear induced by longitudinal loads is determined from the rulebook BM.
- For twin-hulled craft, the transverse BM, vertical shear force, transverse torsional moment and longitudinal torsional moments are determined through empirical relations.
- These loads are then combined in the following manner to determine the adequacy of the structure:
  - 80% longitudinal BM and shear + 60% longitudinal torsion.
  - 60% longitudinal BM and shear + 80% longitudinal torsion.
  - 70% transverse BM + 100% transverse torsion.
  - 100% transverse BM + 70% transverse torsion.

Lloyd's Register

- The wave-induced longitudinal BM and shear and the dynamic longitudinal BM are determined through empirical relations.
- For twin-hulled craft, the transverse BM, transverse torsional moment, and vertical shear force imposed on the cross-structure are determined.
- The global design is then checked through a combination of these loads in three sea conditions, as follows:
  - Head sea – 10% transverse BM + 100% longitudinal BM + 10% transverse torsional moment.
  - Beam sea – 100% transverse BM + 10% longitudinal BM + 20% transverse torsional moment.
  - Quartering sea – 10% transverse BM + 40% longitudinal BM + 100% transverse torsional moment.
- These strength calculations are to be conducted using a three-dimensional global finite element model (FEM) of the craft.

Bureau Veritas

- Similar to the other Classification Societies, the longitudinal BM and vertical shear force are determined through empiricism.
- Also, the twin-hull transverse BM and transverse torsional moment are determined.
- As is specified in ABS, each load is investigated independently to determine the minimum section modulus required.

The common thread between the approaches followed by the various Classification Societies is that the governing global loads (longitudinal BM, transverse BM, transverse torsion) are developed through empirical relations. However, DNV is the only Society to provide a longitudinal torsion moment. In chapter 3.4, a complete structural design that follows each of the Classification Society's rules is accomplished to provide a background for the first-principles-based structural design methodology that is being developed as part of this project.

4.2 Route or Mission-Based Determination of Design Criteria

The determination of the success of the structural design hinges on the determination of the loads to which it will be exposed and the specification of a reasonable probability level for its survival. The environmental loads imposed on the structure will have to be determined from an analysis of the modes of operation of the vessel and its environment, and then, making use of this information, by defining a number of deterministic load conditions for analysis. Each of these load conditions is to be assigned a probability of occurrence and compounded to develop a single long-term probability distribution for each type of load. A failure in the accurate determination of structural load can have significant impact on the design and operation of the vehicle. Underestimation of the loads can result in structural failure or can limit operations. Overestimation of loads, on the other hand, will make the vessel carry excess structural weight, resulting in reduced operational range and payload. Hence, a rational approach to loads determination is important.

5.0 DEVELOPMENT OF A ROUTE/MISSION-BASED STRUCTURAL DESIGN METHODOLOGY

The loads experienced by an ocean-going ship depend upon a very large number of influences; they vary with time in a random manner; they never occur in exactly the same way twice. Some of the influences are vessel-related such as speed, weight distribution and control settings, and some are dependent on the environment such as wave height and wind speed. The structural designer has to convert this constantly changing scene to a limited number of design load cases which can be used to determine the craft's scantlings.

The method adopted here consists basically of the following steps:

- Analysis of the operational environment.

- Selection of representative loading cases.
- Determination of the probability of occurrence of each of the loading cases.
- Calculation of the loads for each representative case in the form of an average or root mean square value together with a short-term probability distribution to describe the possible variations of loads under these conditions.
- Computation of long-term probability distributions by combining the short-term distributions.
- Selection of design loads.

In order to define the problem, therefore, the first requirement is to define the operational environment.

5.1 Operational Environment

Figure 5.1-1 shows a typical operational envelope for a high-performance vessel; in this case, an early version of a very high-speed amphibious assault SES. The vessel is expected to operate within the speed wave-height envelope shown. The proportion of time spent in each area of the envelope is indicated. The distribution on the wave height axis is derived directly from ocean wave-height data as suggested by Figure 5.1-2. The horizontal distribution along the speed scale was derived from a typical mission profile such as that shown in Figure 5.1-3. The sloping lines dividing the speed zones represent the fact that the vessel's speed must fall off as sea state increases. This particular multihull vessel, for example, could reach 90 knots in calm water, but was not expected to exceed 40 knots in SS4. It was not expected to operate on-cushion in sea states higher than SS4. The loads experienced in this case in SS4, even at 40 knots, were so severe that consideration was given to reducing speed still more in the higher sea states. This consideration is represented by the two lines labeled "structural loads limitations". One point of interest in this diagram is that the percentage of time spent in the most severe conditions is really quite small. 2.2% of the total time is spent in SS4, between wave heights ($H_{1/10}$) of 5.8 and 8.7 feet and between speeds of 25 and 48 knots. However, only a small proportion of this 2.2% is actually spent near the extreme corner of the diagram (at 40 knots in wave heights of 8.7 feet). If this distribution within each area is not taken into account, the results can be misleading. In the example shown in Figure 5.1-1, the cases actually used for computation are shown by the small open circles.

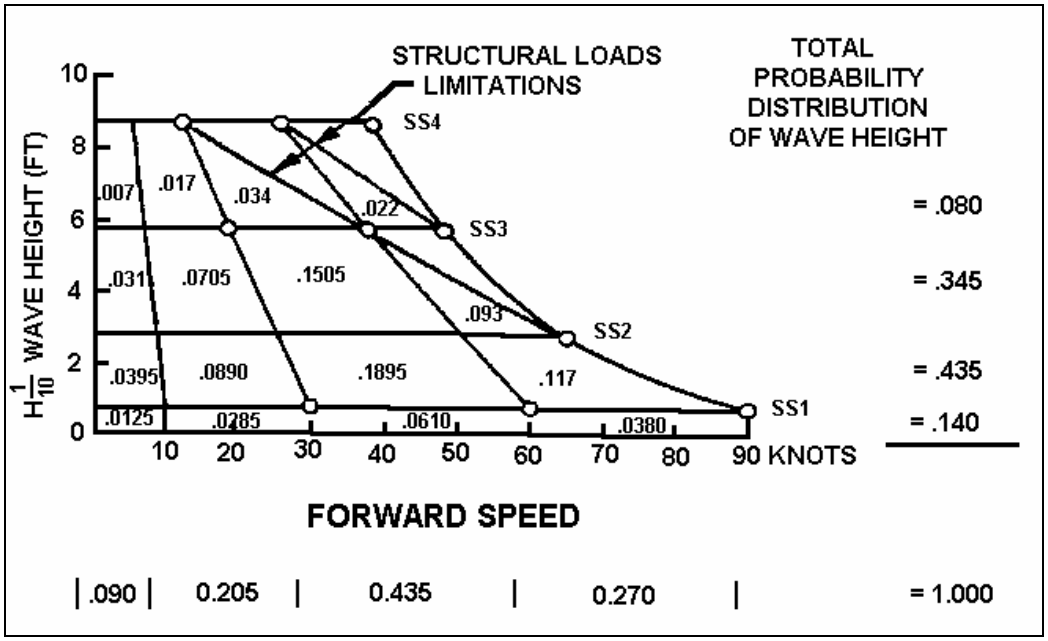

Figure 5.1-1. Typical Operating Envelope for Advanced Marine Vehicles

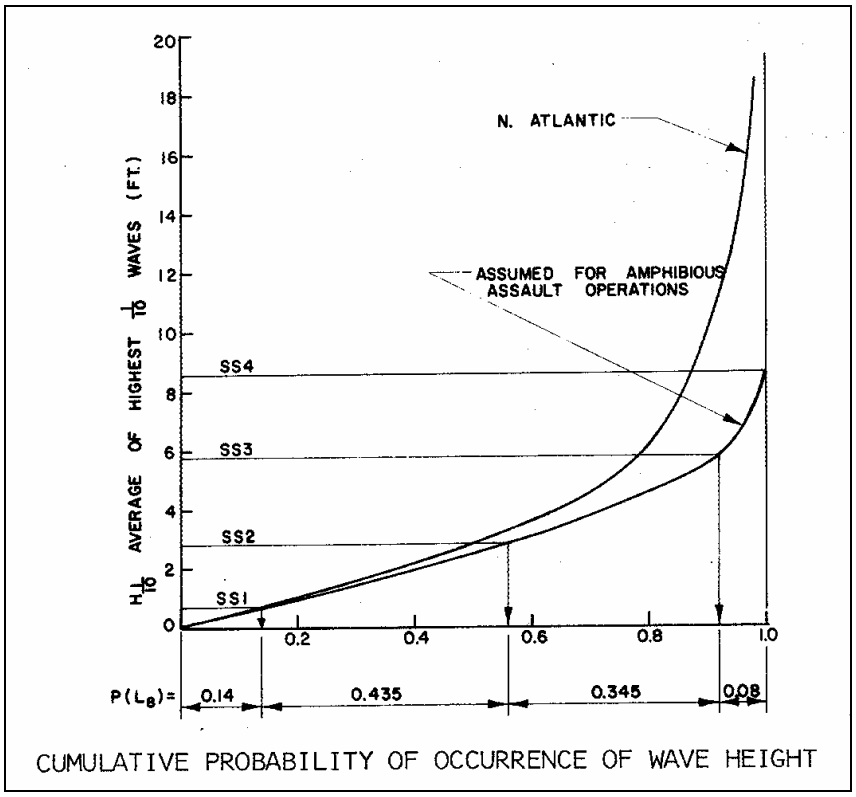

Figure 5.1-2. Sea State Probabilities for Typical Amphibious Assault Mission

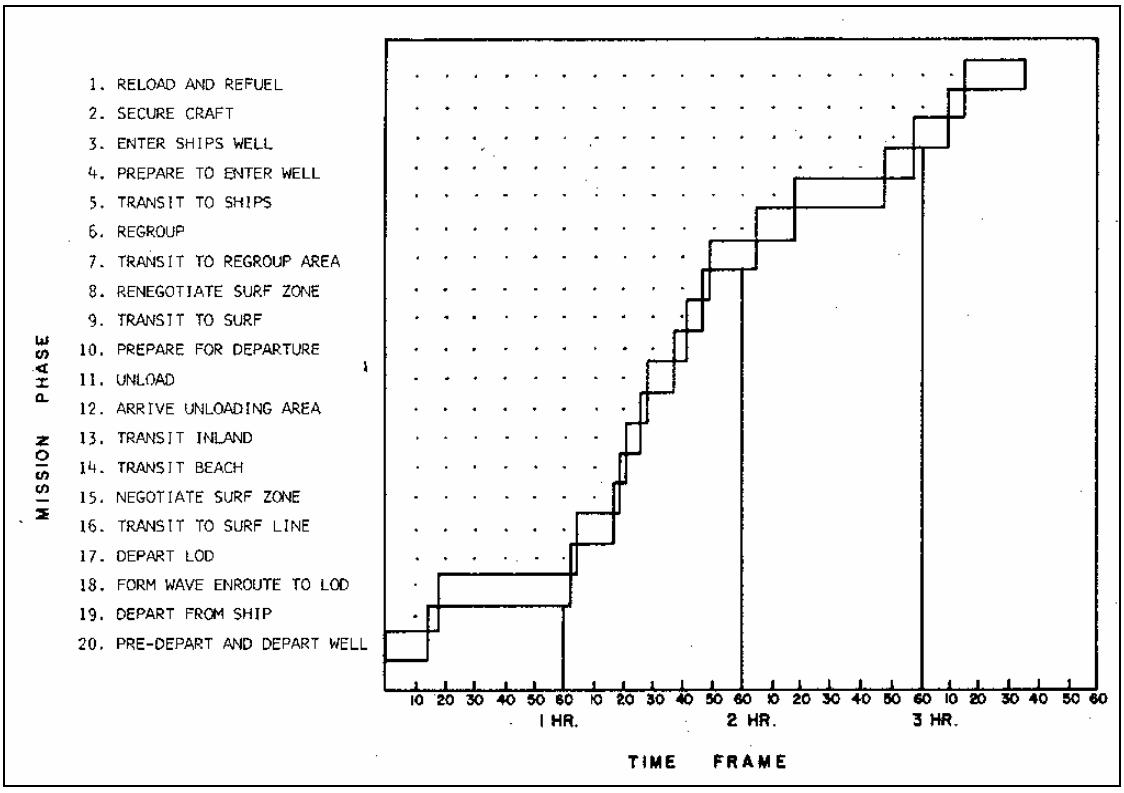

Figure 5.1-3. Analysis of Mission Profile for Amphibious Assault Landing Craft

Speed and sea state are not the only quantities that define the operational environment. Equally important is the need to define the distribution of heading angle to the dominant wave direction and the distribution of gross weight. Typical distributions of these quantities are shown in Figures 5.1-4 and 5.1-5. All headings are normally assumed to be equally probable, and a gross weight distribution can usually be derived by a brief analysis of the typical mission profiles or the top level requirements.

By means of the foregoing considerations, therefore, a formidable matrix of representative cases has been developed. For each case, a set of loads is required which can be generated either by computational methods or by making use of experimental results. In practice, a combination of both sources is often used. For each condition, the designer is interested in a wide variety of load information.

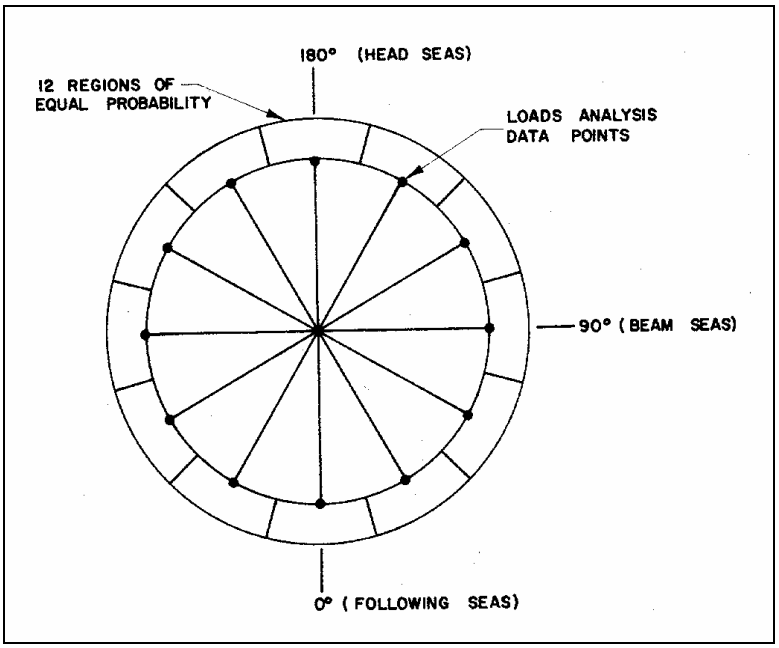

Figure 5.1-4. Assumed Distribution of Ship Heading to Wave Direction

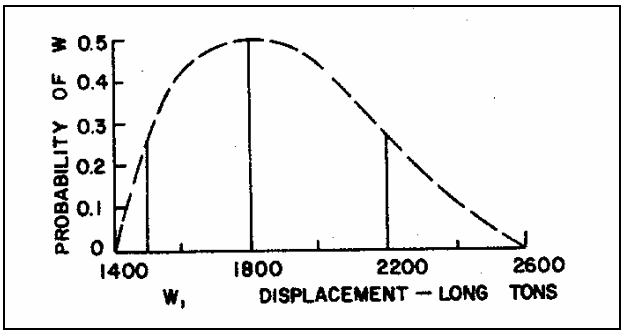

Figure 5.1-5. Assumed Distribution of Gross Weight

5.2 Types of Loads

The designer requires information on a large number of types of loads, including the following:

- Midship vertical bending moment and shear force.
- Longitudinal distribution of bending moment.

- Transverse bending moments.
- Torsional moments.
- Hydrodynamic and hydrostatic pressure distributions.

In all cases, information will be required on limit load and fatigue loads. These loads may be due to a variety of causes, which are normally superimposed on each other. The most significant causes of load are:

- Still-water loads – due to the interaction of buoyancy, lift forces and weight distribution.
- Thermal stresses – due to the different temperatures existing at different components of the structure.
- Wave-induced loads – which are normally the most significant as far as design limit loads are concerned.
- Slam-induced loads – which occur when the cross structure of a multihull hits the water. These loads are normally superimposed on the wave-induced loads.

An interesting illustration of the relative significance of different load types during a single voyage of a merchant ship is shown in Figure 5.2-1 (Reference 8).

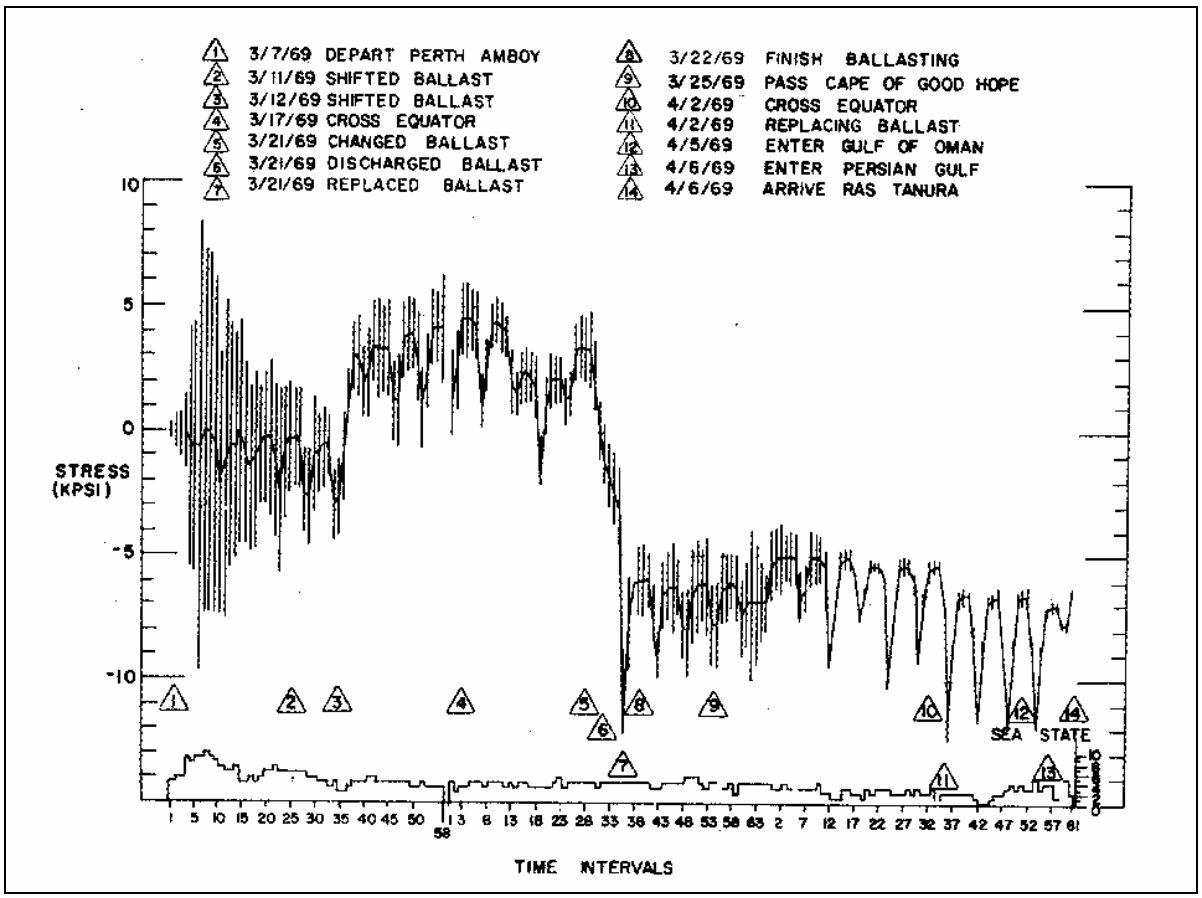

Figure 5.2-1. Typical Variation of Midship Vertical Bending Stress During a Voyage of the S.S.R.G. FOLLIS [8]

An easy to use procedure is required to consider each of these loads in turn, estimate their magnitudes and probability distributions, and to determine to what extent they should be superimposed on each other. The method described here attempts to carry this out. It is inevitable that some of the steps in the method are considerably weaker than others, but the important thing is that it does produce usable numbers for the designer. As time goes on, each step can be re-examined and the validity of the total method can be steadily improved. In order to determine these loads, however, hard data is required on each and every one of the selected cases. The sources of data will be discussed in the next section.

As more and more research and development work is done on an ever-increasing number and variety of advanced marine vehicles, a larger and larger data base becomes available. The advanced marine vehicle community have, perhaps, followed the lead of the conventional ship designers in attempting to replace empirical formulae by rational design procedures, and by extensive full-scale experimentation.

Available sources of information can perhaps be divided into three main groups:

- Analytical load prediction procedures
- Model test results
- Full-scale test results

These will be discussed, in turn, below.

5.3 Load Prediction Procedures

5.3.1 Empirical Formulae

The simplest form of analytical procedure is the empirical formula. It should not be forgotten that until less than forty years ago, many successful ships were designed to formulae. Before the advent of modern computational techniques, this was often the only procedure available to most designers. Also, the rules of most Classification Societies, even today, rely heavily on empirical formulae.

5.3.2 Frequency-Domain Simulation

Provided that the response of the vehicle to a seaway can be assumed to be linear, then frequency-domain analysis can provide load and motion information in a reasonably economical fashion. The response amplitude operators for the quantity in question (midship bending moment, pitch motion, etc.) can be computed (as with SHIPMO) by treating the hydrodynamic and hydrostatic forces acting on the vehicle as linear systems. The standard deviation σ or root mean square (rms) response of each quantity can then be determined for any specific condition of operation.

In spite of the fact that most advanced ship response systems are very obviously nonlinear, it has been found, experimentally, that the agreement between rms responses measured in the model tank and those predicted by frequency-domain simulation is surprisingly good, even for operation in severe sea states. Unfortunately, a great deal of the experimental work carried out on advanced marine vehicles is either classified or proprietary, so that these comparisons cannot be shown here. It should be emphasized, however, that it is only the rms values that correspond to the predicted values. As the responses are nonlinear, especially in high sea states, the distribution of peak responses do not follow the Rayleigh distribution, and the maximum values predicted by using the Rayleigh distribution constants do not, in general, match experimental values.

The great advantage of the frequency-domain simulation, such as SHIPMO, is that it is simple, flexible and inexpensive. As it has now been proven, many times, to yield usable values of rms response, it provides a very valuable design tool.

5.3.3 Time-Domain Simulation

A great deal of effort has been devoted to developing very comprehensive time-domain simulations of ships, but at the present state-of-the-art, for high-speed ships in particular, it does have some disadvantages. Firstly, it is a very elaborate procedure to use, so that when engineering time and computer hours are taken into account, it is very expensive to operate. Secondly, due to the expense involved, it is not usually possible to run the program for long enough to obtain a reasonable statistical sample. By its nature, the time-domain model is deterministic whereas the real world of wave-induced loads (even in the model tank) is probabilistic. The current tendency seems to be to use time-domain models for specific, time-constrained, transient events rather than for steady-state operation.

5.3.4 Impact Simulation

A much less ambitious time-domain simulation approach, that has proven itself useful for many years, is the impact program which has been used by BLA in different versions to generate impact load time histories for the SES-100A, the JEFF-A Landing Craft, the Arctic SEV study, the Litton and Rohr 2K and 3KSES designs and many other high-speed ship designs since. The impact analysis makes use of the assumption that the normal operation of an advanced marine vehicle is more or less impact-free, so that impacts of the hard structure of the hull or wet deck on the water surface are comparatively rare events. It follows that the motion of the vehicle prior to the slam can be predicted satisfactorily by a frequency-domain simulation. By using the characteristic parameters of the Rayleigh (or Weibull or generalized gamma, etc.) distribution, the probabilities of a slam occurring at any point on the ship at any particular velocity can be determined. A slam event is illustrated by Figure 5.3.4-1. The impact program logic converts the probabilistic information of the frequency-domain program into a deterministic scenario represented by Figure 5.3.4-2. Wave heights and lengths are chosen to be compatible with the frequency-domain information and other parameters are chosen to provide representative situations. Considerable effort has been expended, over the years, in studying the sensitivity of the final results to the assumptions made. When necessary, ranges of values have been used to provide multiple simulations. By treating each element of the wetted impact area as a section of an impacting wedge, defined by effective trim and deadrise angles, and by applying modified versions of classical water-impact theory, it is possible to generate a pressure map of the impact area. Integration of the pressure yields total load at each instant of time and, consequently, the vehicle response can be calculated. A typical time history is illustrated in Figure 5.3.4-3.

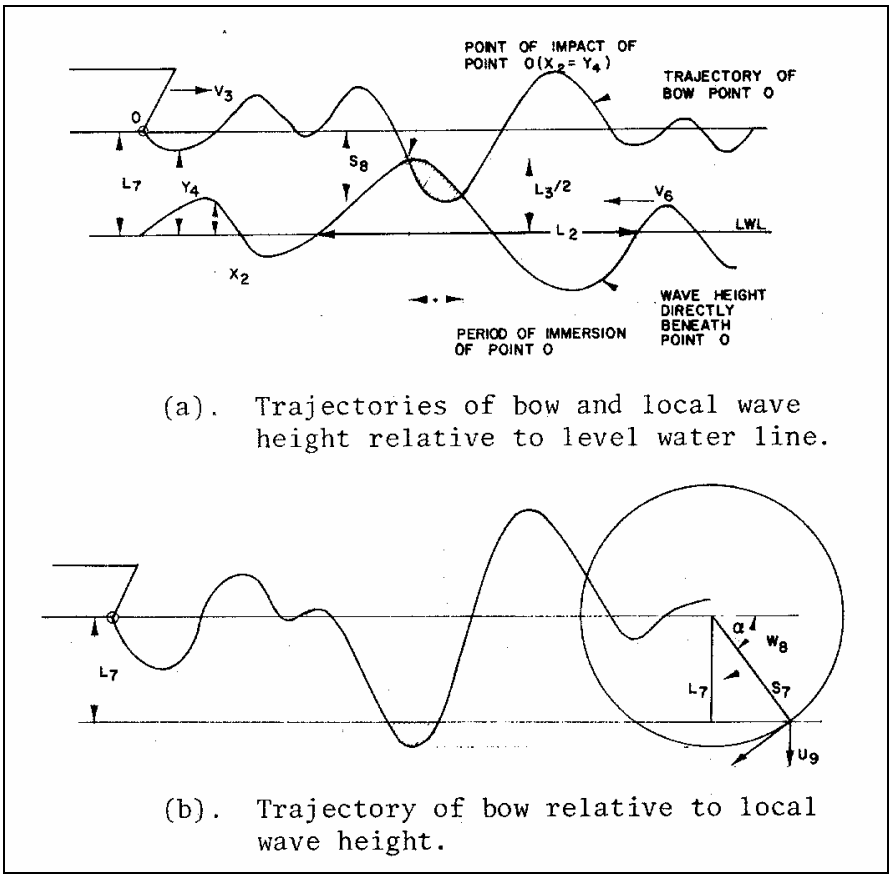

Figure 5.3.4-1. Diagram Showing Impact Event Occurring on a Typical SES Bow

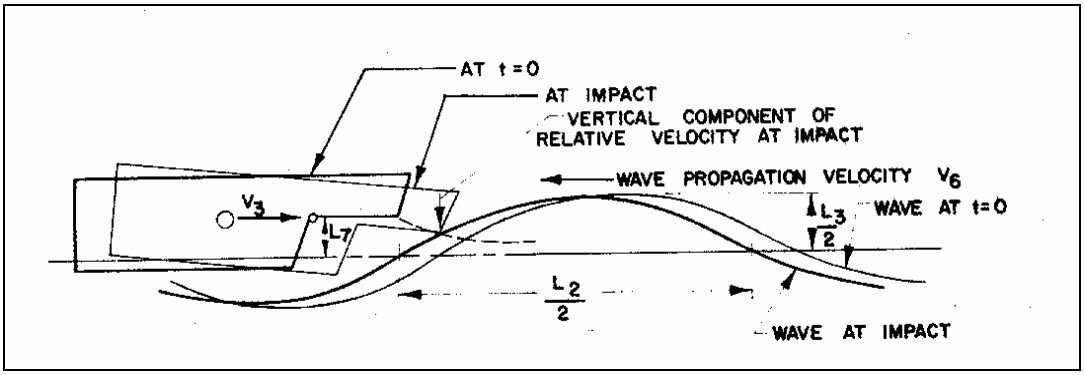

Figure 5.3.4-2. Diagram Representing Bow Impact of a Typical SES

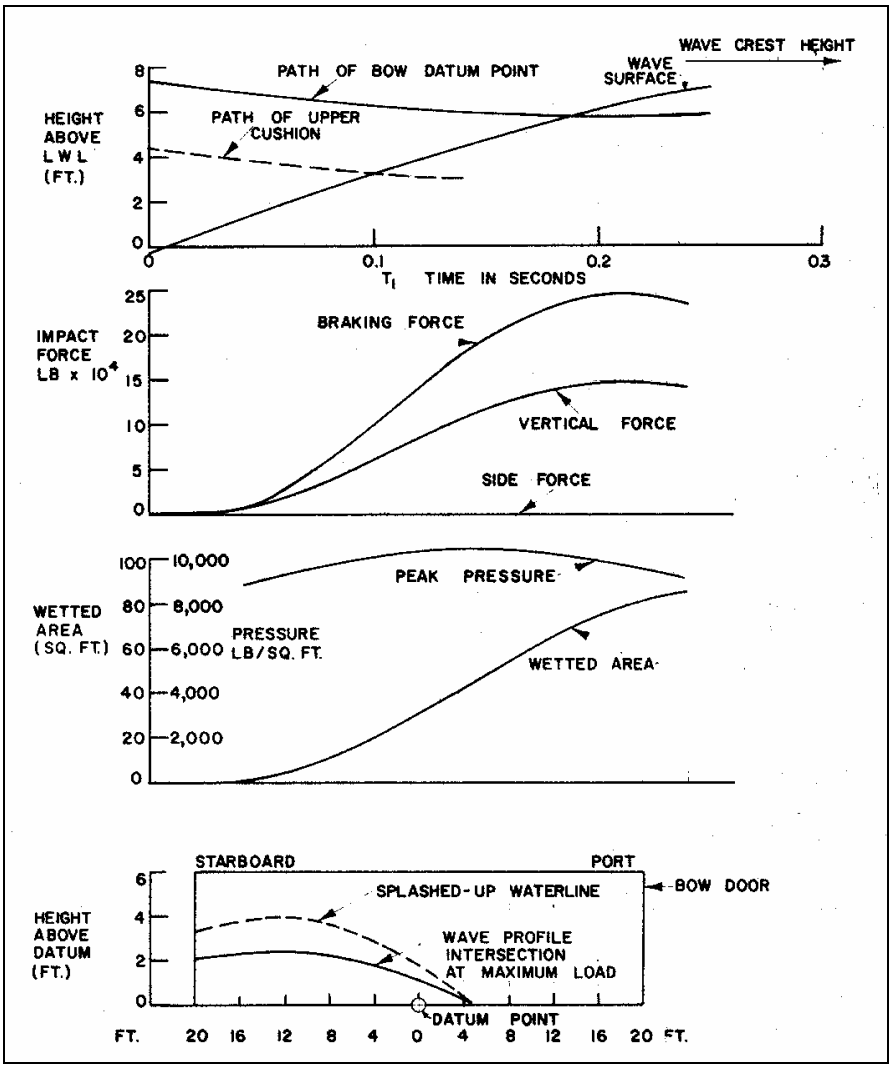

Figure 5.3.4-3. Time History of an AALC Impact in SS4 at 38 knots at 45^{o} Heading to Waves

By carrying out a number of these impact calculations, each of which is associated with a specific frequency of occurrence, it is possible to generate a long-term, probabilistic picture of the impact loads that any vehicle may experience during its lifetime. This procedure will be discussed later in this section.

5.3.5 Model Tests

A number of structural model test techniques have been developed over the years and the application of these techniques to the advanced marine vehicle field has yielded a very significant amount of useful data. Unfortunately, almost all of this data is still classified or proprietary in one way or another, so that all that can be mentioned here are the techniques.

Segmented models have been instrumented to provide measures of shear force and bending moments at one or two hull stations. These models have been tested in head seas and in impact drop tests. These models are similar to those that have been used in tests of conventional ship models.

A rigid, vinyl modeling technique has been developed at DTNSRDC which allows modeling of structural response as well as structural loads. This is achieved by using the fact that the elastic modulus of the rigid vinyl is such that its elastic properties scale properly for 1/30-scale models of aluminum prototypes or

1/28-scale of steel prototypes. This method was used to build a model of the CPIC which was tested at DTNSRDC.

A similar technique has also been developed in which scale models have been built by using a segmented model whose component segments are attached to a carefully designed, scaled structural grillage. This method has been very successful in measuring response of complex models in head and oblique seas. A segmented model of a trimaran was recently tested by the HSS Innovation Cell at CDNSWC.

In the same way as in the field of full-scale testing, the amount of experimental model data available has changed abruptly from the situation a few years ago when almost nothing was available to the present situation where there is almost an embarrassing amount of data and insufficient time to analyze it all.

5.3.6 Full-Scale Trials

In the last few years, particularly in the multihull field, the situation with regard to full-scale structural loads data has improved dramatically. For example, Figure 5.3.6-1 shows vertical accelerations measured on an SES when running, on-cushion, in head seas. The asymmetric nature of the data is at once apparent. The peak upward accelerations tend to be larger than the down. Figure 5.3.6-2 shows similar data taken on an SES plotted on Weibull probability paper. Straight lines on this paper represent cumulative Weibull distributions. The cumulative Weibull distribution function is given by:

$$P(x) = \exp [- (\lambda x)^c]$$

where λ is a constant and the index, c, is numerically equal to the gradient of the straight lines on Figure 5.3.6-2. If the index, c (gradient), is 1.0, then the distribution is exponential, and if it is 2.0, the distribution is Rayleighan as both of these distributions are special cases of the Weibull distribution. The experimental points lie consistently between these two extremes. In Figure 5.3.6-3, the corresponding trough accelerations are plotted, showing that, in the head sea case, at least, a considerable difference exists between trends of peak and trough accelerations. This is consistent with Figure 5.3.6-1. Figure 5.3.6-4 shows plots of bending stress which exhibit very much the same characteristics as the acceleration data. The great advantage of full-scale testing is that the test runs can be several times longer than is possible in sub-scale model testing in towing tanks, so that the statistical samples obtained are much larger. Disadvantages of full-scale testing are that wave heights and other test conditions cannot be known very precisely and may vary considerably even during quite a short run. The full-scale tests, however, are run in those conditions for which prototype ships must be designed so that a degree of realism is achieved that cannot be achieved in the model tank, and the problems of scaling are very much less than those that were involved in scaling from an 8-foot model to, say, a 1000 T ship.

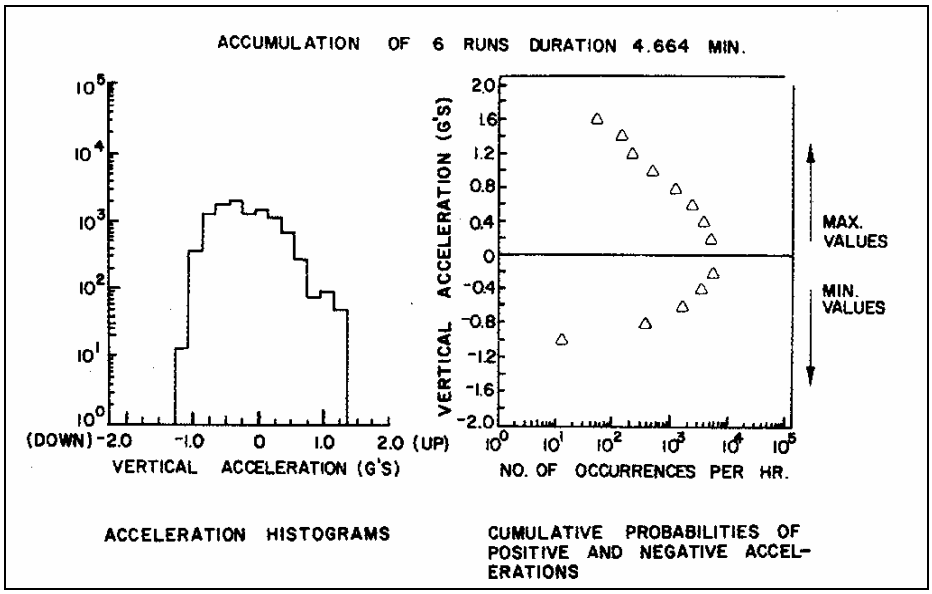

Figure 5.3.6-1. SES Vertical Acceleration at C.G.

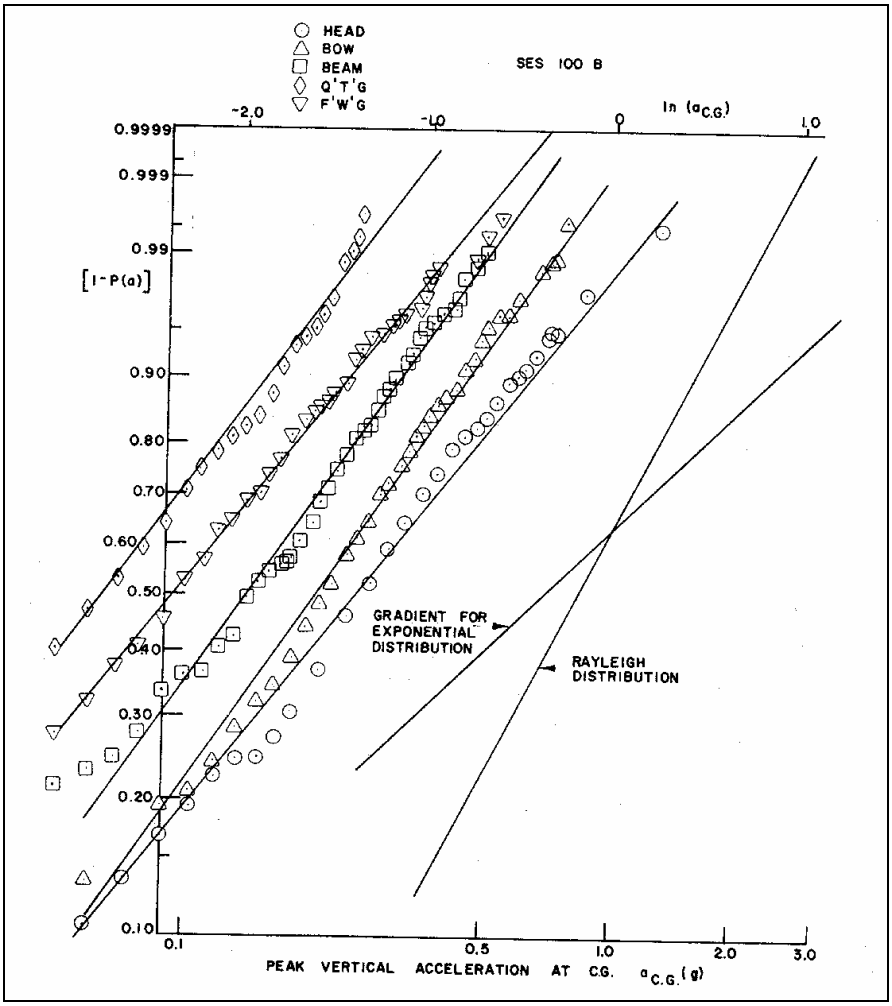

Figure 5.3.6-2. Peak (Upward) Vertical Accelerations Measured at C.G.

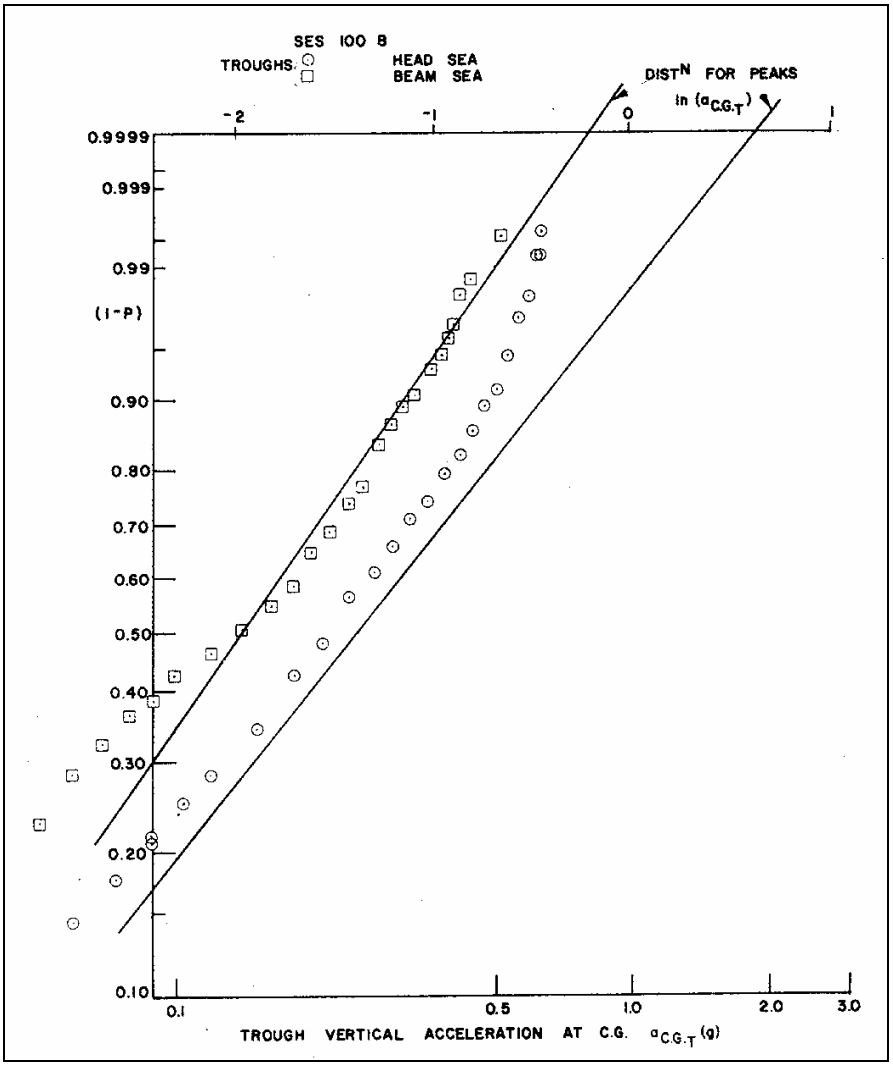

Figure 5.3.6-3. Measured Trough (Downward) Acceleration Data

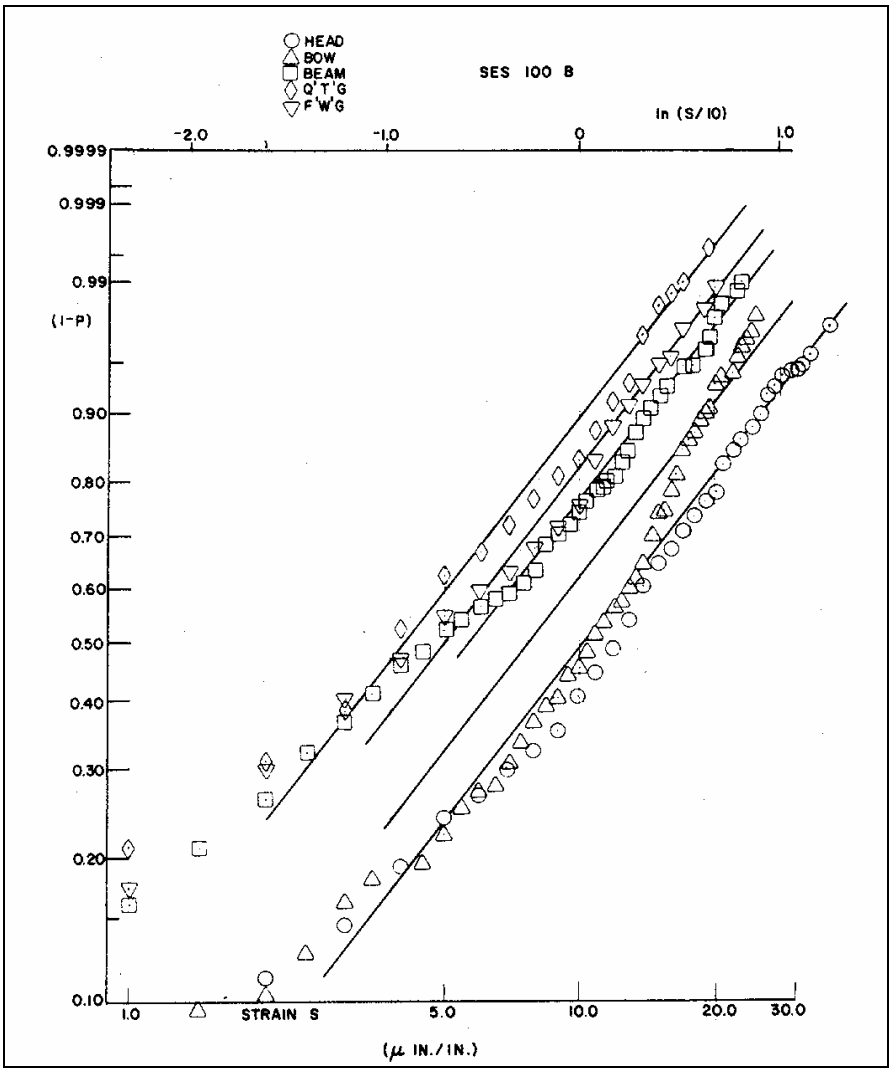

Figure 5.3.6-4. Measured Peak Bending Stress Data

5.4 Prediction of Full-Scale Loads

The structural designer requires specific information so that he can design his ship. He would like to know the largest midship bending moment, for example, to which his ship will be subjected within a twenty-year operational life. The hydrodynamicist cannot provide him with this deterministic figure. Instead, however, he can provide the structural designer with a bending moment which has only a ten percent, or one percent, probability of being exceeded during the lifetime of the ship. Once the probabilistic criteria (in this case the ship's life and the acceptable probability of exceedance) have been specified, a single limit design bending moment can be calculated.

The methods of calculation vary. In broad terms, there are two schools of thought:

(a) One method is to design for the "worst expected sea condition." This method proposes to design the ship by analyzing the ship's response to the "worst storm" that it is likely to encounter. It is well known that the waves encountered in severe storms are very dissimilar to those of lesser storms. The duration of extreme storms is normally so limited that the seas do not have time to become anywhere near fully developed. Figure 5.4-1 illustrates this. The time required to "fully develop" the seas corresponding to the higher sea states exceeds the probable time that the sea state exists in one year. In this method,

therefore, the design loads are determined by exposing the ship, analytically or experimentally, to seas corresponding to the worst storm records available. The main drawback to this method is that the available records of such storms are very limited in number. The statistical sample used as a base is, thus, very limited and, in any case, recorded data shows that the maximum loads probably do not necessarily occur in the worst sea states.

(b) The second method is the statistical method in which extreme loads are postulated by extrapolating from a larger data base using all available sea state data. The weakness of this method is that there is no guarantee that the extrapolations are valid. Historical evidence, however, tends to support this procedure. It may be argued that a conventional ship is basically a linear system, whereas most advanced ships are not, but it is suggested here that, provided suitably flexible probability distributions are used to describe the available data, the nonlinearities do not affect the validity of the method. This method, at least, allows prediction to be made from data that is generally available or obtainable and is flexible enough to allow refinement as time goes on. It can also make use of the data provided by the extreme sea state cases and provides a method for properly ordering and weighting such contributions.

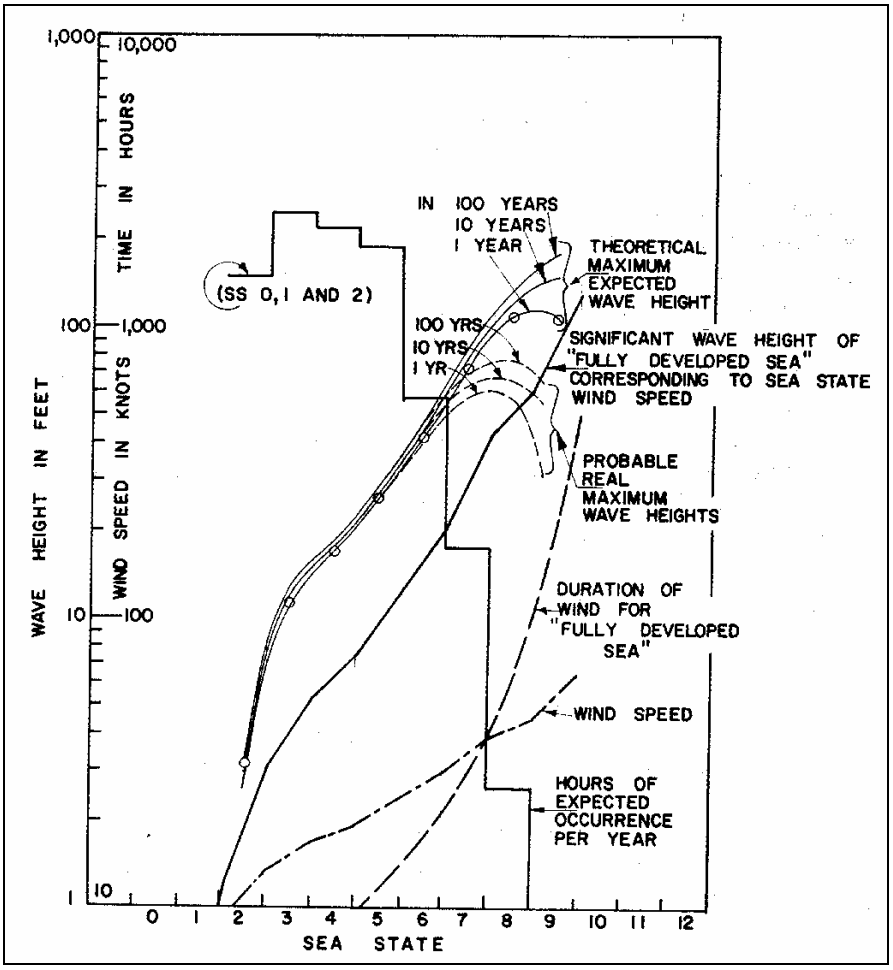

Figure 5.4-1. Theoretical Sea State Characteristics

5.4.1 Short-Term Statistics

In order to predict extreme values of loads or motions, it is necessary, therefore, to be able to extrapolate from available samples of experimental or analytical evidence. In general, the experimental samples are

very small compared with the expected life of the ship, so that the extrapolation process must be done with considerable care. Figures 5.3.6-2, 5.3.6-3 and 5.3.6-4 show typical peak value distributions from SES experience. The distribution used here to approximate the data is the Weibull distribution, which is a special two-parameter case of the three-parameter, generalized gamma distribution. Results of testing SES structural models have exhibited reassuringly similar tendencies, but these data are still proprietary.

The effect of the choice of distribution on the long-term loads, moments and stresses may be seen most graphically in Figure 5.4.1-1, which shows the long-term distributions of x/x_{rms} for various c values. At the higher levels of probability, which are those of interest in establishing extreme values, the long-term cumulative distribution curves fan out over a wide range for different values of the Weibull parameter c.

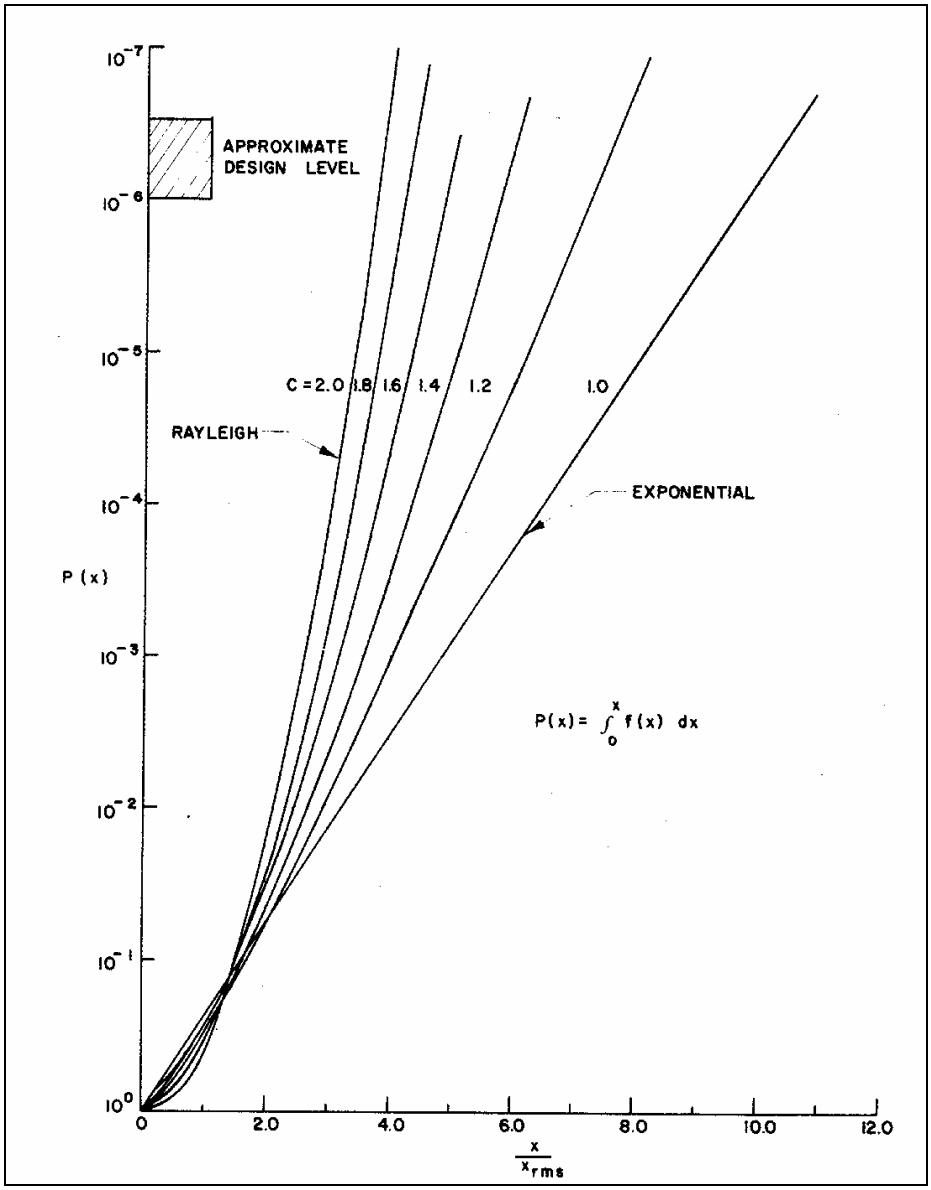

Figure 5.4.1-1. Cumulative Weibull Probability Distributions for a Range of Values of the Index c

On the basis of the evidence in Figures 5.3.6-2 - 5.3.6-4, it is suggested that the Weibull distribution may be said to represent the data in a reasonable manner, and that it is a clear improvement on either the exponential or the Rayleigh distributions which are, in turn, one-parameter special cases of the Weibull

distribution (see Figure 5.3.6-2). The Weibull distribution is also acceptable from the point of view that it is closely related to the Rayleigh distribution which is generally accepted as representative of wave heights and wave-induced phenomena. The theory of extremes from which the first asymptotic distribution is derived is not really applicable to this type of data. The theory of extremes should be applied to the distribution of single extreme values from unrelated events (for example, the highest flood tide in each year or the highest single stress measured in each of a set of different storms or test runs). It should not be applied, therefore, to a series of peak values from a single continuous record, which is the extent of the majority of the data presently available. If a large enough number of runs were made on models, it would be very relevant to examine the maximum values of each run by means of the statistics of extremes. This has not yet been attempted as the number of rough-water test runs on models is still too limited.

5.4.2 Long-Term Statistics

Each run in the test tank or of the full-scale ship is necessarily a short-term event. During each short-term event, it is assumed that the ship's speed and heading and the sea state remain constant. The operational life of a ship can be considered as a summation of a very large number of short-term events. If the behavior in each short-term event is known, and also if the manner of distribution of short-term events throughout the ship's life is known, then a long-term picture of the vehicle's life can be built up.

This is the method that is used here to predict the long-term behavior of the ship so that, eventually, a single long-term distribution of each applied load or stress can be built up to represent the ship total experience in all speeds, sea states, headings and loading conditions. In order to accomplish this, use is made of the description of the operational environment given earlier in this section.

If the probability of exceeding a given wave-induced load x at a speed V in sea-state S at heading H and gross weight W is $P_{VHSW}^{(x)}$, then the total probability P(x) of exceeding the load x is given by summing the component probabilities for all conditions.

$$P(x) = \sum_V \sum_H \sum_S \sum_W P_V P_H P_S P_W P_{VHSW}^{(x)}$$

where P_V, P_H, P_S, P_W are the probabilities of occurrence of each velocity, heading, sea state and gross weight.

Combined loads can be treated in the same way. Suppose, for example, that the probable occurrence of a still water load x_{SW_i} (or thermal load, or etc.) is $P(x_{SW_i})$, and that this distribution is independent of the wave-induced load, then the total combined probability $P_c(x)$ of exceeding the same load x is given by:

$$P_c(x) = \sum_i P(x_{SW_i}) P(x - x_{SW_i})$$

In fact, neither still-water loads nor thermal loads are normally independent of wave-induced loads, but this only provides a slight complication that can readily be resolved by computational procedures.

By basing the short-term extrapolations on experimentally measured stresses, the effects of the combined components of wave-induced loads are taken into account. The complex combinations of vertical and transverse bending moment and torsion can be represented in the model and full-scale tests in an adequate manner.

The number of cases selected from the operational envelope shown in Figure 5.1-1 is limited by the test and computational time available. As mentioned before, it may be misleadingly conservative to use the points at the top right-hand corner of each section of the operational envelope to define the conditions pertaining within that segment.

Instead, it is usually assumed that the distribution within each segment is uniform and a correction is applied based on this assumption. Figure 5.4.2-1, for example, shows the effect on the long-term probability of exceeding a value x_j of a uniform spread of short-term Weibull distributions with rms values ranging from x_{rms_2} (upper limit) to x_{rns_1} (lower limit). The larger the value of x, and the smaller the ratio x_{rms_1} / x_{rms_2}, the greater the effect on the total probability. The ordinate $P'(x_j)_{AB}$ in Figure 5.4.2-1 is the ratio of the probability of exceeding x_j due to the uniformly distributed set of distributions to the probability of exceeding x_j due to a single distribution at x_{rms_2}.

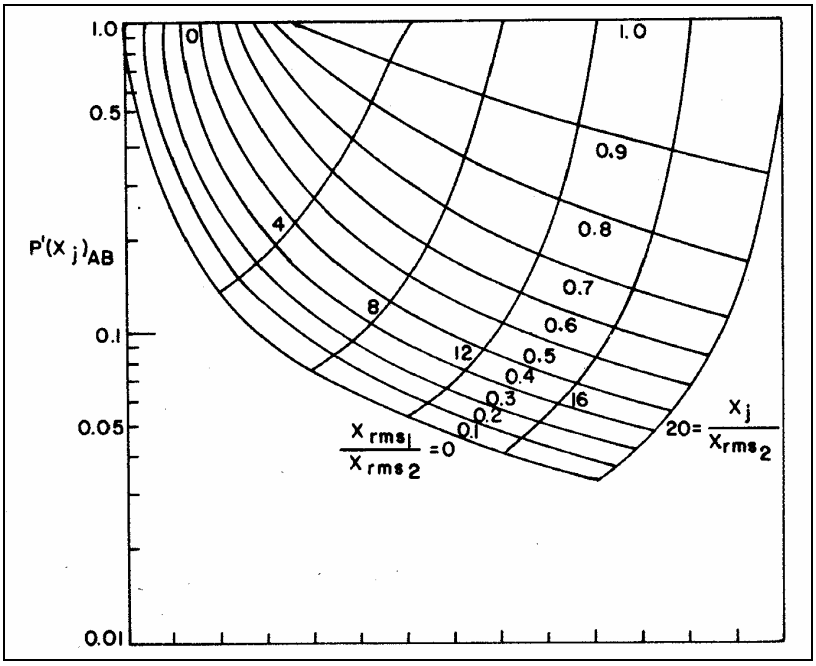

Figure 5.4.2-1. Cumulative Distribution Characteristics of the Weibull Distribution (c = 1.0)

5.4.3 Selection of Design Limit Loads

By using the summation and integration procedures outlined in the previous sections, it is possible to generate a single, long-term probability distribution of each type of load or stress such as the familiar curves illustrated in Figure 5.4.3-1.

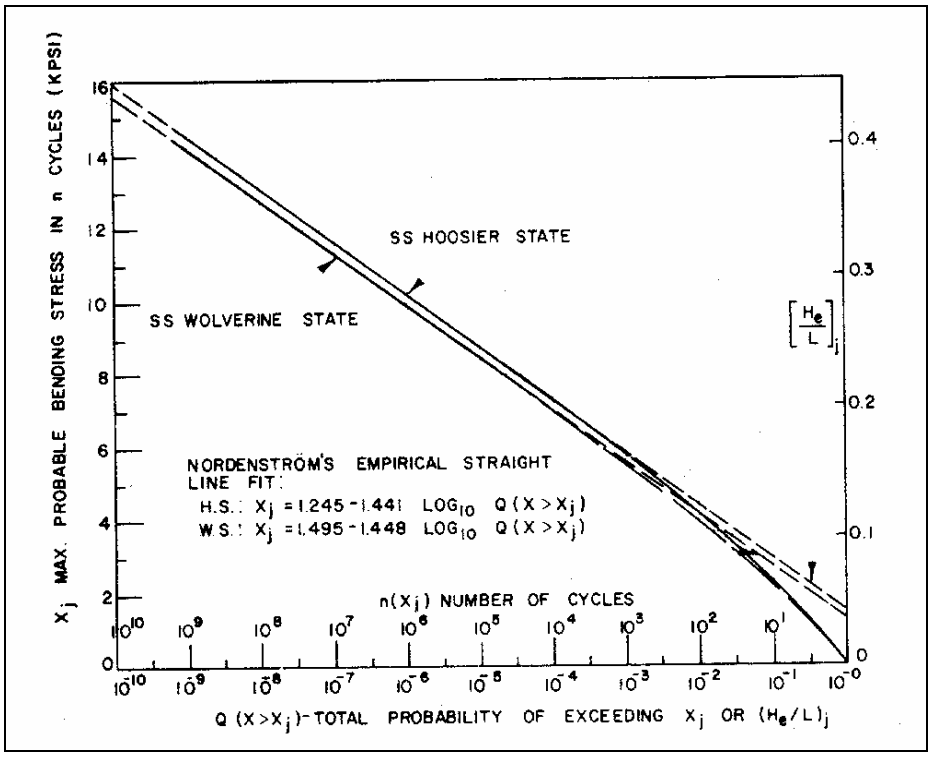

Figure 5.4.3-1. Comparison of Long-Term Probability Curves for Actual Weather, S.S. WOLVERINE STATE and S.S. HOOSIER STATE [9]

The abscissa is a logarithmic scale that may represent probability of exceedance in each stress cycle, or number of cycles per return period, which may be readily converted to ship life in years. The left-hand end of this curve is relevant to rarely occurring limit loads and the right-hand end to multiple-cycle fatigue loads.

The design limit load may be read off this curve at one, ten and one-hundred ship lives. It is simple to show that by selecting one-hundred ship lives as the return period, then each ship has a one-percent chance of exceeding this design load during its operational life. Fortunately, the increase in stress level between one, ten or one-hundred lives is, normally, not very large so that a conservative choice may be made without too great a penalty. The sensitivity of a typical design SES bending moment to some of the principal parameters involved is shown in Figures 5.4.3-2, 5.4.3-3 and 5.4.3-4. In Figure 5.4.3-2, the effect of operational life is seen to be rather small compared with the effect of the Weibull parameter c. Figure 5.4.3-3 shows the effect of limiting the maximum sea state, and Figure 5.4.3-4 shows, for this multihull, the slight alleviation that can be achieved by allowing a deviation in heading in severe sea states. In all cases, the Weibull parameter, c, is seen to dominate the result so that considerable care should be devoted to its proper evaluation.

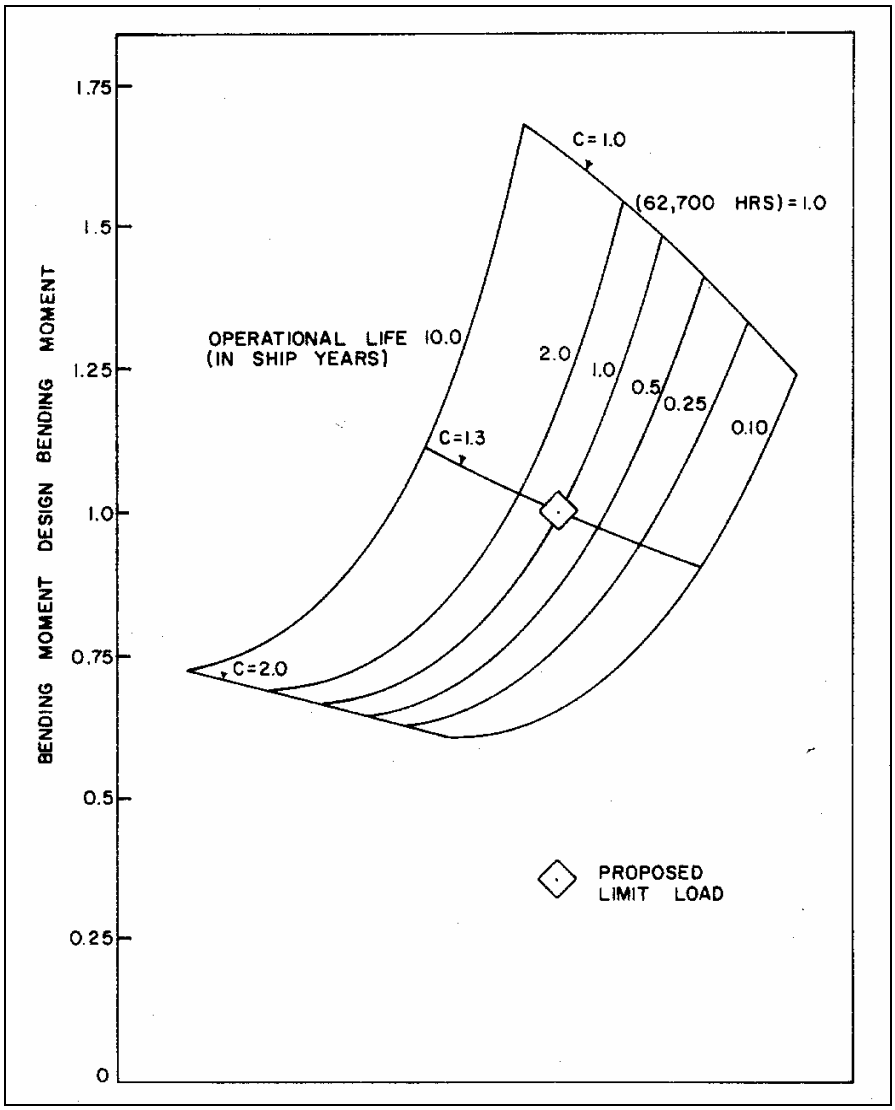

Figure 5.4.3-2. Sensitivity of On-Cushion Design Bending Moment to Selected Return Period and Weibull Parameter c

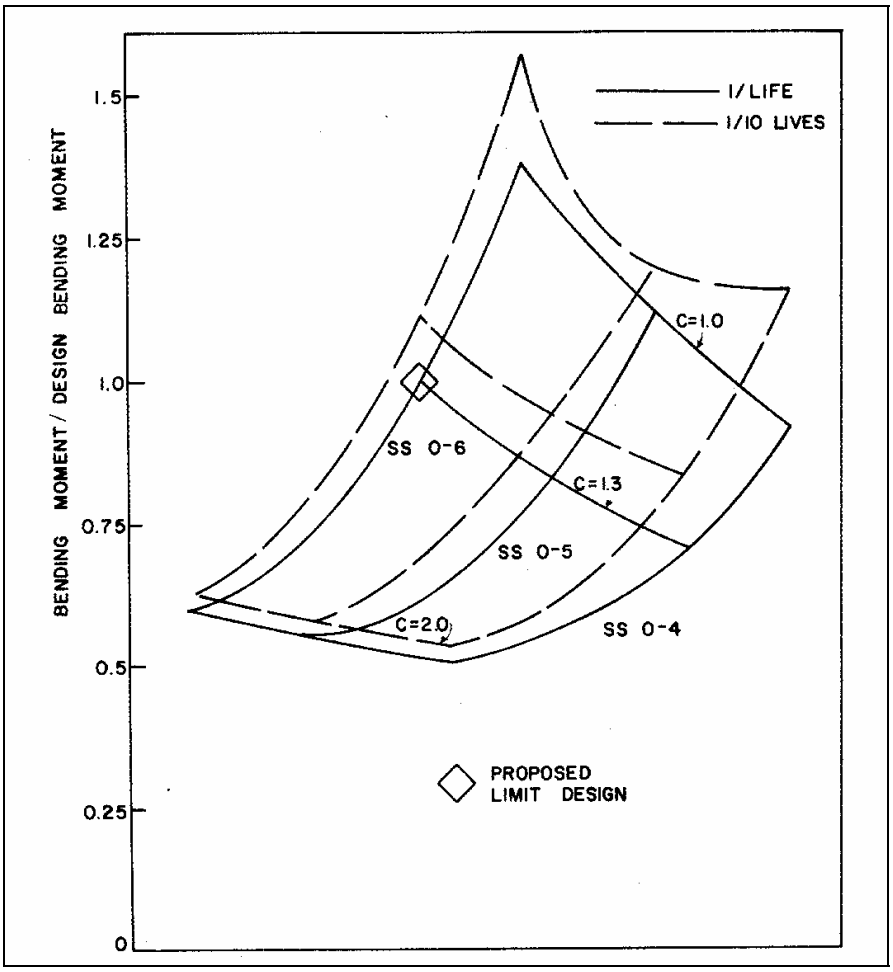

Figure 5.4.3-3. Sensitivity of Design Bending Moment to Limit On-Cushion Sea State and Weibull Parameter c

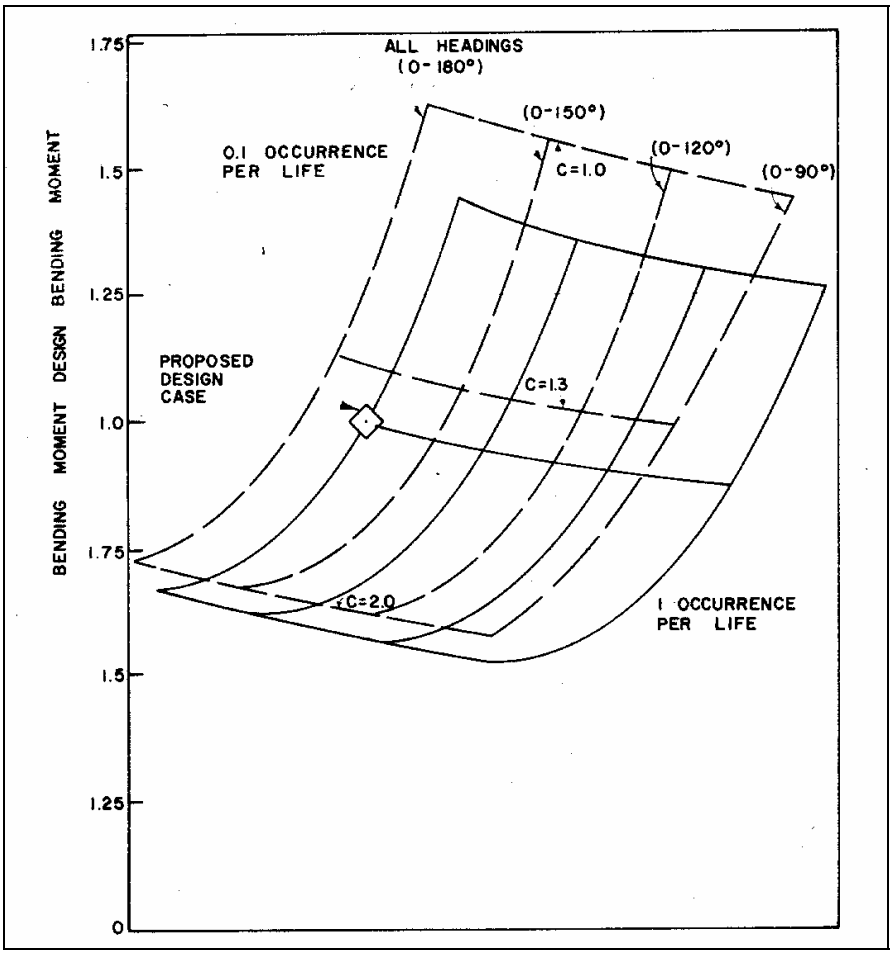

Figure 5.4.3-4. Sensitivity of Design Bending Moment to Range of Heading Angle and Weibull Parameter c

5.4.4 Structural Fatigue

Cyclic fatigue loads will occur in a number of situations and in a number of different elements of the structure. The principal causes of repetitive cyclic loading are the following:

- Still-water bending loads varying once per voyage, or per refueling cycle due to changes in payload, stores, fuel load or ballast.
- Diurnal thermal stresses due to changes of air temperature from day to night and from sunlight to shade.
- Occasional severe slamming loads which may occur every few minutes under storm conditions.
- Wave bending loads which will occur at wave encounter frequency.
- Vibrational loads caused by structural response to slamming (“whipping”), wave-induced loads (“springing”) or by machinery-induced vibration.
- Flow-induced vibration due to turbulence or cavitation of immersed appendages.

A single slam may result in a large number of stress reversals due to the whipping response of the structure. While little data is available for high performance ships, a great deal of data exists for

conventional ships. Figure 5.4.4-1 is an example of this. The bending stress at the midship section in this example takes more than sixty cycles and twenty seconds to decay to one-quarter of the maximum value measured at the slam. These stress reversals can be of considerable importance when considering fatigue and cyclic loading.

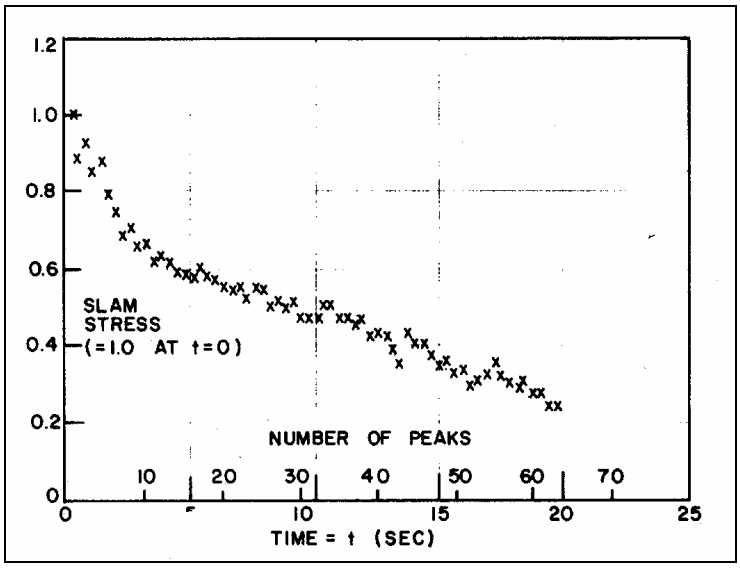

Figure 5.4.4-1. A Typical Decay Curve of Whipping Stress

The machinery vibrations are often difficult to predict during the design stage and will be best treated by making adequate provisions for shock mounting and insulation. Flow-induced vibrations should be avoided as much as possible by careful hydrodynamic design.

The most critical of the cyclic loads are probably the wave-induced loads, as they occur with far greater frequency than the basically diurnal thermal effects or the load change cycles.

An illustration of the relative magnitudes and frequencies of the various types of loads acting on a conventional ship is shown in Figure 5.2-1. The stress record in this figure covers an entire voyage of a large tanker. Three types of load variation are apparent:

1. The vertical lines represent the wave bending stresses which were sampled for a comparatively short time every four hours. The higher frequency wave bending and vibrational loads cannot be properly represented on this scale. The ship evidently encountered a severe storm soon after leaving Perth Amboy.

2. Large changes are apparent in the mean stress level due to changes in ballast.

3. Superimposed on the mean time variation throughout the voyage are the daily variations due to temperature changes from day to night. These temperature effects are most apparent after passing around the Cape of Good Hope when the wave loads are very small. In the North Atlantic, when the wave loads are largest, the temperature effects are rather small.

An indication of the variation of severity of load with frequency of occurrence is shown in Figure 5.4.4-2. The example shown is for a conventional ship. Each dot on the figure represents the root mean square of a sample of the hull bending stress on the S.S. HOOSIER STATE, taken every four hours during fourteen voyages. A large concentration of values are recorded at lower stresses and a very few at high stresses. By an extrapolation technique explained in Reference 9, it was possible to predict stress occurrences over a much longer time span. This result is shown in Figure 5.4.3-1, which plots the maximum stress

against its probability of occurrence. Similar data for high performance ship impact loads can be computed analytically using the type of impact program described earlier. Figure 5.4.4-3 shows a result typical of such analyses. The right-hand end of the curve of loads occurring every few seconds provides data for fatigue analysis, while the loads occurring at the left-hand end of the curve provide data for rarely occurring maximum loads.

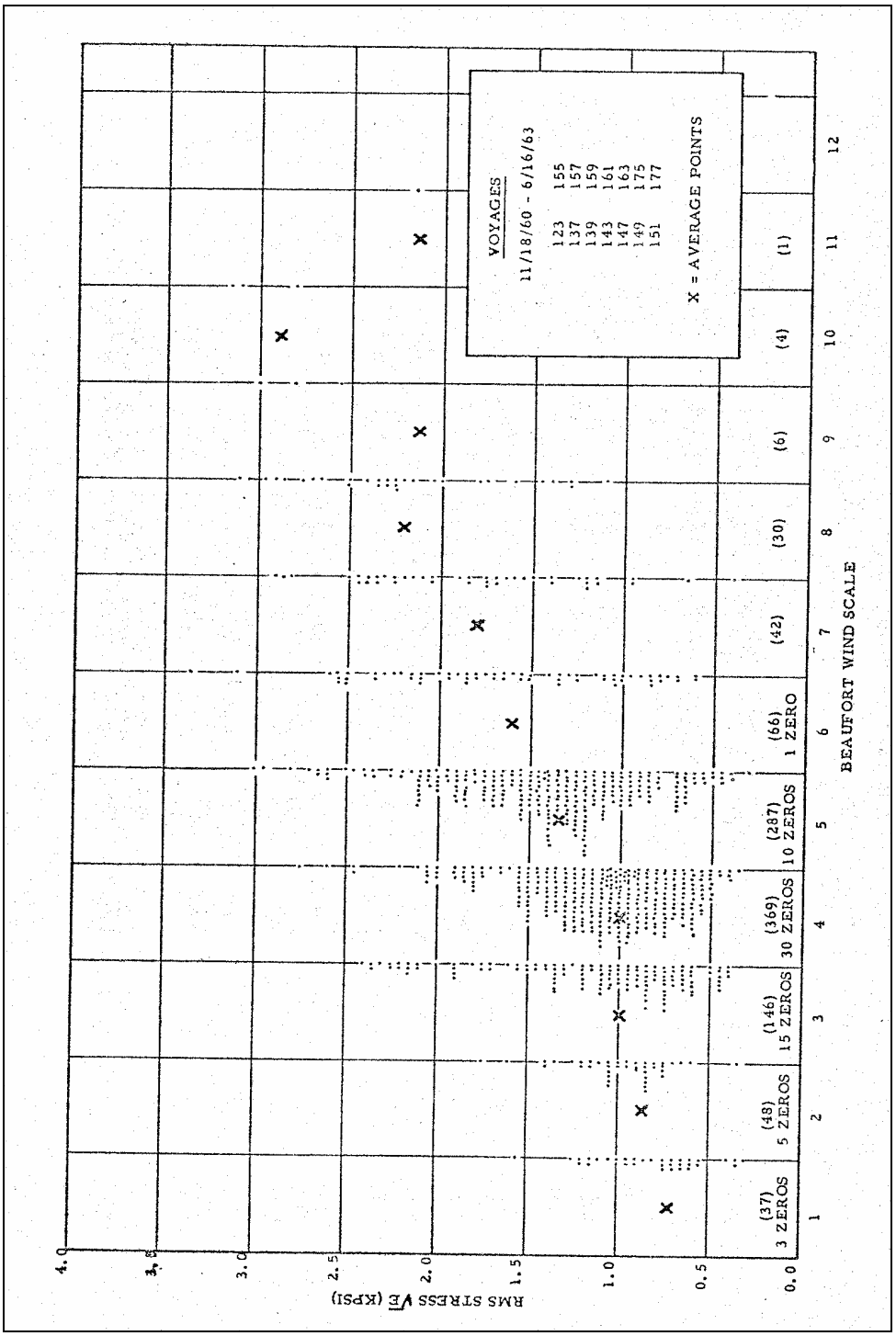

Figure 5.4.4-2. RMS Stress vs. Sea State, S.S. HOOSIER STATE (Port, Coastwise and Channel Data Excluded)

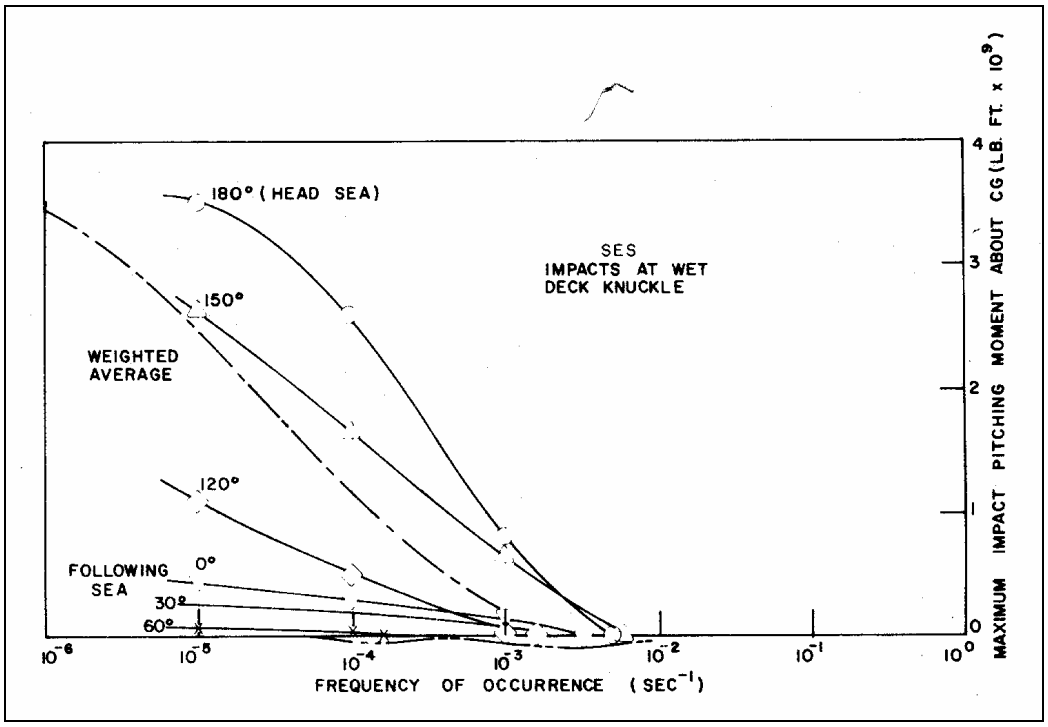

Figure 5.4.4-3. Frequencies of Occurrence of Pitching Moments During Impact

The problem of achieving a proper design providing full protection against damage from the type of cyclic loading to which ships are exposed is a very serious one to which a great deal of attention is being paid, but no adequate analytical treatments are yet available.

The following approach should be adopted until sufficient stress data is available from some of the experimental high performance ships:

a) Calculate the long-term probability distribution of stresses in critical components (main hull, girders, plating in impact areas, etc.) due to wave bending, slamming and thermal stresses. A series of curves similar to those in Figure 5.4.3-1 will then be obtained. When plotted against number of cycles, the long-term probability curve is usually referred to as the cyclic loading spectrum.

b) Experience with conventional ships suggests that the cyclic loading spectrum due to wave bending is slightly more severe than that due to whipping as described above. Figure 5.4.4-4 compares these two spectra for the case of the WOLVERINE STATE. The two spectra are nearly enough equal to suggest that the dynamic spectra may prove to be critical in a high performance vessel, but until such information is available, it is proposed to assume that the dynamic effects are not more severe from considerations of cyclic loading than the wave bending effects, which are more readily predictable.

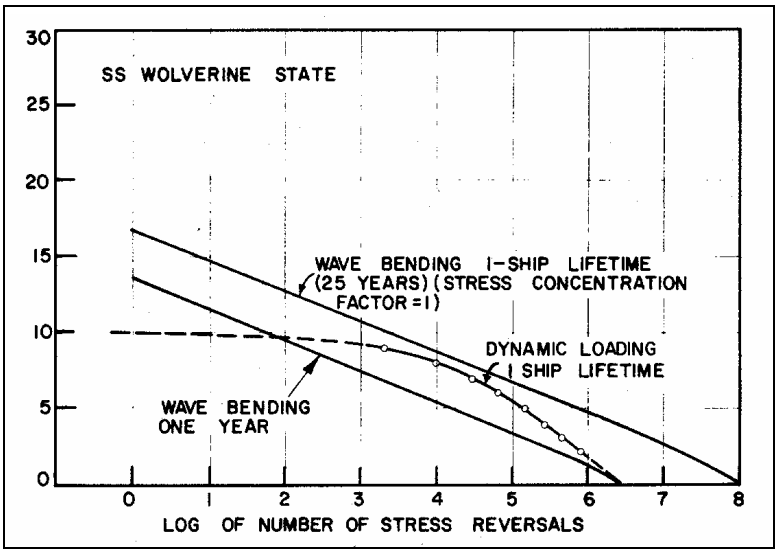

Figure 5.4.4-4. Cyclic Loading "Spectra", S.S. WOLVERINE STATE

Results of ACV and SES model tank tests reveal that in regular waves, a great deal of response is generated at frequencies other than the wave encounter frequency as a result of their inherently nonlinear response characteristics. The higher frequency components of these responses may well be significant for considerations of fatigue. The relative importance of the various harmonic components are sketched in Figure 5.4.4-5. Typical second harmonics can have an amplitude of more than one-half of the fundamental and will occur twice as frequently, so that the long-term probability curve is displaced to the right by a factor of two on Figure 5.4.4-5. Similarly, the third harmonic curve is displaced to the right by a factor of 3. By inspection of Figure 5.4.4-5, however, and by comparison with typical fatigue strength characteristics as sketched in Figure 5.4.4-6, it does not appear that the harmonic components of the wave-induced bending loads can have a critical effect. The dominant characteristic of the wave-induced bending appears to be the maximum and minimum value which, therefore, simplifies calculation procedures.

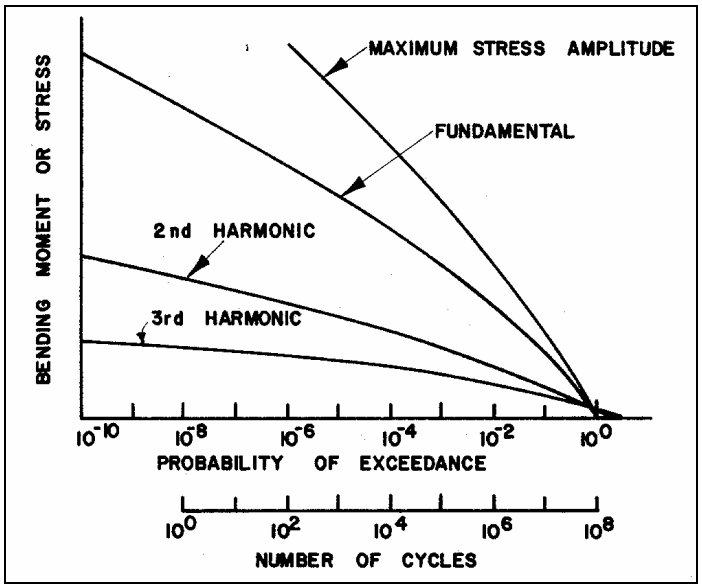

Figure 5.4.4-5. Cyclic Loading Spectra for Typical SES Model Showing Harmonic Components of Total Stress

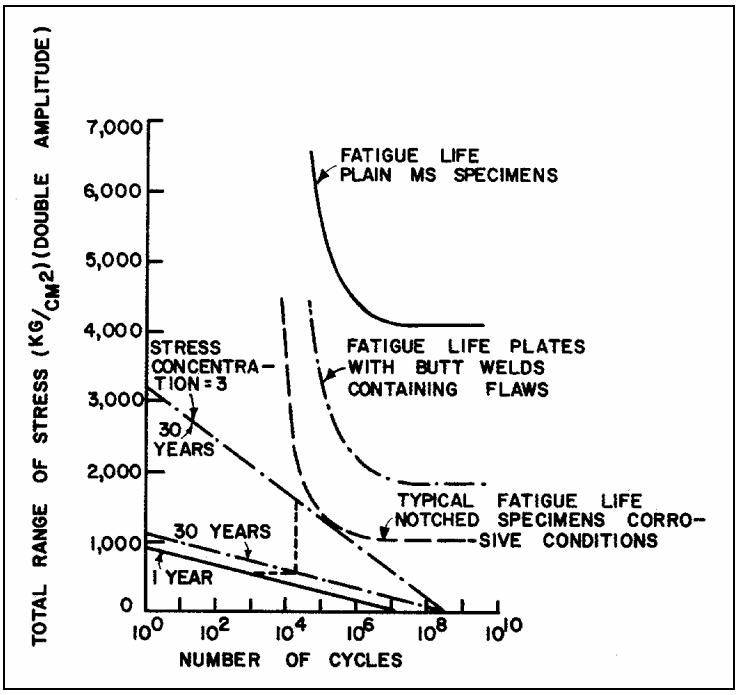

Figure 5.4.4-6. Example of Application of Cyclic Loading Curves to Study of Fatigue

Thus, a methodology has been described for extrapolating from analytical, model test or full-scale test, data to determine rational design loads and moments. It is further contended that:

i) Based on a small number of comparable cases, the rms values of frequency-domain analysis and tank test experiments have rather satisfactory agreement. It is, therefore, assumed that it is equally valid to determine rms values from frequency-domain modeling or model tank data. The frequency-domain model (such as SHIPMO) is clearly very much more economical to run.

ii) The frequency-domain analytical model cannot take into account load combinations. These can, however, be modeled satisfactorily in the tow tank or analytically as proposed in our Phase II program of work.

Thus the precise nature of the loadings, pressure distributions, time durations, etc. can be determined as described in this section by using procedures such as the proposed (Phase II) impact program to match design load cases selected from the long-term probability analyses.

In the absence of the effect of slamming, to be determined from the Phase II effort, the design loads for an example vessel can be determined as shown in the next section. Since the complete load prediction process has not yet been established, what follows is a limited application of what is to be developed in Phase II.

5.5 East Coast AutoFerry (Example)

For this example exercise, the operational characteristics of a proposed AutoFerry service were chosen to represent a vessel that can operate successfully in competition with existing modes of transportation. A preliminary estimate of the transport capabilities of the proposed service, such as speed, range and payload capacity, was developed based on the capabilities of the AutoTrain (provided in Appendix F). The speed requirement of the AutoFerry was based on the transit time of the AutoTrain between Sanford and Lorton. This required that the ferry cover the 800 NM distance between Port Canaveral and Norfolk

at an average speed of 40 knots to be comparable with the AutoTrain. The AutoTrain's maximum payload capacity of 200 cars and 450 passengers was used as the payload capacity for the proposed service. The proposed service is designed to operate 7 days a week for 10 months of the year with a load factor of 75% for both cars and passengers. A ferry route from Port Canaveral to Norfolk to New York City was deemed ideal in that service would be provided beyond that offered by the AutoTrain.

Catamaran AutoFerry

PASS™ was used to develop the design space and determine an optimal design for a catamaran AutoFerry. There are several catamarans in operation with load-carrying capabilities similar to those described in Table 5.5-1, and the principal characteristics of these vessels were used as a guide to assess available design space for the AutoFerry. However, it must be stated that most of the fast catamarans in service do not possess ranges in excess of 500 NM, and a majority of the catamarans operate in coastal ferry routes and kind sea conditions. For the AutoFerry, craft length was varied from 225 ft to a maximum of 350 ft, with demihull length-to-beam ratios varying from 15 to 20. The selection of a design point for the AutoFerry is made by determining a choice of principal parameters that provides for efficient mission performance, i.e., load, carry and unload 200 cars for the lowest cost while providing the requisite operational speed and passenger comfort. The variation of the total installed propulsion power with waterline length and demihull length-to-beam ratio was plotted to identify regions of low installed power (and, hence, lower operational cost), as seen in Figure 5.5-1. Also indicated on the surface are lines of constant draft (T) and a design point indicating minimum power.

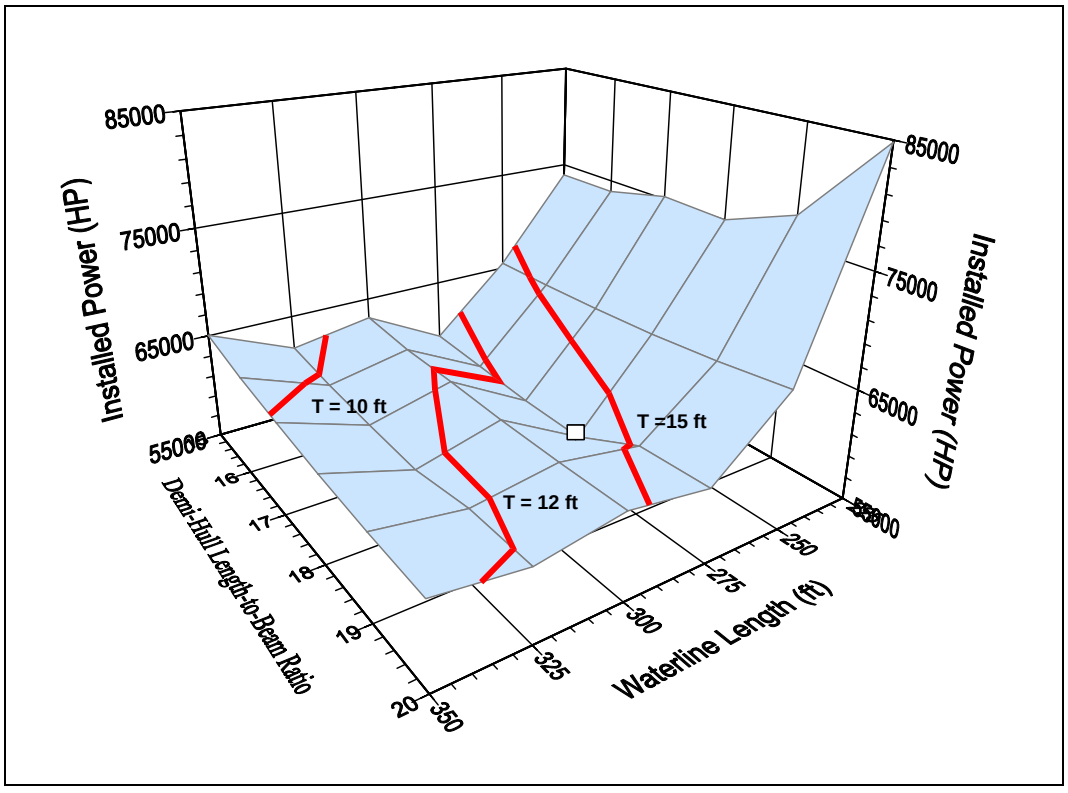

Figure 5.5-1. Variation of Propulsion Power as a Function of Waterline Length and Demihull Length-to-Beam Ratio

Table 5.5-1 identifies the principal parameters for the chosen design for the catamaran AutoFerry. The AutoFerry is capable of carrying 200 cars on two decks with 7 car lanes on each deck. The two decks are accessible through a single stern ramp at the lower level for loading. Ramps on the outer lanes at the forward end of the craft connect the two decks for convenience in drive-through loading.

Table 5.5-1

Catamaran AutoFerry Principal Characteristics

Length Overall (ft)	291.60
Waterline Length (ft)	270.0
Beam Overall (ft)	72.13
Draft (ft)	13.74
Depth (ft)	33.60
Full-Load Displacement (LT)	1666
Passengers/Cars	450/200
Prime Movers (Gas Turbines)	4 @ 14,563
Propulsors (Waterjets)	4.30 ft

5.6 Route & Environmental Description

Typically, the environmental description of the route is presented in terms of significant wave properties over the route, typically divided into sections, where environmental data is available from historical measurements or compiled weather almanacs. Along the Atlantic seaboard, the Gulf Stream current dominates the wave climate. The magnitude and meander of the Gulf Stream are presented graphically in Figure 5.6-1 using both current vectors and sea surface temperature plots. As seen in Figure 5.6-1, the current speeds can be on the order of 2 m/s (1 knot = 0.5144 m/s).

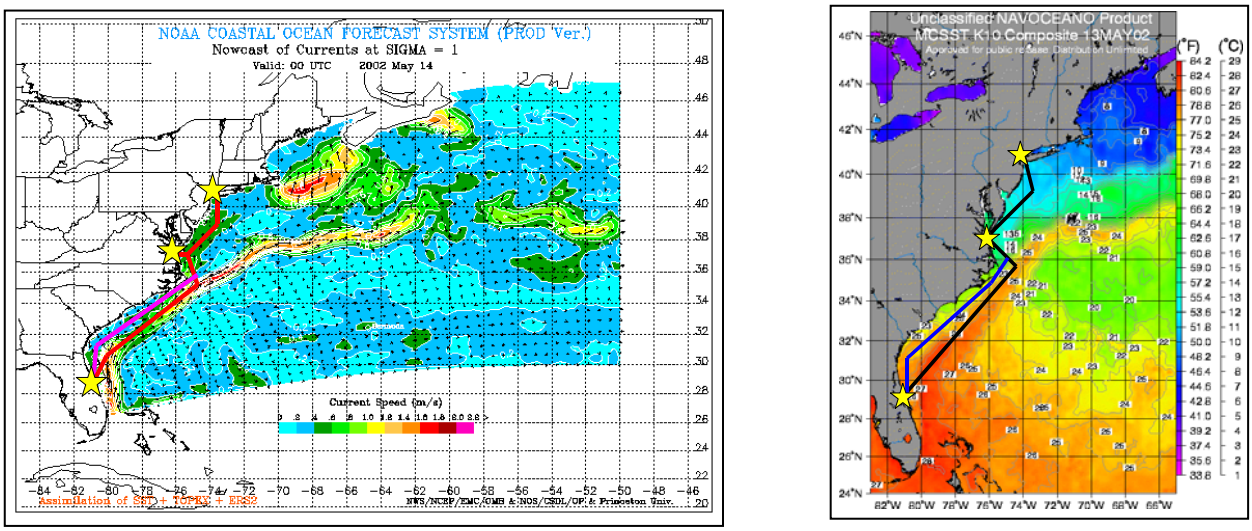

Figure 5.6-1. Magnitude and Extent of the Gulf Stream Current

The AutoFerry route between Port Canaveral, Norfolk and New York is depicted in Figure 5.6-2 for both the northbound and southbound segments. Overlaid on the route is the meander of the Gulf Stream, which significantly impacts the wave climate on the route. In Figure 5.6-2, markers representing buoys on the route are highlighted. Data from these buoys in terms of the statistical descriptions of wave heights and modal periods are presented in Appendix G and represent data collected for over 20 years.

Data from the buoys along the AutoFerry route have been summarized in Table 5.6-1. Included are data on both the average values of significant wave height and period, as well as the extreme measured values of the same.

The data from Table 5.6-1 have been used to develop a multi-segmented route for the AutoFerry. The route has been discretized into 15 voyage segments for both the northbound and southbound routes. Table 5.6-1 represents data for the northbound route and highlights the segment distance, vessel speed in the segment, the time spent in each segment as a fraction of the total voyage time, and identifies the buoy name for each segment.

The data shown in Tables 5.6-1 and 5.6-2 form the basis of the route description module that is being developed. When complete, the module will be capable of identifying the suitable data sources, extracting the requisite environmental data, and processing and delivering the data in suitable form for use in developing the input conditions for motions modeling.

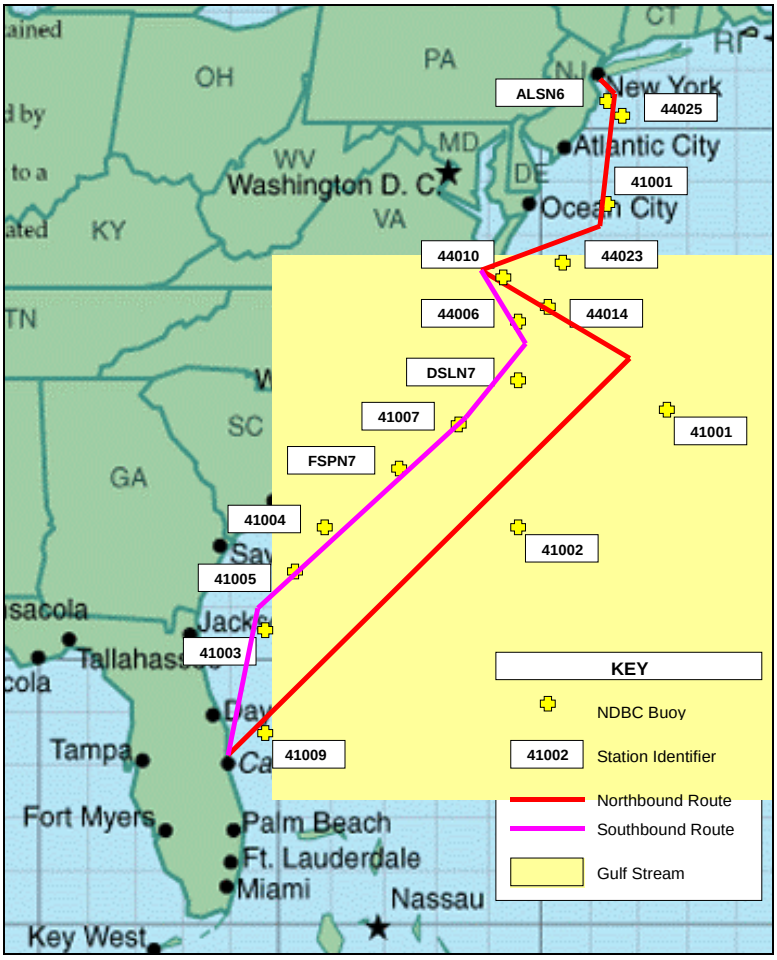

Figure 5.6-2. Atlantic AutoFerry Route and Locations of Wave Buoys

Table 5.6-1

Environmental Data Compilation for Atlantic Route AutoFerry (from TM 727-6)

ROUTE BASED ENVIRONMENTAL DATA FOR NOTIONAL EAST-COAST CATAMARAN PASSENGER / CAR FERRY "AUTOCAT"														
NBDC Buoy or C-MAN Station	Location			Sample Duration	Historical Significant Wave Height Data					Historical Dominant Wave Period Data				
	General Description	Latitude	Longitude		Avg Yearly	One Sigma		Extreme		Avg Yearly	One Sigma		Extreme	
						High	Low	Max	Min		High	Low	Max	Min
		(deg)	(deg)	(years)	(m)	(m)	(m)	(m)	(m)	(sec)	(sec)	(sec)	(sec)	(sec)
41009	CANAVERAL - 20M East of Cape Canaveral FL	28.50 N	80.18 W	5.25	1.2	1.7	0.6	6.2	0.2	8.3	10.0	6.5	20.0	2.5
41002	S. HATTERAS - 250M East of Charleston SC	32.27 N	75.42 W	18.50	1.9	2.7	1.0	16.0	0.0	8.1	10.0	6.1	20.0	2.5
41001	HATTERAS - 150M East of Cape Hatteras NC	34.68 N	72.23 W	17.50	2.0	3.0	1.0	10.4	0.0	8.0	9.9	6.1	20.0	3.0
44014	VIRGINIA BEACH - 64M East of Va Beach VA	36.58 N	74.84 W	3.17	1.4	2.1	0.7	8.2	0.5	7.8	9.9	5.6	20.0	2.5
44010	Chesapeake Bay Entrance	36.90 N	75.70 W	1.00	0.9	1.3	0.6	3.6	0.1	6.8	8.8	4.7	17.0	2.5
44023	100M NE of Va Beach VA	37.50 N	74.40 W	1.00	1.5	2.2	0.8	5.0	0.1	7.8	9.8	5.9	14.0	2.8
44001	100M NE of Ocean City MD	38.70 N	73.60 W	15.50	1.4	2.0	0.7	7.8	0.0	7.5	9.6	5.3	12.5	0.0
44025	LONG ISLAND - 33M South of Islip NY	40.25 N	73.17 W	2.67	1.2	1.9	0.5	9.3	0.0	7.0	9.2	4.7	20.0	0.0
ALSN6	Ambrose Light NY	40.46 N	73.83 W	4.00	0.9	1.4	0.5	7.4	0.0	7.7	10.6	4.9	20.0	0.0
44006	Northern Outer Banks - 60M SE of Va Beach VA	36.30 N	75.40 W	7.08	1.2	1.7	0.6	4.3	0.3	8.2	10.7	5.7	17.0	2.5
DSLN7	Diamond Shoals Light NC	35.15 N	75.30 W	5.08	1.5	2.2	0.8	10.8	0.3	7.8	9.8	5.9	20.0	2.8
41007	75M East of Wilmington NC	34.20 N	76.50 W	1.00	1.7	2.4	1.1	4.4	0.6	8.2	9.7	6.6	12.5	3.0
FPSN7	Frying Pan Shoals NC	33.49 N	77.59 W	1.00	1.6	2.3	0.9	4.8	0.4	7.8	9.8	5.8	14.0	2.8
41004	EDISTO - 41M SE of Charleston SC	32.50 N	79.10 W	13.58	1.3	1.9	0.7	6.6	0.2	7.2	9.1	5.3	16.5	2.3
41005	100M SE of Savannah GA	31.70 N	79.70 W	1.25	1.4	2.0	0.7	5.2	0.3	7.2	9.5	5.0	17.0	2.5
41003	80M East of Jacksonville FL	30.40 N	80.10 W	2.25	1.2	1.7	0.7	4.4	0.2	7.1	9.4	4.8	17.0	2.5

Table 5.6-2

Operational Profile for the Northbound Leg of the AutoFerry Route (from TM727-6)

OPERATIONAL PROFILE OF NOTIONAL EAST-COAST CATAMARN PASSENGER / CAR FERRY "AUTOCAT"									
	Voyage Segment	Description	Approx Segment Distance	Vessel Speed	Time on Segment	% Total Voyage Time	NBDC Buoy or C-MAN Station	Avg Significant Wave Height	Avg Dominant Wave Period
			(nm)	(knots)	(hours)			(m)	(sec)
NORTHBOUND LEG	1 N	Port Canaveral Terminal (Onload / Offload)	0.0	0.0	18.00	17.0	N/A	0.0	0.0
	2 N	Transit Port Canaveral Harbor	3.0	6.0	0.50	0.5	N/A	0.0	0.0
	3 N	Port Canveral to GS 110M NE of Daytona Beach	120.0	40.0	3.00	2.8	**41009**	1.2	8.3
	4 N	Daytona Beach to GS 180M SE of Wilmingrton NC	400.0	40.0	10.00	9.4	**41002**	1.9	8.1
	5 N	Wilmington to GS 100M East of Cape Hatteras	130.0	40.0	3.25	3.1	**41001**	2.0	8.0
	6 N	Cape Hatteras to Virginia Beach (50M Offshore)	100.0	40.0	2.50	2.4	**44014**	1.4	7.8
	7 N	Virginia Beach Offshore to Chesapeake Bay Entrance	50.0	40.0	1.25	1.2	**44010**	0.9	6.8
	8 N	Transit Norfolk Harbor	3.0	6.0	0.50	0.5	N/A	0.0	0.0
	9 N	Norfolk Terminal	0.0	0.0	6.00	5.7	N/A	0.0	0.0
	10 N	Transit Norfolk Harbor	3.0	6.0	0.50	0.5	N/A	0.0	0.0
	11 N	Chesapeake Bay Entrance to 50M NE Virginia Beach	50.0	40.0	1.25	1.2	**44010**	0.9	6.8
	12 N	NE Virginia Beach to 75M SE of Ocean City MD	90.0	40.0	2.25	2.1	**44023**	1.5	7.8
	13 N	Ocean City to 50M East of Atlantic City NJ	90.0	40.0	2.25	2.1	**44001**	1.4	7.5
	14 N	Atlantic City to Outer New York Harbor	90.0	40.0	2.25	2.1	**44025**	1.2	7.0
	15 N	Transit New York Harbor	3.0	6.0	0.50	0.5	**ALSN6**	0.9	7.7

5.7 Numerical Modeling of AutoFerry Motions & Loads Determination

The utilization of frequency-domain seakeeping prediction software allows the rapid generation of rational first-principles motions and wave-induced loads based on actual route-specific operational data. In addition, data can be gathered to support the development of wave impact loads and secondary hull-girder response loads, such as springing and whipping, by generating relative velocities at various discrete points on the multihull's demihulls and cross-structure. Relative velocities refer to the difference in vertical velocity between a specified point on the craft and the surface of the seaway, and are, therefore, a key component in the dynamic pressures acting on the vessel's structure. Typically, a slam occurs when the relative velocity exceeds 20 ft/sec.

Frequency-domain modeling results in motions and loads data that are represented as short-term single amplitude statistics based on a user-supplied wave energy spectrum. Thus, this approach is fundamentally linked to a robust analysis of the environmental conditions inherent to the proposed route. Short-term statistical descriptions of the frequency-domain data are then extrapolated into expected lifetime structural loads. Time-domain modeling will allow the investigation of specific non-linear response occurrences over a specified discrete time series and is considered a more rigorous and, thus, more accurate approach. However, the investment in computing power and time required for direct non-linear time-domain modeling is extensive. In Phase II of this project, we propose to utilize a Fast Fourier Transform (FFT) to transition from the frequency-domain to the time-domain. The FFT procedure will afford us the ability to develop a time series, and will significantly reduce the complexity and the required investment in time that time-domain modeling requires. However, the process will lack some of the accuracy of performing the motion calculations directly in the (non-linear) time-domain, as phase information is lost in the transition. The underlying assumption behind the proposed approach is that the accurate determination of phase will become statistically insignificant as the length of the sample duration (i.e. length of the time series) is increased to represent the lifetime loads on the notional AutoFerry.

5.7.1 Computer Model Development

The AutoFerry motions model was developed in SHIPMO, incorporating the lessons learned from the extensive program validation performed during this project. Hull dimensions, geometry, and general design data such as the SWBS weight breakdown, powering and subsystem design characteristics were generated based on the optimized PASS™ model for the notional AutoFerry. The remaining key element for the motions model taken from PASS™ is the longitudinal weight distribution, which is critical to the development of realistic environmentally-induced structural loads. PASS™ utilizes a simplified notional weight distribution that generally follows the buoyancy distribution of the underwater hullform, producing a situation in which the longitudinal centers of buoyancy and gravity are in alignment for a zero-trim operating condition, a reasonable assumption in craft of this type and application. PASS™ also performs all calculations at the full-load displacement or departure condition, which may or may not produce the limiting structural loads in a seaway.

The weight and buoyancy distribution developed for the notional AutoFerry is shown in Figure 5.7.1-1 in addition to the PASS™-generated still water (static) bending moment. To develop a realistic lightship weight distribution and allow the variation of individual load items to determine the limiting structural load condition, known loads can be extracted from the full-load data as shown in Figure 5.7.1-2. As the intent of this analysis is largely to illustrate procedure rather than perform a fully detailed design of the AutoFerry, only the full-load weight distribution has been investigated to date. In Phase II of this project, specific loads will be broken out and varied according to location along the notional route to produce realistic lifetime load statistics and determine the limiting load conditions for this particular application.

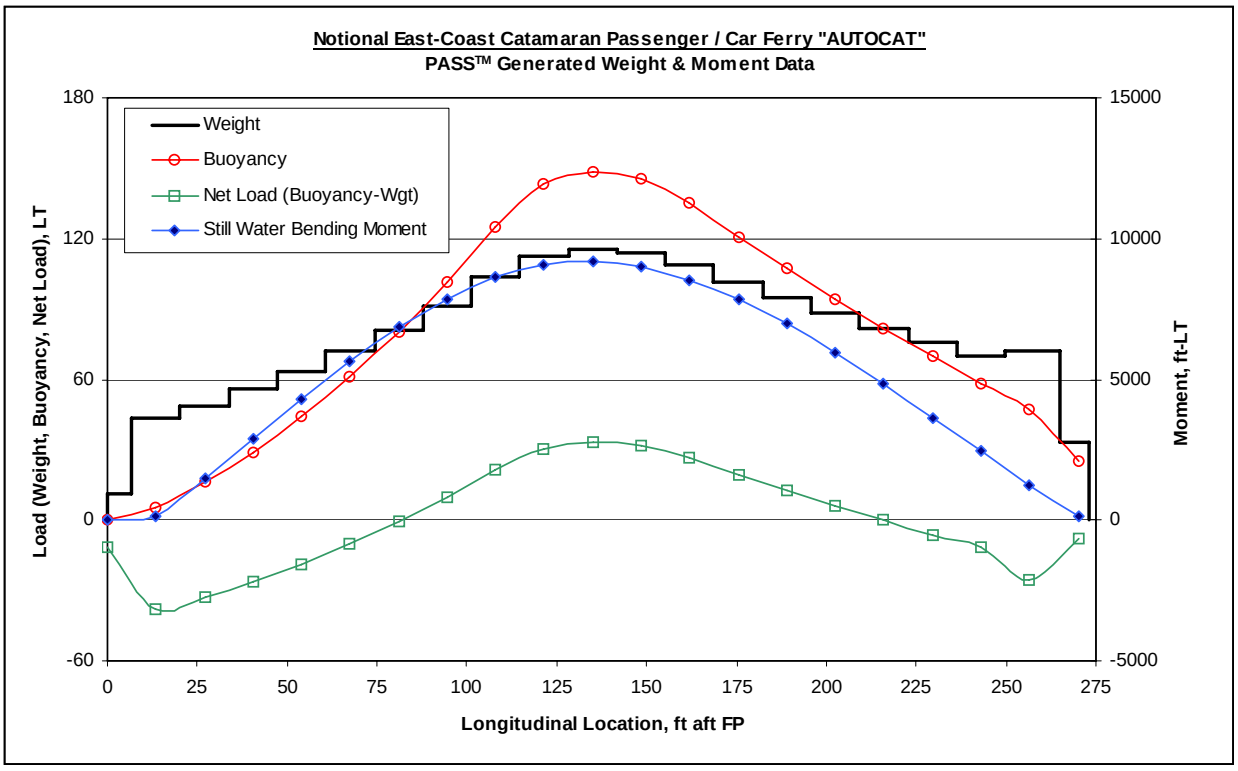

Figure 5.7.1-1. PASS™-Generated Weight, Buoyancy and Static Moment at Full-Load

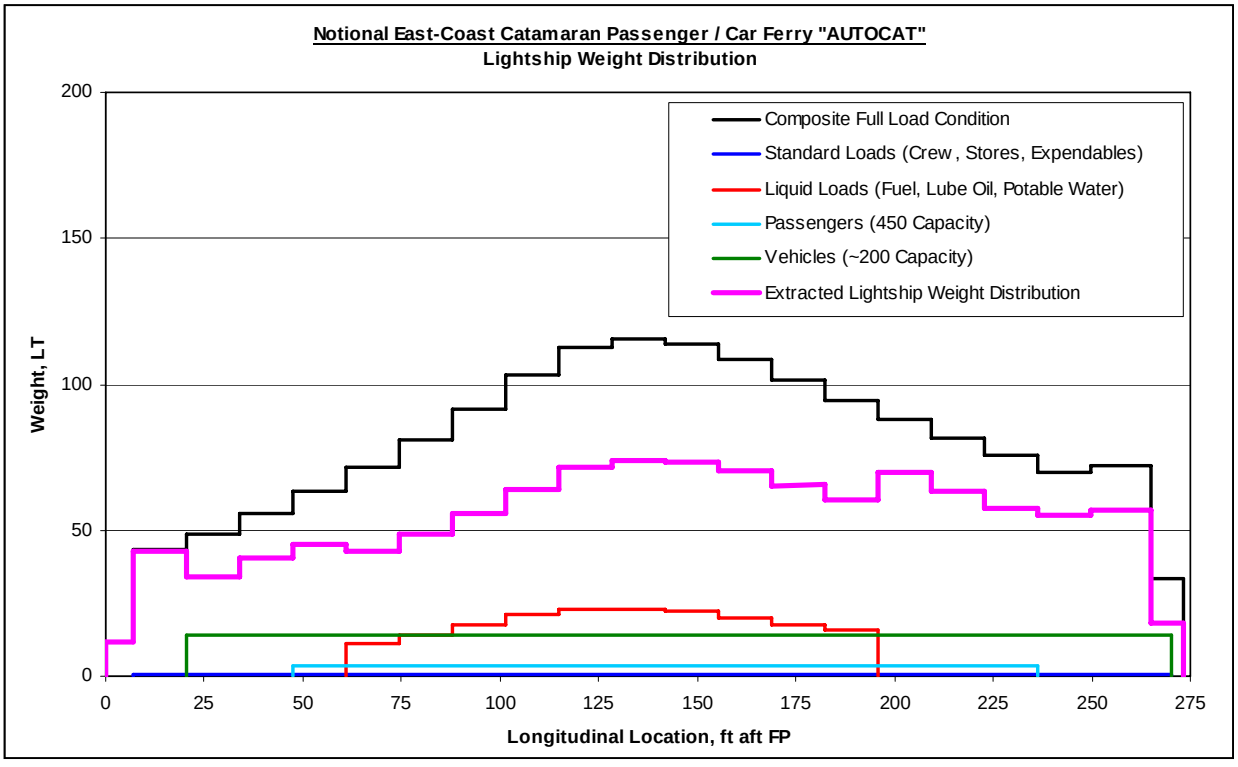

Figure 5.7.1-2. Extraction of Lightship Weight Distribution Based on Known Loads

Environmental Conditions

All motions modeling performed to date utilizing SHIPMO is based on an ITTC two-parameter wave spectrum (modified Bretschneider). Characteristics of the idealized spectrum are developed through a user-supplied significant wave height and modal period. This is the same basic data compiled in the historical database of NDBC buoys along the proposed AutoFerry route off the eastern coast of the United States.

All motions modeling has been performed for the buoys on the AutoFerry route that were deemed to be representative of limiting operational criteria. NDBC stations 41001 and 41002 off the coast of Cape Hatteras were thus chosen. These buoys are located in the vicinity where the cold water of the Labrador currents being swept down from the northern latitudes meet the warm waters of the Gulf Stream, producing relatively robust seaway conditions including larger waves, stronger winds, and a characteristic fog as compared to the more protected and benign seas along the remaining sections of the route. In addition to displaying very similar sea conditions, these buoys encompass a substantial portion of the total distance covered by the AutoFerry in typical operation (~530 miles or 25% of the total transit distance).

While Phase II of this project entails a more detailed statistical description of loads along the entire AutoFerry route, for the time being motions have been modeled for the mean (M) and mean-plus-one standard deviation (M+1σ) yearly significant wave height at the extreme buoys to provide a range of comparison against the parallel 'rulebook' designs. In considering the M+1σ wave height case (3m), approximately 84% of all wave encounters are expected to be less than or equal to the design values at these extreme buoys based on a normal distribution, as shown in Figure 5.7.1-3.

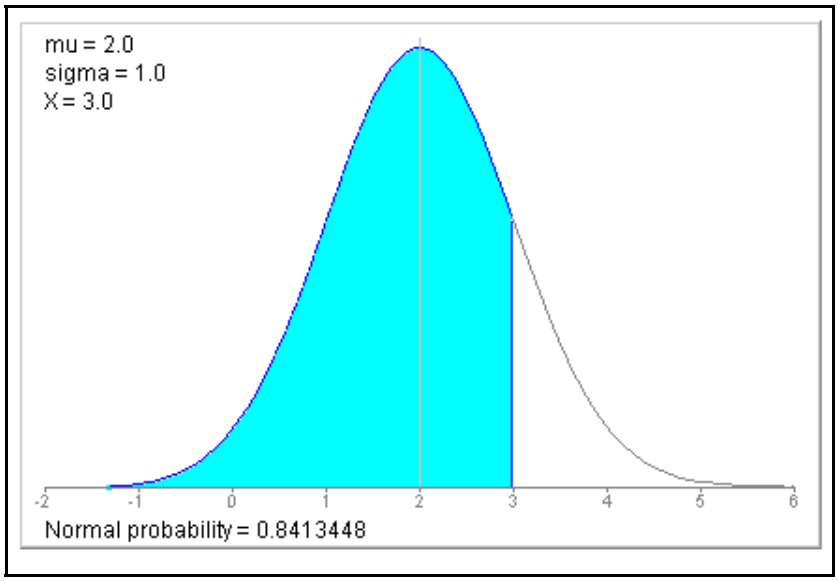

Figure 5.7.1-3. Characteristics of a Normal Distribution at Mean-Plus-One Standard Deviation

While, at first glance, covering 84% of expected occurrences may appear deficient, a simple compounding of probabilities demonstrates that utilization of the M+1σ wave actually represents a less than 0.5% total probability of exceedance over the lifetime of the AutoFerry. This is due to various factors, including the fact that 75% of the AutoFerry route is in sea conditions less severe than those at the limiting buoys, in addition to the fact that the design loads are developed at the worst vessel heading, while it is presumably fair at this point in the analysis to assume an equal probability of all headings. The calculation of a composite probability of occurrence is shown in Table 5.7.1-1. It should also be noted

that reported loads represent single significant amplitude statistics, or the average of only the highest 1/3 encounters.

Table 5.7.1-1

Calculation of Composite Probability of Exceedance for M+1σ Wave Height

0.159	Probability of Exceedence Based on Normal Distribution (1.000 - 0.841)
x 0.250	Route Based Probability (Percent of Operation At or Near Limiting Buoys)
x 0.125	Heading Probability (Assumes Equal Probability of All Headings at 45^{o} Increments)
0.00497	**Composite Probability of Exceedence of M+1σ Design Wave**

The low probability of exceedance at the M+1σ design wave provides a high level of confidence that the structural loads developed to design the vessel structure using first-principles and frequency-domain modeling are adequate, particularly following the addition of a reasonable safety margin. However, it must also be noted that it only requires a single severe exceedance of the design load to place the vessel in potential danger. This consideration is, again, where modeling non-linear motions and loads directly in the time-domain produces the most benefit, as specific response occurrences can be examined over a specified period of time in operation to identify the maximum loads.

Vessel motions and design loads have been compiled for both longcrested and shortcrested irregular seas. Longcrested seas imply that all waves propagate from the same direction, a relatively idealized assumption that allows the user to identify particular headings and encounter frequencies that may result in excessive motions and structural loads, generally in resonant conditions. The shortcrested seas case is far more representative of physical reality, as a directional spectrum is applied to the seaway, resulting in wave directions that are randomly varied around a single principal or dominant direction. Directionality is applied to the spectrum utilizing a cosine squared spreading function and is accepted procedure. The utilization of shortcrested seas tends to filter the resonant responses, as the likelihood of multiple resonant oscillations is low given the varying wave direction and irregular wave frequency associated with this assumption. Figure 5.7.1-4 (from Principles of Naval Architecture, Vol 3., Ed. E. Lewis) presents a surface contour map of a sample sea condition generated from stereo photos, demonstrating the high degree of irregularity and the lack of directionality in a typical seaway.

In this analysis, the longcrested sea data was generally utilized in an investigation of the resonance characteristics of the proposed AutoFerry. Resonance occurs when the forcing frequency of the encountered seaway matches the natural frequency of the hullform, a condition resulting in potentially large amplitude motions and thus loads. An investigation to identify particular headings at the design speed of 40 knots in which resonance was likely in heave, pitch or roll was performed. These headings could then be singled out for further analysis as the dominant wave direction in a more realistic shortcrested sea.

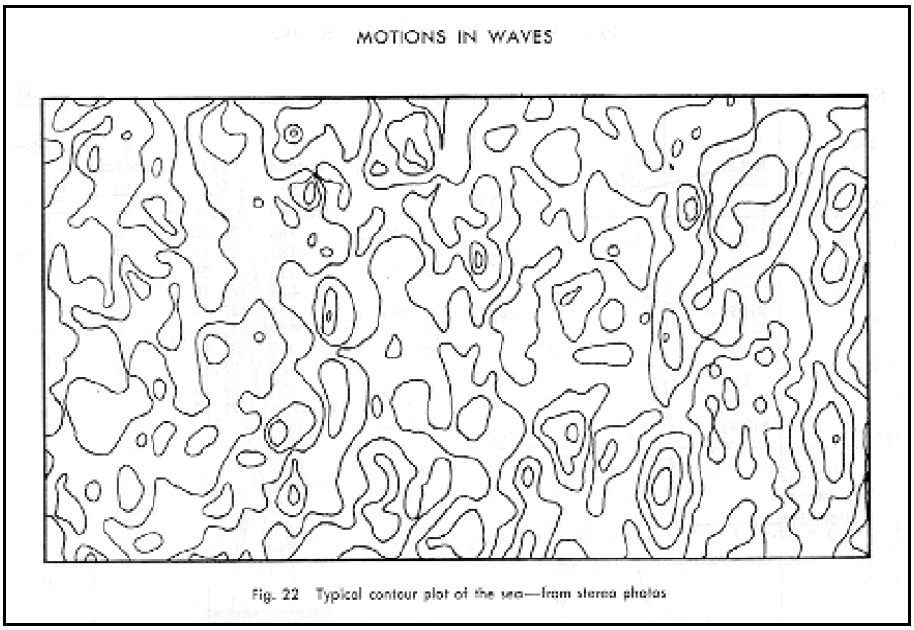

Figure 5.7.1-4. Contour Plot of a Seaway, Demonstrating the Typical Level of Irregularity (from Principles of Naval Architecture, Vol 3., Ed. E. Lewis)

The natural periods of the proposed AutoFerry were calculated using equations 1 through 3 below:

(1) Heave $$T_h = 2\pi\sqrt{\frac{T \times C_B\left(\frac{B}{3T}+1.2\right)}{g \times C_{WP}}}$$ (metric units)

(2) Pitch $$T_\theta = \frac{2\pi k_{YY}}{\sqrt{g \times GM_L}}$$

(3) Roll $$T_\phi = \frac{2\pi k_{XX}}{\sqrt{g \times GM_T}}$$

Natural periods computed utilizing these equations were converted to frequencies and subsequently plotted along with the encounter frequency (wave frequency corrected for forward vessel speed and direction) of the AutoFerry at design speed in headings covering the full range from head to following seas. Encounter frequencies were calculated for the dominant wave frequency at the limiting buoys on the proposed route in addition to the high and low ends of a one-standard-deviation range. This data is shown in Figure 5.7.1-5. Note that a negative encounter frequency simply implies that the forward speed of the vessel results in a situation where the AutoFerry is overtaking following waves (i.e. following seas at 40 knots).

The colored vertical bands overlaying Figure 5.7.1-5 indicate the headings in which the maximum load responses (in both the vertical and lateral planes) were calculated based on the idealized longcrested sea assumption. As expected, these extreme loads correspond with encounter frequencies in which resonant conditions are likely. As a result of this investigation, headings of 105 degrees (region of maximum lateral loads) and 150 degrees (region of maximum vertical loads) were singled out for analysis in more realistic shortcrested seas, along with a typical investigation of all headings at 45-degree intervals. As alluded to earlier in this section, the transition to shortcrested seas tends to filter these resonant responses, and the

response maxima shifted to more intuitive headings in which the limiting vertical loads occur in head and following seas and the maximum lateral loads occur in beam seas. All design loads currently in use for this analysis are based on data from simulations using a shortcrested sea.

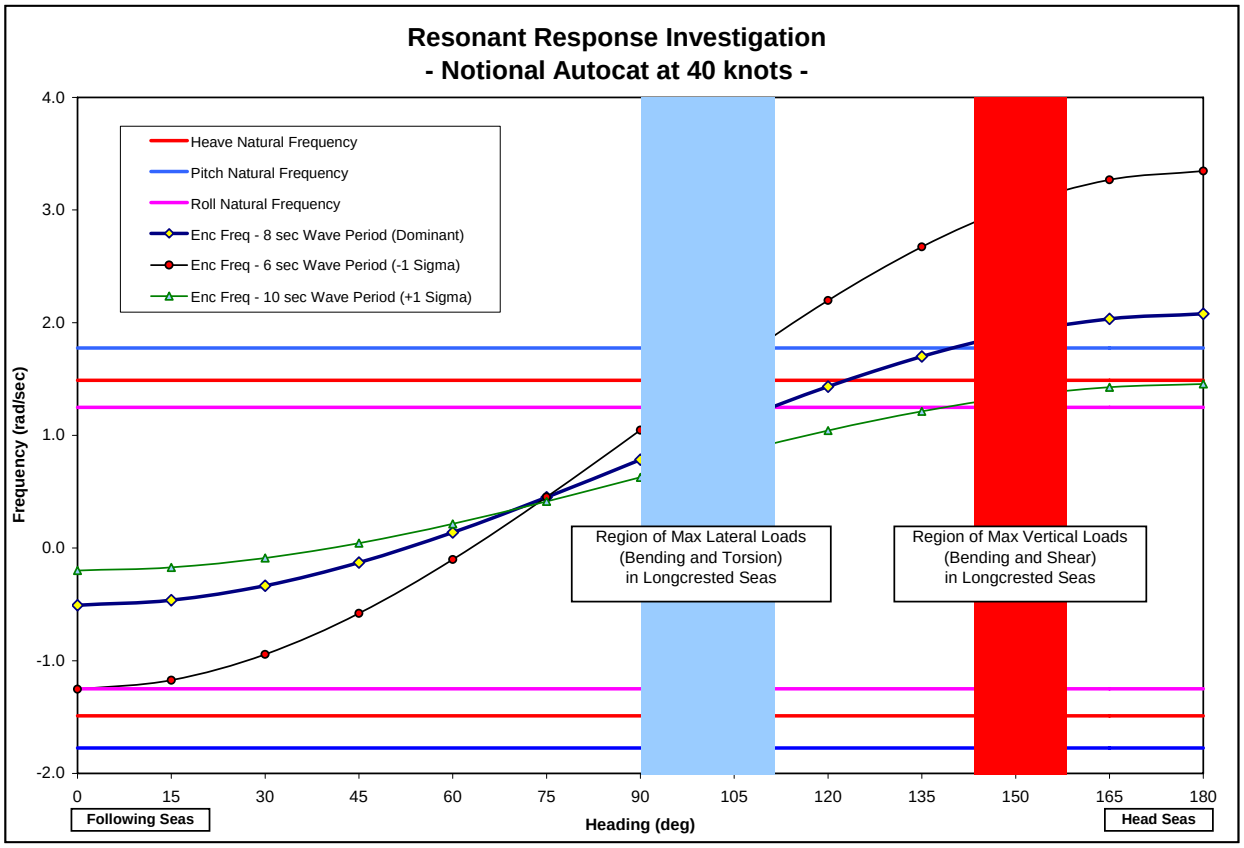

Figure 5.7.1-5. Identification of Resonant Conditions

Ideally, a designer always strives to design away from any chance of resonance in normal operation. However, in a vessel of this size operating at relatively high speed in an open-ocean environment, this is effectively impossible given the assumption of equal probability of all wave headings. In operation, resonant conditions can always be averted by minor changes in speed and heading as well.

Numerical Modeling of AutoFerry Motions

Since the primary intent of this analysis is the development of rational route-based structural loads, the vessel motions are integral to the generation of these loads. Vessel motions also play an integral role in the comfort and effectiveness of crew and passengers, the safety of cargo, and the longevity of onboard equipment. Applicable vessel motions and accelerations for the proposed AutoFerry are displayed as polar plots in Figures 5.7.1-6 and 5.7.1-7 for all headings at the design speed of 40 knots for the Mean and M+1σ design wave cases.

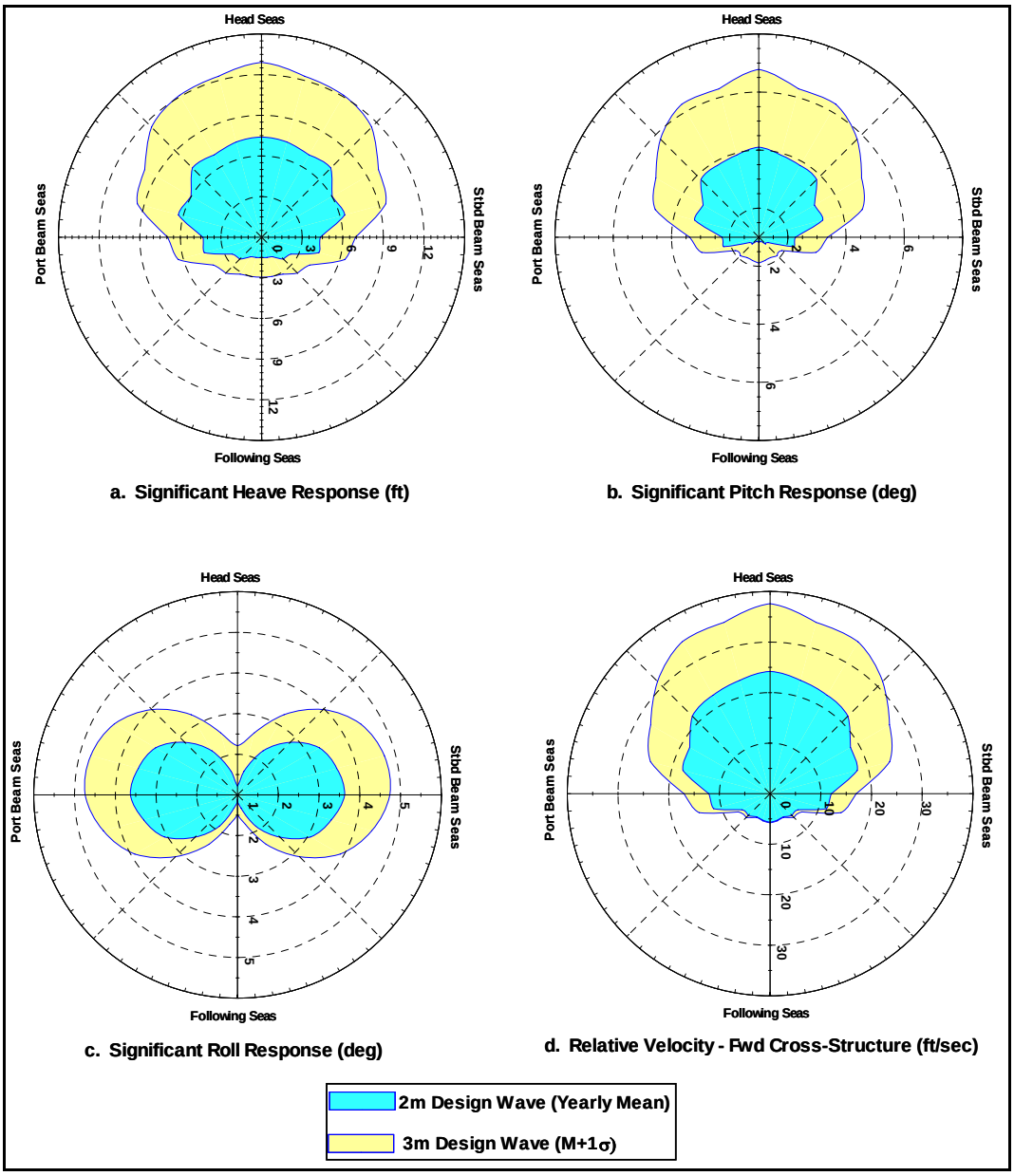

Figure 5.7.1-6. Significant Single Amplitude Motions Data for Notional AutoFerry at 40 knots

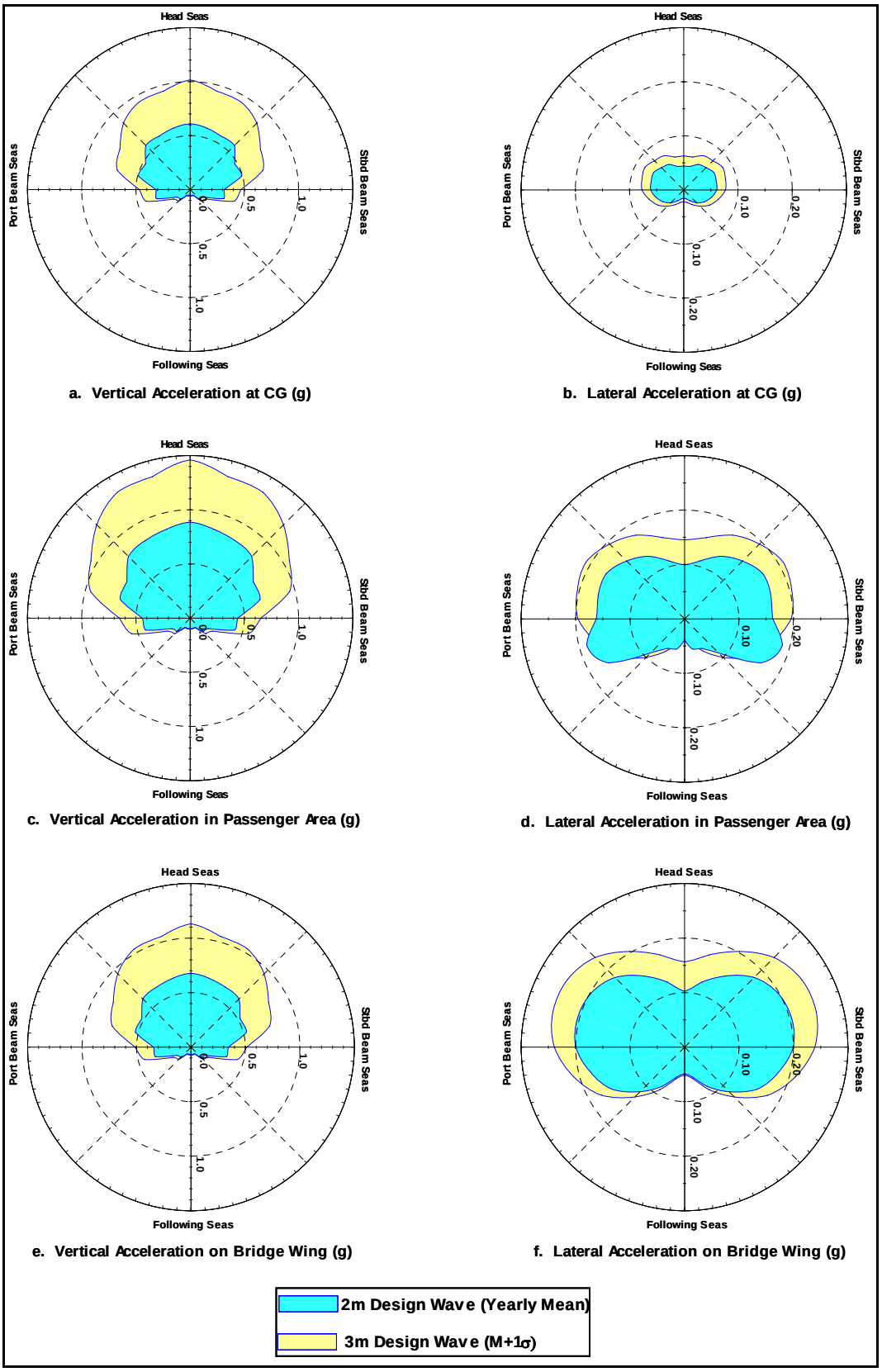

Figure 5.7.1-7. Single Significant Amplitude Accelerations Data for Notional AutoFerry at 40 knots

Several vital pieces of information can be extracted from the data contained in the AutoFerry polars. For instance, it is clearly evident that the extreme vessel motions and accelerations in the vertical plane (i.e. pitch, heave, and vertical acceleration) are developed in the head sea condition. However, the maximum wave-induced regular loads in the vertical plane occurred in the following sea case, in which vessel motions and accelerations are relatively benign, but the vessel is typically subjected to lower frequencies of encounter which drive up the global bending loads. This suggests that the development of the hull-girder response loads (whipping and springing) and the slam impact loads, slated for Phase II of this project, will be of utmost importance in determining not only the true magnitude of the total extreme loads on the vessel, but also the operational conditions (vessel headings) which produce these limiting loads. It must also be noted, however, that the Seakeeping Committee of the 16th ITTC (International Towing Tank Conference) has previously reported substantial disagreement between calculated results and experimental investigations of vertical wave loads in following waves utilizing strip theory, which is primarily applicable to higher frequency analysis. More investigation is required to assess the legitimacy of the calculated loads in following seas, as the body of model data for use in the validation effort is far less robust than in the case of head and bow quartering seas. In the case of the lateral plane, more uniformity is evident as the maximum vessel motions, accelerations, and loads occur consistently in beam sea conditions.

Another interesting observation that can be extracted from data contained in the AutoFerry polars is the generally large magnitude of the motions and accelerations in the vertical plane. Even in the case of the 2 m design wave, the vertical plane motions and accelerations are slightly in excess of what would be considered typical operational criteria, even for military applications. This would suggest that some form of ride-control system would be required for the AutoFerry, which could potentially take the form of a forward T-foil, active stabilizer fins, passive canards, or a combination of all three systems. It should be noted that most fast catamarans currently in operation worldwide employ some form of ride-control, even though operations are typically confined to seas much less extreme than those required by the proposed AutoFerry route. In the case of the 3 m design wave, vertical motions and accelerations are farther in excess of typical operational criteria. However, these predictions are not deemed unreasonable by any means for a relatively small vessel in mid sea-state 5 conditions at 40 knots. Operationally, some concession of speed or heading would certainly be required in these conditions. However, it remains important to develop the loads based on the worst-case vessel motions which may be experienced in the event of failure or loss of the ride-control systems employed.

Design Loads

Design loads for analyses completed to date have been compiled for both the average (mean) yearly significant wave height at the limiting buoys and the mean-plus-one standard deviation case (M+1σ) to provide a range of comparison against the 'rulebook' designs. The applicable design loads are shown in Table 5.7.1-2. The loads displayed represent both the significant single amplitude (average of the highest 1/3), as well as the average of the 1/10 highest responses at the worst heading. The complete set of compiled loads in longcrested and shortcrested seas at all headings, from which the design values were extracted, is shown in Tables 5.7.1-3 and 5.7.1-4.

Table 5.7.1-2

AutoFerry Design Loads at 40-knot Design Speed

STATIC LOAD		
Still-Water Bending Moment (Midship)	LT-ft	8564.29

WAVE-INDUCED LOADS		Mean Signf. Wave Height - 2m -		Mean + 1σ Signf. Wave Height - 3m -	
		Avg. 1/3	Avg. 1/10	Avg. 1/3	Avg. 1/10
Vertical Bending Moment (Midship)	LT-ft	10446.42	13319.19	31696.42	40412.94
Lateral Bending Moment (Midship)	LT-ft	5883.92	7502.00	7178.58	9152.58
Torsional Bending Moment (Midship)	LT-ft	1517.86	1935.27	1794.64	2288.17
Vertical Shear (Midship)	LT	56.16	71.60	83.22	106.11
Lateral Shear (Midship)	LT	31.70	40.42	37.32	47.58

Design Values Developed Assuming Shortcrested Irregular Seas (ITTC Two-Parameter Wave Spectrum).
Pertinent Parameters (Wave Height and Modal Period) Consistent With Historical Data for NDBC Buoys 41001 & 41002.

Table 5.7.1-3

Compiled Loads Data for Notional AutoFerry in 2m Seas

Still-Water Bending Moment (Midship) 8564.29 LT-ft

Significant Wave Height	2.0 m
Dominant Wave Period	8.0 sec
Average Wave Period	5.83 sec

Yearly Averages for NDBC Buoys 41001 & 41002

LONGCRESTED SEAS

- ITTC Two-Parameter Wave Spectrum (Longcrested) -
Short Term Statistics Based on Avg Yearly Wave Height & Period Data for Buoys 41001 & 41002

Heading (0 - Following Seas, 180 - Head Seas)	Vertical Bending Moment (LT-ft)				Lateral Bending Moment (LT-ft)				Torsion (LT-ft)				Vertical Shear (LT)				Lateral Shear (LT)			
(deg)	RMS	Avg	Signf	Avg 1/10	RMS	Avg	Signf	Avg 1/10	RMS	Avg	Signf	Avg 1/10	RMS	Avg	Signf	Avg 1/10	RMS	Avg	Signf	Avg 1/10
0	2178.57	2723.21	4357.14	5555.35	0.00	0.00	0.00	0.00	0.00	0.00	0.00	0.00	27.32	34.15	54.64	69.67	0.00	0.00	0.00	0.00
15	2290.18	2862.73	4580.36	5839.96	741.07	926.34	1482.14	1889.73	207.14	258.93	414.28	528.21	27.32	34.15	54.64	69.67	8.93	11.16	17.86	22.77
30	2066.96	2583.70	4133.92	5270.75	1508.93	1886.16	3017.86	3847.77	415.18	518.98	830.36	1058.71	26.43	33.04	52.86	67.40	16.29	20.36	32.58	41.54
45	2803.57	3504.46	5607.14	7149.10	2482.14	3102.68	4964.28	6329.46	566.96	708.70	1133.92	1445.75	27.23	34.04	54.46	69.44	18.48	23.10	36.96	47.12
60	4464.29	5580.36	8928.58	11383.94	2593.75	3242.19	5187.50	6614.06	633.93	792.41	1267.86	1616.52	29.78	37.23	59.56	75.94	16.12	20.15	32.24	41.11
75	2308.04	2885.05	4616.08	5885.50	1500.00	1875.00	3000.00	3825.00	347.76	434.70	695.52	886.79	35.67	44.59	71.34	90.96	15.00	18.75	30.00	38.25
90	843.75	1054.69	1687.50	2151.56	4410.71	5513.39	8821.42	11247.31	651.79	814.74	1303.58	1662.06	8.35	10.44	16.70	21.29	7.10	8.87	14.20	18.10
105	1258.93	1573.66	2517.86	3210.27	4120.54	5150.68	8241.08	10507.38	1258.93	1573.66	2517.86	3210.27	10.36	12.95	20.72	26.42	16.70	20.88	33.40	42.59
120	1754.46	2193.08	3508.92	4473.87	2584.82	3231.03	5169.64	6591.29	955.36	1194.20	1910.72	2436.17	13.30	16.63	26.60	33.92	13.79	17.24	27.58	35.16
135	2272.32	2840.40	4544.64	5794.42	1549.11	1936.39	3098.22	3950.23	750.00	937.50	1500.00	1912.50	16.96	21.20	33.92	43.25	11.88	14.85	23.76	30.29
150	5089.29	6361.61	10178.58	12977.69	901.78	1127.23	1803.56	2299.54	491.07	613.84	982.14	1252.23	38.13	47.66	76.26	97.23	14.38	17.98	28.76	36.67
165	3093.75	3867.19	6187.50	7889.06	504.46	630.58	1008.92	1286.37	233.93	292.41	467.86	596.52	25.09	31.36	50.18	63.98	5.80	7.25	11.60	14.79
180	2901.79	3627.24	5803.58	7399.56	0.00	0.00	0.00	0.00	0.00	0.00	0.00	0.00	23.04	28.80	46.08	58.75	0.00	0.00	0.00	0.00

SHORTCRESTED SEAS

- ITTC Two-Parameter Wave Spectrum (Shortcrested w/ $\cos^2$ Spreading Function) -
Short Term Statistics Based on Avg Yearly Wave Height & Period Data for Buoys 41001 & 41002 (Heading corresponds to Principal Wave Angle)

Principal Wave Direction (0 - Following Seas, 180 - Head Seas)	Vertical Bending Moment (LT-ft)				Lateral Bending Moment (LT-ft)				Torsion (LT-ft)				Vertical Shear (LT)				Lateral Shear (LT)			
(deg)	RMS	Avg	Signf	Avg 1/10	RMS	Avg	Signf	Avg 1/10	RMS	Avg	Signf	Avg 1/10	RMS	Avg	Signf	Avg 1/10	RMS	Avg	Signf	Avg 1/10
0	5223.21	6529.01	10446.42	13319.19	1544.64	1930.80	3089.28	3938.83	383.04	478.80	766.08	976.75	28.08	35.10	56.16	71.60	15.85	19.81	31.70	40.42
45	4089.29	5111.61	8178.58	10427.69	2241.07	2801.34	4482.14	5714.73	531.25	664.06	1062.50	1354.69	27.05	33.81	54.10	68.98	15.49	19.36	30.98	39.50
90	3616.07	4520.09	7232.14	9220.98	2941.96	3677.45	5883.92	7502.00	758.93	948.66	1517.86	1935.27	20.63	25.79	41.26	52.61	14.43	18.04	28.86	36.80
135	3008.93	3761.16	6017.86	7672.77	2406.25	3007.81	4812.50	6135.94	669.64	837.05	1339.28	1707.58	23.21	29.01	46.42	59.19	13.66	17.08	27.32	34.83
180	3348.21	4185.26	6696.42	8537.94	1276.79	1595.99	2553.58	3255.81	468.75	585.94	937.50	1195.31	25.89	32.36	51.78	66.02	10.09	12.61	20.18	25.73

Table 5.7.1-4

Compiled Loads Data for Notional AutoFerry in 3m Seas

Still-Water Bending Moment (Midship)	8564.29	LT-ft

Significant Wave Height	3.0 m	+1σ Data for NDBC Buoys 41001 & 41002
Dominant Wave Period	10.0 sec	
Average Wave Period		

LONGCRESTED SEAS

Heading	- ITTC Two-Parameter Wave Spectrum (Longcrested) - Short Term Statistics Based on Yearly +1σ Wave Height & Period Data for Buoys 41001 & 41002																			
0 - Following Seas 180 - Head Seas	Vertical Bending Moment (LT-ft)				Lateral Bending Moment (LT-ft)				Torsion (LT-ft)				Vertical Shear (LT)				Lateral Shear (LT)			
(deg)	RMS	Avg	Signf	Avg 1/10	RMS	Avg	Signf	Avg 1/10	RMS	Avg	Signf	Avg 1/10	RMS	Avg	Signf	Avg 1/10	RMS	Avg	Signf	Avg 1/10
0	3941.96	4927.45	7883.92	10052.00	0.00	0.00	0.00	0.00	0.00	0.00	0.00	0.00	37.81	47.26	75.62	96.42	0.00	0.00	0.00	0.00
15	6785.71	8482.14	13571.42	17303.56	1138.39	1422.99	2276.78	2902.89	254.91	318.64	509.82	650.02	37.41	46.76	74.82	95.40	11.12	13.90	22.24	28.36
30	5133.93	6417.41	10267.86	13091.52	2276.79	2845.99	4553.58	5805.81	500.00	625.00	1000.00	1275.00	37.81	47.26	75.62	96.42	20.13	25.16	40.26	51.33
45	5443.43	6804.29	10886.86	13880.75	3419.64	4274.55	6839.28	8720.08	678.57	848.21	1357.14	1730.35	37.19	46.49	74.38	94.83	23.21	29.01	46.42	59.19
60	5491.07	6863.84	10982.14	14002.23	3334.82	4168.53	6669.64	8503.79	745.54	931.93	1491.08	1901.13	34.96	43.70	69.92	89.15	19.73	24.66	39.46	50.31
75	2308.04	2885.05	4616.08	5885.50	1674.11	2092.64	3348.22	4268.98	415.18	518.98	830.36	1058.71	34.87	43.59	69.74	88.92	15.67	19.59	31.34	39.96
90	870.54	1088.18	1741.08	2219.88	4553.57	5691.96	9107.14	11611.60	696.43	870.54	1392.86	1775.90	8.66	10.83	17.32	22.08	7.23	9.04	14.46	18.44
105	1397.32	1746.65	2794.64	3563.17	5089.29	6361.61	10178.58	12977.69	1428.57	1785.71	2857.14	3642.85	11.61	14.51	23.22	29.61	17.32	21.65	34.64	44.17
120	2129.46	2661.83	4258.92	5430.12	3781.25	4726.56	7562.50	9642.19	1245.54	1556.93	2491.08	3176.13	16.43	20.54	32.86	41.90	16.34	20.43	32.68	41.67
135	2941.96	3677.45	5883.92	7502.00	2540.18	3175.23	5080.36	6477.46	1017.86	1272.33	2035.72	2595.54	21.70	27.13	43.40	55.34	14.82	18.53	29.64	37.79
150	8169.64	10212.05	16339.28	20832.59	1513.39	1891.74	3026.78	3859.14	669.64	837.05	1339.28	1707.58	60.71	75.89	121.42	154.81	21.43	26.79	42.86	54.65
165	4732.14	5915.18	9464.28	12066.96	852.68	1065.85	1705.36	2174.33	342.86	428.58	685.72	874.29	37.23	46.54	74.46	94.94	6.56	8.20	13.12	16.73
180	4343.75	5429.69	8687.50	11076.56	0.00	0.00	0.00	0.00	0.00	0.00	0.00	0.00	33.13	41.41	66.26	84.48	0.00	0.00	0.00	0.00

SHORTCRESTED SEAS

Principal Wave Direction	- ITTC Two-Parameter Wave Spectrum (Longcrested) - Short Term Statistics Based on Yearly +1σ Wave Height & Period Data for Buoys 41001 & 41002																			
0 - Following Seas 180 - Head Seas	Vertical Bending Moment (LT-ft)				Lateral Bending Moment (LT-ft)				Torsion (LT-ft)				Vertical Shear (LT)				Lateral Shear (LT)			
(deg)	RMS	Avg	Signf	Avg 1/10	RMS	Avg	Signf	Avg 1/10	RMS	Avg	Signf	Avg 1/10	RMS	Avg	Signf	Avg 1/10	RMS	Avg	Signf	Avg 1/10
0	15848.21	19810.26	31696.42	40412.94	2156.25	2695.31	4312.50	5498.44	459.82	574.78	919.64	1172.54	41.61	52.01	83.22	106.11	18.66	23.33	37.32	47.58
45	7544.64	9430.80	15089.28	19238.83	2816.96	3521.20	5633.92	7183.25	616.07	770.09	1232.14	1570.98	35.31	44.14	70.62	90.04	18.21	22.76	36.42	46.44
90	7901.79	9877.24	15803.58	20149.56	3589.29	4486.61	7178.58	9152.69	897.32	1121.65	1794.64	2288.17	27.99	34.99	55.98	71.37	16.65	20.81	33.30	42.46
105	4598.21	5747.76	9196.42	11725.44	3558.04	4447.55	7116.08	9073.00	897.32	1121.65	1794.64	2288.17	29.11	36.38	58.21	74.22	18.04	22.55	36.08	46.00
135	4250.00	5312.50	8500.00	10837.50	3062.50	3828.13	6125.00	7809.38	825.89	1032.36	1651.78	2106.02	32.28	40.35	64.56	82.31	16.61	20.76	33.22	42.36
150	4642.86	5803.58	9285.72	11839.29	2584.82	3231.03	5169.64	6591.29	763.39	954.24	1526.78	1946.64	35.58	44.48	71.16	90.73	13.71	17.14	27.42	34.96
180	5267.86	6584.83	10535.72	13433.04	1919.64	2399.55	3839.28	4895.08	629.46	786.83	1258.92	1605.12	38.84	48.55	77.68	99.04	13.21	16.51	26.42	33.69

5.8 Structural Design of AutoFerry

As a point of comparison to the rational structural design paradigm developed through this project, two rulebook structural designs were investigated for the catamaran AutoFerry. The American Bureau of Shipping (ABS) Guide for Building and Classing High-Speed Craft (HSC), issued February 1997, and Det Norske Veritas (DNV) Rules of Classification of High-Speed, Light Craft and Naval Surface Craft, issued January 2001, were employed. The AutoFerry structural design was assessed using the ABS guide, and a precursory look at the required plating thickness and global loads based on DNV was completed and is described.

5.8.1 First-Principles Structural Design of AutoFerry

The first-principles-based approach relies on the development of realistic design loads based on the intended route of the AutoFerry. Using a seakeeping model and buoy data along the route of the craft, the design loads were developed and are shown in Table 5.7.1-2. Based on this data and an allowable stress of 80% of the welded strength of aluminum, the section modulus requirements for the AutoFerry were determined and are shown in Table 5.8.1-1.

Table 5.8.1-1

Global Sectional Property Requirements

	2 m Wave Height		3 m Wave Height	
	Avg 1/3	**Avg 1/10**	**Avg 1/3**	**Avg 1/10**
Minimum Longitudinal Bending SM at Midship (ft^3)	19.15	22.04	40.55	49.33
Minimum Transverse Bending SM along CL (ft^3)	5.93	7.56	7.23	9.22
Minimum Transverse Torsional SM (ft^3)	1.53	1.95	1.81	2.30

5.8.2 Structural Design of AutoFerry Using ABS Rules

Following the general procedure outlined in Section 4.5.1, the first step in the structural design was to define the craft geometry. The definitions used for the AutoFerry are shown in Table 5.8.2-1.

Table 5.8.2-1

Craft Particulars as Defined by ABS

Rule Length, L (ft)	259.2
Breadth, B (ft)	30.86
Molded Depth, D (ft)	35.10
Draft, T (ft)	13.74
Displacement, (LT)	1,693
Design Speed, V (kts)	40
Deadrise @ LCG, $_{cg}$ (°)	15

The length defined in Table 5.8.2-1 is given as 96% of the length on the waterline, and the breadth is taken as the sum of the breadth of the individual hulls.

After the craft particulars were set, the design of the plating and internals comprising the bottom hull, side hull, wet deck (cross-structure), and cargo decks of the midship section were completed. A summary of the plate thickness required by ABS and the plate thickness chosen for each area of the craft cross-section is shown in Table 5.8.2-2. Note that the chosen thickness for each plate was dictated by nominal plate sizes that are commonly available. For the purpose of this study, it was assumed that plates of 1/16" thickness intervals were readily available.

Table 5.8.2-2

Midship Section Plating Requirements

Description	**Required Thickness (in)**	**Design Thickness (in)**
Bottom Hull	0.384	0.438
Lower Side Hull[1]	0.340	0.375
Upper Side Hull[2]	0.302	0.313
Wet Deck Cross-Structure	0.352	0.375
Main Deck	0.249	0.25
2nd Deck	0.249	0.25

[1] The lower side hull is defined as all plating below the lower girder, shown in Figure 5.8.2-1.
[2] The upper side hull is defined as all plating above the lower girder, shown in Figure 5.8.2-1.

In designing the plates shown in Table 5.8.2-2, the following observations were made:

- The slamming pressures strictly governed the bottom hull plate thickness.
- For side hull plates, the hydrostatic pressure determined the plate thickness for the lower portion while the wave slap loads dictated the plate thickness above that.
- The wet deck design pressures were a linear function of the clearance between the waterline and the structure. For the AutoFerry, the wet deck clearance was 9.15 ft.
- The main deck and 2nd deck were both assumed to carry the intended cargo for the craft – automobiles. A worst-case two-ton car load was assumed with the weight evenly distributed over the four wheels. Even with this extreme loading, it was found that the deck plating thickness was governed by the minimum allowable plate thickness for strength decks.

As the plating for each deck was designed, a parallel design of the internals supporting each deck was also completed. The same governing principles that were observed in the plating design were also applicable to the internal design. Table 5.8.2-3 shows the ABS requirements for the internals and the section modulus of the stiffener chosen to meet these requirements. Figure 5.8.2-1 accompanies Table 5.8.2-3 to show the location of the stiffeners and their relative size.

Upon completion of the local structure design, the global hull-girder section properties of the midship section were determined to compare with the requirements imposed by ABS. Table 5.8.2-4 shows the global loads as determined using the ABS HSC Guide.

The section modulus (SM) and moment of inertia of the midship section were found to be 99.0 ft^3 and 1832.0 ft^4, respectively. The values dictated by the local design present global factors of safety of 3.1 and 5.4 for the section modulus and hull-girder moment of inertia.

In addition to the longitudinal bending check, the transverse strength of the cross-structure was checked to verify that it would withstand the global loads imposed on it. The maximum bending and shear stresses induced in the cross-structure due to the global loads were 8,132 psi and 1,209 psi, respectively. Based on the allowable stresses provided by ABS, these represent safety factors of 2.1 and 8.2 in bending and shear.

Following the same guidelines established in the design of the midship section, a section forward of the midship was also designed. The section chosen was 71.7 feet from the forward perpendicular, at approximately 0.25*L. Figure 5.8.2-2 summarizes the results of this analysis.

Table 5.8.2-3

Design of Internal Structural Elements

Description	Required Section Modulus (in^3)	Design Section Modulus (in^3)
Bottom Hull		
CL girder	131.9	135.4
Outboard girder	131.5	135.4
Longitudinal stiffeners	11.0	11.9
Inboard transverse web	20.1	21.4
Outboard transverse web	18.8	21.4
Side Hull		
Lower girder	88.3	89.5
Middle girder	65.8	66.0
Upper girder	63.0	66.0
Longitudinal stiffeners	4.55	4.60
Transverse web below lower girder	29.6	29.8
Transverse web below middle girder	25.7	29.4
Transverse web below upper girder	27.1	29.4
Transverse web below main deck	27.1	29.4
Transverse web above main deck	58.1	66.0
Wet Deck		
Longitudinal stiffeners	5.90	6.30
Transverse web	101.3	105.6
Main Deck		
Longitudinal stiffeners	1.40	1.60
Inboard transverse web	45.9	46.2
Outboard transverse web	25.7	28.9
2nd Deck		
CL girder	101.1	101.6
Outboard girder	88.3	89.3
Longitudinal stiffeners	1.40	1.60
Inboard transverse web	45.9	46.2
Outboard transverse web	25.7	28.9

Table 5.8.2-4

Global Loads and Craft Sectional Property Requirements

Longitudinal Bending Moment (LT-ft)	31721
Vertical Shear due to Longitudinal BM (LT)	210.1
Transverse BM (LT-ft)	3415
Transverse Torsional Moment (LT-ft)	7805
Vertical Shear due to Transverse Loads (LT)	60.2
Minimum Longitudinal Section Modulus at Midship (ft^3)	31.84
Minimum Hull-girder Moment of Inertia at Midship (ft^4)	340.7
Minimum Transverse Bending Section Modulus along CL (ft^3)	4.17
Minimum Transverse Torsional Section Modulus (ft^3)	8.39

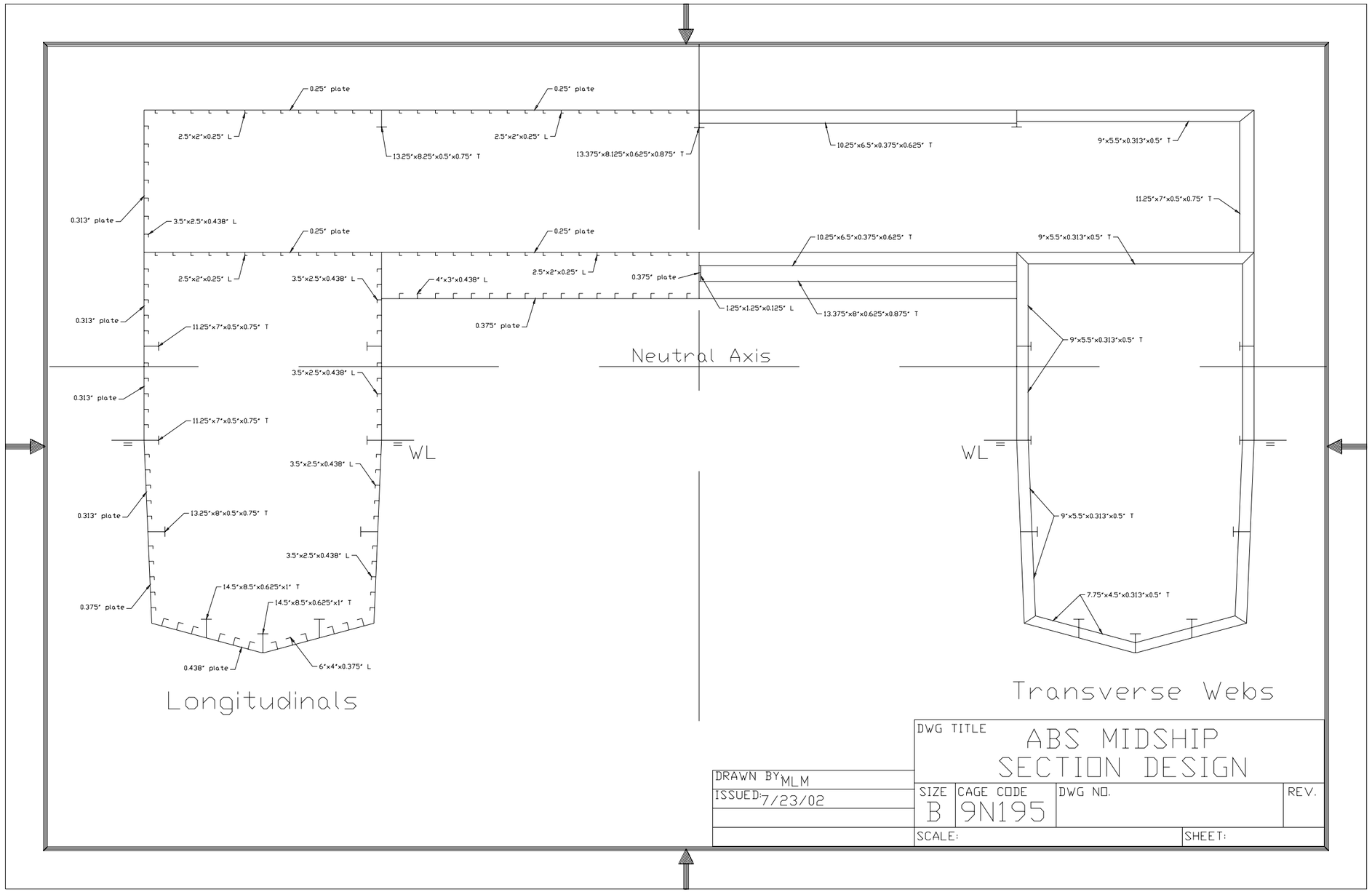

Figure 5.8.2-1. Midship Section Structural Design

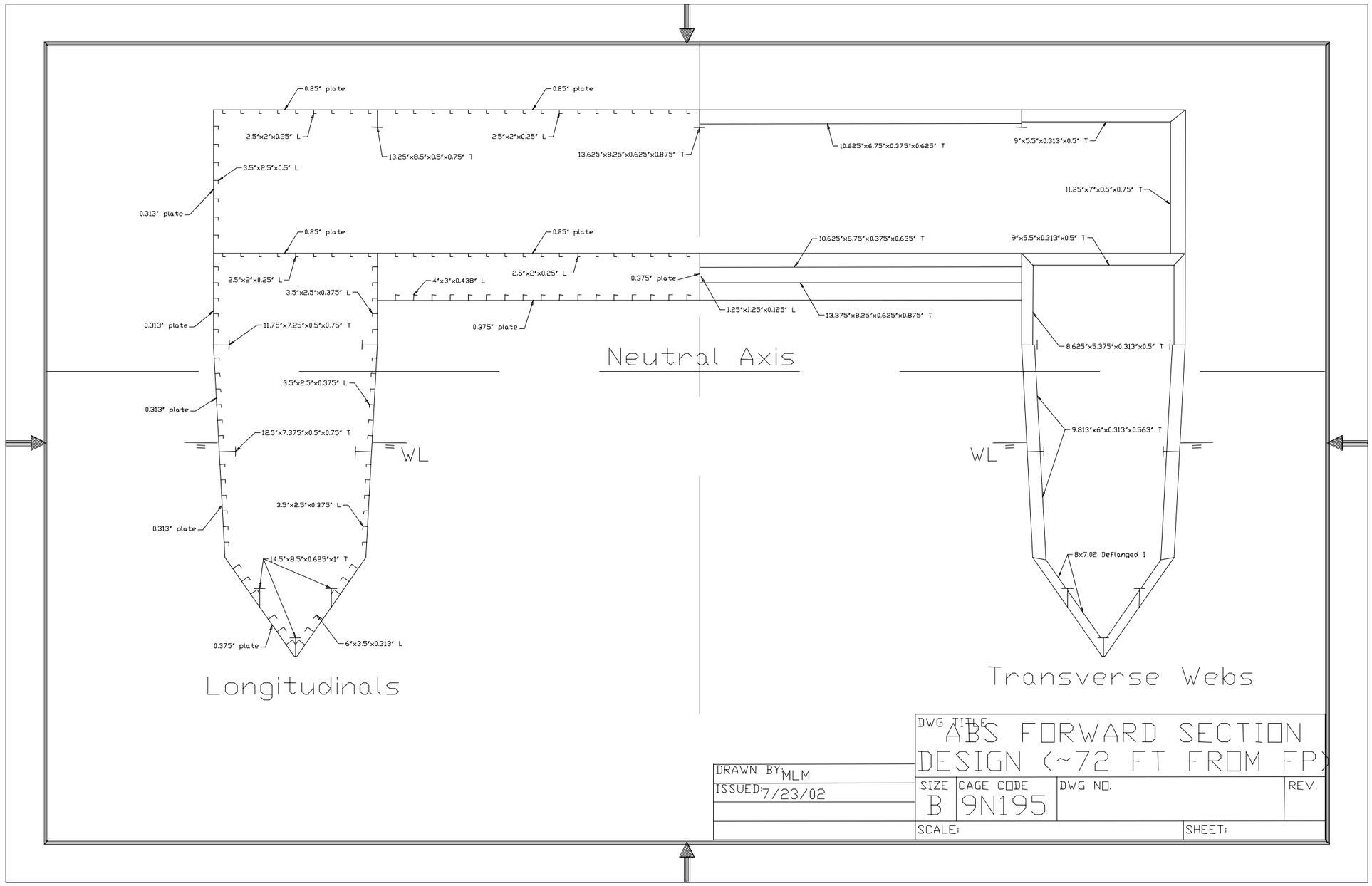

Figure 5.8.2-2. Forward Section (71.7 ft from FP) Structural Design

5.8.3 Structural Design of AutoFerry Using DNV Rules

In order to make a fair comparison, the arrangement (stiffener spacing and location) employed in the ABS design was maintained for the DNV design. A summary of the plate thickness requirements based on DNV and the thickness chosen for each location are shown in Table 5.8.3-1 for the midship section.

Table 5.8.3-1

Midship Section Plating Requirements

Description	Required Thickness (mm)	Design Thickness (mm)
Bottom Hull	12.91	13.0
Lower Side Hull[1]	7.32	8.0
Upper Side Hull[2]	6.79	7.0
Wet Deck Cross-Structure	6.79	7.0
Main Deck	8.54	9.0
2nd Deck	8.54	9.0

[1] The lower side hull is defined as all plating below the middle girder, shown in Figure 5.8.2-1.
[2] The upper side hull is defined as all plating above the middle girder, shown in Figure 5.8.2-1.

For the bottom hull plating and cargo deck plating, the DNV requirements result in a thicker plate than those using ABS. The opposite is true for the side hull and wet deck cross-structure. Based on these observations, it appears that the total weight of the plates comprising the decks analyzed will be approximately equal.

Finally, the global loads were determined using the DNV requirements and are summarized in Table 5.8.3-2.

Table 5.8.3-2

Global Loads for AutoFerry

Longitudinal Bending Moment (kN-m)	261448
Vertical Shear due to Longitudinal BM (kN)	12708
Longitudinal Torsional Moment (kN-m)	71755
Transverse BM (kN-m)	68882
Transverse Torsional Moment (kN-m)	170840
Vertical Shear due to Transverse Loads (kN)	4152

5.9 Route/Mission-Based Structural Design – Conclusions

The following conclusions can be drawn regarding the seakeeping performance of the AutoFerry:

- Maximum AutoFerry motions and accelerations in the vertical plane occur in head seas and bow seas, whereas the maximum wave-induced regular loads are developed at the low encounter frequencies associated with following seas. This suggests that the development of the hull-girder response loads (whipping and springing) and the slam impact loads, slated for Phase II of this project, will be of utmost importance in determining not only the true magnitude of the total extreme loads on the vessel, but also the operational conditions (vessel headings) which produce these limiting loads.

- Some form of ride-control system would be required for the intended AutoFerry application. This is typical of existing high-speed ferries currently in operation worldwide, and may consist of a forward retractable T-foil, active stabilizer fins, passive canards, or a combination of these various systems. In lieu of the incorporation of ride-control to mitigate the motions in the more severe conditions along the proposed AutoFerry route, the vertical plane motions and accelerations are in excess of typical seakeeping criteria, even for military applications.

The following conclusions regarding the structural loads and design can be drawn:

- The first-principles-based global loads for seas with significant wave height of 2 m and 3 m are close to those obtained through application of the ABS HSC guide. A safety margin of 20% on allowable stress was used for the first-principles approach under the assumption that the loads obtained from motions modeling represent a realistic assessment of the loads that are expected to be encountered along the intended route of the AutoFerry. If a greater level of confidence can be achieved, the margin could be reduced accordingly.

- For smaller craft, local loads due to slamming generally drive the structural design. In order for global loads to take precedence, the craft must be large or slender (high L/B). Although the AutoFerry is a relatively large craft by rulebook definition, the structural design according to ABS showed that the local slamming and hydrostatic pressures on individual structural elements were the governing factors for structural design. Thus, the global hull-girder requirements were inherently met and exceeded by the local design, with a safety factor of 3.1 for the midship section modulus. Thus, the need for a first-principles-based local slamming model to accurately determine the slamming pressures is further emphasized.

6.0 CONCLUSIONS & RECOMMENDATIONS

The specific objective of the study reported herein was to develop a route or mission-dependent approach to predict structural loads for high-speed multihulls. This is being created in a two-phased program of work to produce an easy to use ship motion and dynamic load calculation program and an overall statistical methodology that is suitable for use by Designers, Classification Societies, and the U.S. Navy. The specific work reported here is for Phase I of the program.

Under the Phase I effort, a 2D hydrodynamics and strip theory approach was used to develop an easy to use but reliable frequency-domain ship motion and dynamic loads prediction method for high-speed multihulls. As part of this process, the strip theory-based ship motion program, SHIPMO, was validated against several experimental investigations on the motions of high-speed catamarans. Overall, the strip theory frequency-domain model was found to provide an acceptable level of fidelity for motions data. The model performance degrades with increasing Froude number and is a result of the limitations of the underlying two-dimensional hydrodynamics theory. However, the ease of use, low computational cost, and the unavailability of any reliably validated computational techniques for the seakeeping modeling of high-speed multihulls renders the SHIPMO program, with its intrinsic capability to model multihulls, a very viable option.

The motions modeling of a notional trimaran hullform has also been attempted using SHIPMO. The conclusions derived from the validation effort suggested that the interference effects between the hulls has little significance in influencing ship motions in the vertical plane. The complete accuracy of the trimaran motion predictions is, as yet, undetermined.

The program has been successfully combined with a route/mission statistical module to combine short-term wave load predictions into a long-term (ship lifetime) load prediction, and to identify segments of the mission that are likely to be of concern from a ship slamming standpoint. The example of an AutoFerry operating between Port Canaveral, FL to New York has been used to develop both a notional route/mission module as well as the determination of statistical descriptions of seaway loads on a notional design for a catamaran operating on this route. The resultant statistical description of the seaway loads

(wave-induced loads) has been determined and compared to rulebook-based design criteria for a multihull craft.

Based on the analysis of the catamaran motions and wave-induced loads data, it is clearly evident that the extreme vessel motions and accelerations in the vertical plane (i.e. pitch, heave and vertical acceleration) occur in the head sea condition.

Based on these conclusions, and the potential for a very significant contribution to the state-of-the-art in the development of a rational approach to structural design for high-performance ships, we present here a brief outline of and recommendations for the continuation of this effort into the second phase, as outlined earlier. Highlights of the work to be accomplished in Phase II are as follows:

Under Phase II efforts, the frequency-domain motions/loads prediction program will be combined with a deterministic time-domain structural slamming program to establish a prediction for overall loads (see Section 5). A standard procedure and rationale will be established to apply these extreme loads to practical ship structure design. The complete prediction program will be verified and validated against several sets of available sea trials and experimental data. The technical approach for the proposed effort is fully integrated with that of the Phase I effort. In broad terms, the Phase II approach can be described in the following steps:

- Study the latest background literature and references covering developments in the area of the water entry (impact or slamming) problem for ships.

- A rationale will be developed to identify the most probable combinations of operational elements, i.e., speed, heading, and sea-states for the prescribed route/mission, that will lead to any considerable impact and slamming loads based on certain threshold values of slamming parameters. The extreme value statistics of dynamic loads and motions obtained from the Phase I frequency-domain program (SHIPMO) will be identified for the probable combinations of operational elements leading to slamming.

- An impact and slam load prediction program will be developed through the development of a deterministic time-domain model (Section 5). The time-domain model will be simulated for the selected operational element combinations to obtain the extreme values of slamming parameters. These extreme slam pressures can then be converted to both local and global lifetime maximum loads, as described in Section 5.

- The time-domain slamming program will be integrated into the overall route and mission-dependent program developed in Phase I.

- A rational prediction process will be developed to use the calculated load statistics and estimated extreme loads in practical ship structure design. The most appropriate load case combinations will be investigated to form the basis for the ultimate load design methods. A probabilistic approach will also be completed for a reliability-based structure design standard.

7.0 REFERENCES

1) Balasubramanian, S., Cullina, J.C. & Mish, W.H. (2001). "Performance and Cost-Based Design Discrimination for Fast-Ferry Hullform Selection," Proceedings, 17th Fast Ferry Conference, New Orleans.

2) Beck, R.F. and Troesch, A. W. (1990). "Documentation and User's Manual for the Computer Program SHIPMO.BM", Department of Naval Architecture and Marine Engineering Report No. 89. University of Michigan.

3) Bertram, V. (2000). "Practical Ship Hydrodynamics", Butterworth Heinemann, Oxford, UK.

4) Bhattacharyya, R. (1978). “Dynamics of Marine Vehicles. A Volume in Ocean Engineering”, A Wiley

5) Series Edited by Michael E. McCormick. John Wiley & Sons, Inc., New York, 1978.

6) Chapman, R.B. (1975). “Free Surface Effects for Yawed Surface Piercing Plates”, Journal of Ship Research, 20, pp. 125-132.

7) Salvesen, N., Tuck, E.O., and Faltinsen, O. (1970). “Ship Motions and Sea Loads”, Transactions, SNAME 78, pp.250-287.

8) Lewis, E.V., Hoffman, D., Maclean, W.M., van Hoof, R., and Zubaly, R.B. “Load Criteria for Ship Structural Design.” SSC-240 (1973).

9) Band, E.G.U. “Analysis of Ship Data to Predict Long-Term Trends of Hull Bending Moments.” American Bureau of Shipping, New York (1966).